TOWARDS UNDERSTANDING THE ANCESTRAL ROLE OF INSULIN-LIKE PEPTIDES (ILPS) IN *HYDRA*

Dissertation

Zur Erlangung des Doktorgrades
der Mathematisch-Naturwissenschaftlichen Fakultät
der Christian-Albrechts-Universität zu Kiel

Vorgelegt von

Xiaoyu Xiang

Kiel, im August 2016

Erster Gutachter: Prof. Dr. Dr. h.c. Thomas Bosch
Zweiter Gutachter: Prof. Dr. Hinrich Schulenburg

Tag der mündlichen Prüfung: 25th Oktober 2016
Genehmigung zur Veröffentlichung: 1st November 2016

Prof. Dr. Natascha Oppelt, Dekanin

Meinen Eltern

Content

I. Summary

Insulin/Insulin-Like Peptides (ILPs) and their signalling pathways are evolutionary conserved pathways regulating metabolism, growth, stress resistance, reproduction and lifespan of animals. However, the ancestral roles of ILPs in early emerged multicellular organisms remain unknown. The present thesis explores the origin of ILPs among basal metazoans and investigates the function of ILPs in a basal organism *Hydra*.

The *in silico* search for ILPs in published databases revealed the presence of *ilp* genes in Placozoa, Cnidaria and Bilateria phyla, whereas no *ilp* genes were detected in Choanozoa, Porifera and Ctenophora. This indicates that *ilps* emerged after the radiation of major Metazoa groups and consistent with multiple origins of the nervous systems. Interestingly, every organism checked contained different numbers of *ilps*: 7 *ilps* in *Nematostella vectensis*, 6 *ilps* in *Acropora digitfera*, 4 *ilps* in *Aurelia aurita* and 3 *ilps* in *Hydra*, indicating that intensive radiation of *ilps* (adaptation) on a genus level. Exploring pattern of gene expression along *Hydra* body revealed that 3 *ilps* from *Hydra vulgaris AEP* named *hyilp-A*, *hyilp-B* and *hyilp-C*, were highly expressed in the head region, while *hyilp-B* and *hyilp-C* were expressed in the foot region. Moreover, *hyilp-B* also exhibited a dynamic expression pattern at the budding region during bud development. Strikingly, *hyilp-A* and *hyilp-B* turned out to be expressed in neurons at both transcription and protein levels.

Starvation and knockdown of *Hydra insulin receptor* (*hyinsr*) gene promoted high expression of *hyilp-A*, indicating that HyILP-A plays a putative role in the nutrient sensing and potentially is regulated by HyINSR signalling. Inhibition of GSK-3 suppressed the expression of *hyilp-A* and *hyilp-C*, indicating *hyilp-A* and *hyilp-C* may be downstream genes of *Hydra* Wnt signalling, which is known to be crucial for pattern formation. To dissect HyILP-B functions, transgenic *Hydra* polyps were generated using either HyILP-B overexpression or HyILP-B knockdown constructs. Population growth rate analysis revealed that HyILP-B overexpression leads to *Hydra* population growth delay. Interestingly, cell cycle dynamics was not influenced. HyILP-B knockdown did not affect population growth rate. In contrast to insulin in mammalians, HyILP-B appears not to be proteolytically cleaved during maturation. Taken together, the present study reveals that HyILPs as neuron secreted peptides, most possibly play

roles in nutrient regulation and growth control through HyINSR signalling pathways in *Hydra*.

II. Zusammenfassung

Einblicke in die angestammte Rolle der Insulin-ähnlichen Peptide (ILPS) in *Hydra*

Insulin/Insulin-ähnliche Peptide (ILPs) und ihre Signalwege sind evolutionär konserviert und regulieren den Stoffwechsel, Wachstum, Stressresistenz, Reproduktion, und die Lebensdauer in Tieren. Die ursprünglichen Funktionen der ILPs in früh entstandenen multizellulären Organismen verbleiben unklar. Die vorliegende Arbeit erforscht den Ursprung von ILPs in basalen Metazoen und untersucht die Funktion der ILPs in dem basalen Organismus *Hydra*.

Die in silico Suche nach ILPs in publizierten Datenbanken zeigte die Anwesenheit von ilp Genen in den Stämmen Placozoa, Cnidaria und Bilateria. Hingegen wurden in Choanozoa, Porifera und Cternophora keine ilps gefunden. Das deutet darauf hin, dass ilps nach der Abspaltung von der großen Gruppe der Metazoa und einheitlich mit vielen Ursprüngen des Nervensystems entstanden sind. Jeder Organismus der überprüft wurde besaß interessanterweise eine unterschiedliche Anzahl an ilps: 7 ilps in *Nematostella vectensis*, 6 ilps in *Acropora digitifera*, 4 ilps in *Aurelia aurita* und 3 ilps in *Hydra*, was darauf hindeutet, dass weitere Abspaltungen von ilps (Anpassungen) auf der Ebene der Gattung entstanden sind.

Erforschung des Genexpressionsmusters entlang der Körperachse von Hydra zeigte, dass 3 ilps in *Hydra vulgaris* AEP, hyilp-A, hyilp-B und hylip-C, stark in der Kopfregion exprimiert werden, während hyilp-B und hylip-C nur in der Fußregion exprimiert werden. Außerdem wies hyilp-B ein dynamisches Expressionsmuster in der Knospungsregion bei der Knospenentwicklung auf. Interessanterweise wurden hyilp-A und hylip-B auf Transkriptions- und Proteinebene in den Neuronen exprimiert.

Hungern und Ausschalten des Insulinrezeptor Genes von *Hydra* (*hyinsr*) führte zu erhöhten Expression von hyilp-A, was vermuten lässt, dass HyILP-A eine wichtige Rolle in der Verarbeitung von Nährstoffen spielt und möglicherweise durch HyINSR Signalisierung reguliert wird. Inhibierung von GSK-3 verminderte die Expression von hyilp-A und hyilp-C, was auf hyilp-A und hyilp-C als nachgeschaltete Hydra Wnt-Signalweg Gene deutet, welcher entscheidend für die Musterbildung ist.

Zur Analyse der Funktionen von HyILP-B wurden transgene *Hydra* Polypen generiert mit entweder einer HyILP-B Überexpression oder HyILP-B Knock-down Konstrukten. Untersuchungen des Populationswachstums zeigten, dass HyILP-B Überexpression

zur Verzögerung des Populationswachstums in *Hydra* führte. Interessanterweise wurde der Zellzyklus nicht beeinflusst. Der Knockdown von HyILP-B führte hingegen zur keiner Veränderung des Populationswachstums. Im Gegensatz zum Insulin der Säugetiere wurde HyILP-B während der Maturation proteolytisch nicht gespalten. Zusammengefasst zeigt diese Arbeit, dass HyILPs als Neuronen sekretierte Peptide sehr wahrscheinlich eine Rolle in der Verarbeitung von Nährstoffen und in der Kontrolle der Größe durch den HyINSR Signalweg in *Hydra* spielen.

III. Abbreviations

% (v/v)	Volume concentration (volume/volume)
% (w/v)	Mass concentration (weight/volume)
A	Adenine
aa	Amino acids
Amp	Ampicillin
AP	Alkaline Phosphatase
ASW	Artificial Seawater
AS160/TBC1D4	Akt substrate of 160 kDa / TBC1 domain family member 4
AC	Activating adenylyl cyclase
ALP	Alsterpaullone
b	Base
BCIP	5-Brome-4-Chlor-3-Indolylphosphate
BLAST	Basic Local Alignment Search Tool
bp	Base pairs
BrdU	5-Brom-Deoxy-Uridin
BSA	Bovine Serum Albumin
BAD	Bcl-2-associated death promoter
C	Cysteine or Control
℃	Degree Celsius
cDNA	Complementary DNA
CHAPS	3-[(3-Cholamidopropyl) -Dimethylammonio] -1-Propansulfonate
cm	Centimeter
cAMP	Cyclic adenosine monophosphate
C. elegans	*Caenorhabditis elegans*
CHICO	*Drosophila* insulin receptor substrate
CDS	Coding DNA sequence
CLSM	Confocal Laser Scanning Microscopy
d	Day
DIG	Digoxigenin
DMSO	Dimethylsulfoxid
DNA	Deoxyribonucleic acid
DNase	Deoxyribonuclease
dNTP	Deoxynucleotide triphosphat
D. melanogaste	*Drosophila melanogaster*
DAF2	Abnormal dauer formation protein 2
DIR	*Drosophila* insulin like receptor
dFOXO	Drosophila forkhead box O transcription factor
dILPs	*Drosophila* insulin like peptides
E. coli	*Escherichia coli*

EDTA	Ethylenediaminetetraacetic Acid
EF	Elongation factor 1 alpha
e.g.	Lat.: exempli gratia, engl.: for example
EGF	Epidermal growth factor
ECM	Extracellular matrix
endo	Endoderm
ecto	Ectoderm
endo epi	Endodermal epithelial cells
ecto epi	Ectodermal epithelial cells
F	Forward or Phenylalanine
Fig.	Figure
FOXO	Forkhead box O
G	Glycine
GFP	Green fluorescent protein
GSK3	Glycogen synthase kinase 3
GPCRs	G protein-coupled receptors
gld	Gland cell
h	Hour (s)
H_2O	Millipore water
HCl	Hydrochloric Acid
HyILPs	*Hydra* insulin like peptides
HvAEP	*Hydra vulgaris AEP*
Hm/Hmag	*Hydra magnipapillata*
Ho/Holi	*Hydra oligactis*
Hv/Hvir	*Hydra viridissima*
H+F	Head and Foot
I	Isoleucine
ILPs	Insulin-like peptides
INS	Human insulin
IGFs	Insulin-like growth factors
INSLs	Human Insulin like peptides
INSRs	Insulin receptors
IGFRs	IGF receptors
IRSs	Insulin receptor substrates
ILR	Insulin like receptor
in silico	Via computer simulation
in situ	Natural location
i-cells	Interstitial cells
HyINSRkd	*Hydra* INSR knockdown
JJT	Jones-Thornoton-Taylor

K	Lysine
Kb	Kilo base pairs
kV	Kilovolt
L	Liter or Leucine
LB	Lauria Bertani (bacterial growth broth)
M	Molar or methionine
m	Milli
mA	Milliampère
MAB	Maleic Acid Buffer
MAB-B	Maleic Acid Buffer with BSA
MAB-T	Maleic Acid Buffer with Tween20
MEGA	Molecular Evolutionary Genetic Analysis
mg	Milligram
min	Minute(s)
ml	Milliliter
mm	Millimetre
mM	Millimolar
mRNA	Messenger-RNA
MAPK	Mitogen activated protein kinase
mTOR	Mammalian target of rapamycin
MNCs	Brain median neuron secretory cells
n.s.	Nonsignificant
µ	Micro
µg	Microgram
µl	Microliter
µM	Micromolar
n	Number of replicates
NaOH	Sodium Hydroxide
NBT	Nitro Blue Tetrazolium
NCBI	National Center for Biotechnology Information
ng	Nanogram
Nv	*Nematostella vectensis*
ORF	Open reading frame
P	Proline or peptide
PBS	Phosphate Buffered Saline
PBT	PBS with Tween20
PCR	Polymerase Chain Reaction
PTTH	Protheracicotropic Hormone
PI3K	Phosphoinositide 3-kinase
PKB	Protein kinase B

Phyre2	Protein Homology/analogy Recognition Engine V2.0
qRT-PCR	Quantitative Real-Time PCR
R	Reverse or Arginine
RNA	Ribonucleic Acid
RNAi	RNA Interference
RNase	Ribonuclease
rpm	Rounds per minute
RT	Room Temperature or Reverse Transcription
RT-PCR	Reverse Transcriptions-PCR
RLNs	Relaxins
RXFPs	Relaxin family peptide receptors
S	Serine
SD	Standard deviation
SDS	Sodiumdodecylsulfate
SDS-PAGE	Sodiumdodecylsulfate polyacrylamide gel electrophoresis
sec	Seconds
SEM	Standard Error of the Mean
SMART	Simple Modular Architecture Research Tool
sp.	Species
SP	Signal peptide
T	Thymine
TAE	Tris-Acetate-EDTA-buffer
Taq	*Thermophilus aquaticus*
TBE	Tris-Boric acid-EDTA-buffer
TEMED	N,N,N´,N´- Tetraethylendiamin
T_m	Melting temperature
Tris	Tris-(Hydroxymethyl) -Aminomethane
tRNA	Transfer RNA
TSC1/2	Tuberous sclerosis proteins 1 and 2
U	Units
USP	Ultraspiracle
UTR	Untranslated region
UV	Ultraviolet Light
V	Volt or valine
WT	Wild Type
Y	Tyrosine

1. Introduction

1.1 Evolutionary conserved Insulin/insulin-like growth factor signalling plays a key role in animal development.

Every kind of organism must respond to physiological and environmental cues in order to develop, locate food, keep off toxic or pathological insults, and survive stress. This requires robust regulatory mechanisms that coordinate physiological responses at systematic level. For example, growth, lifespan and reproduction can be adjusted based on nutrient availability and environmental conditions such as temperature (Bosch and David 1984, Littlefield et al. 1991, Fielenbach and Antebi 2008, MacNeil et al. 2013). Although, the genotype of an organism determines its available regulatory mechanisms, organisms' physiological activities, instead of being passively dictated by available resources, are governed by lots of regulatory layers, including neural signalling, hormones, and signal transduction pathways which form logical circuits (Fielenbach and Antebi 2008).

Expanded gene families often come together with an increase in organismal complexity. Gene families are groups of homologous genes descended from a common ancestral gene through gene duplications. The distribution of gene family size varies substantially among species and gene families (Lespinet et al. 2002). Human insulin-like peptides (ILPs) gene family contains 10 members including insulin (INS), insulin-like growth factors (IGFs), relaxins (RLNs) and insulin like peptides (INSLs) (Claeys et al. 2002), while mouse olfactory receptor family, as the largest gene family, contains more than 1000 members (Mombaerts 2001, Zhang and Firestein 2002). The largest family in *Drosophila melanogaster* is the trypsin family containing 111 members (Gu et al. 2002). A gene family is formed by gene duplication, however, members from the same gene family may have distinct functions or even no function. When a new gene emerged from an ancestral gene by gene duplication, it has four evolutionary fates (Zhang 2003). First, the new gene may gain novel functions, which is neofunctionalization. Second, the new gene may maintain the same or similar function as its parental gene in order to provide extra amount of protein or RNA products, or works as a buffer against mutation. Third, each daughter gene adopts part of the functions of their parental gene by subfunctionalization (Hughes 1994, Nowak et al. 1997). Fourth, the new gene turns into a pseudogene that loses its

function because of functional redundancy. Gene duplication provides raw genetic material for novel functional genes as the bases of protein interaction networks (Rubin et al. 2000, Wagner 2001). Therefore, together with structured metabolic networks, protein interaction networks build robust and flexible biological systems in adapting to various environments (Wagner 1994, Wagner 2001, Gu et al. 2003).

ILPs family and its signalling pathways cascades are evolutionary conserved in animal kingdom, regulating metabolism, growth, stress responses, lifespan, reproduction and neuroendocrine processes (Siddle 2011, Bathgate et al. 2013). In human, INS/IGFs signalling pathway is well studied because it plays an essential role in maintaining human health and longevity (Siddle 2011, Sciacca et al. 2012). Meanwhile, there is another set of ILPs signalling in human - the relaxin family signalling pathway. INS/IGFs signalling pathway contains 3 ligands - one INS and two IGFs with different binding affinities to 6 kinds of tyrosine kinase receptors - Insulin receptors (INSRs), IGF receptors (IGFRs) and their hybrid receptors (Sciacca et al. 2012). These ligands bind to the receptors and initiate downstream cascades, which lead to different functional category, metabolic effects and mitogenic effects (Figure 1-1A). First, Insulin receptor substrates (IRSs) or Shc can be recruited to the INSR or IGFRs and get phosphorylated. Second, phosphorylated IRSs or Shc can initiate two independent downstream pathways/cascades - Phosphoinositide 3-kinase (PI3K) / Protein kinase B (PKB or Akt) and Ras / Mitogen activated protein kinase (MAPK) pathways. Finally, key substrates, kinases or transcription factors, can be activated, which lead to distinct physiological responses, including glycogen synthase kinase 3 (GSK3), regulating glycogen synthesis; Akt substrate of 160 kDa / TBC1 domain family member 4 (AS160/TBC1D4), regulating glucose transport; tuberous sclerosis proteins 1 and 2 (TSC1/2) regulating the mammalian target of rapamycin (mTOR) and protein synthesis; the Bcl-2-associated death promoter (BAD) protein, regulating apoptosis; forkhead box O (FOXO) transcription factors, regulating expression of gluconeogenic and longevity genes (Manning and Cantley 2007, Wilicox et al. 2008).

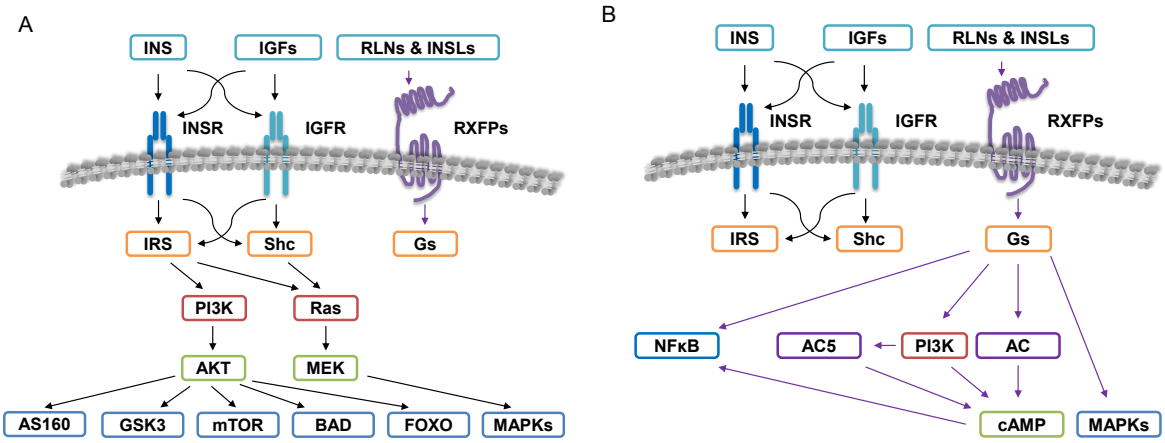

Figure 1-1 ILPs family signalling pathways in human

(A) INS/IGFs signalling pathway: INS and IGFs binds to INSR and IGFR, resulting in recruiting and phosphorylation of IRS or Shc. Downstream cascades are activated through either PI3K/AKT pathway or Ras/MEK pathway. (B) Relaxin family signalling pathway: RLN family ligands bind to RXFPs, which leads to coupling of receptor with specific G proteins (Gs), which later either influencing cAMP accumulation or mediating MAPK signalling and NFκB transcription. The principal components of pathways are indicated: ligands (in light blue), receptors, tyrosine-phosphorylated substrates and coupled G protein (in orange), adaptors and transducers (in red), serine/threonine kinases (in green), adenylyl cyclase (in purple) and serine/threonine phosphorylated substrates and downstream components (in sea blue). See Abbreviations.

Relaxin family signalling pathways are implicated in the regulation of reproduction, cardiovascular system, organ protection, metabolism and neuroendocrine processes (Figure 1-1B) (Bathgate et al. 2013, Yegorov et al. 2014, Halls et al. 2015). There are 7 relaxin ligands, including 3 RLNs and 4 INSLs, and four Relaxin family peptide receptors (RXFPs) (1-4) which belong to G protein-coupled receptors (GPCRs) (Bathgate et al. 2013). Although they belong to ILPs family signalling, Relaxin family signalling pathways regulate their corresponding biological functions through different cascades. In general, relaxins mediate the level of cyclic adenosine monophosphate (cAMP) and downstream targets, such as MAPK signalling and NFκB transcription (van der Westhuizen et al. 2007, van der Westhuizen et al. 2010), through activating adenylyl cyclase (AC) (Hsu 1999, Hsu et al. 2000, Nguyen et al. 2003, Nguyen and Dessauer 2005, Halls et al. 2006, Halls et al. 2007, Halls et al. 2009).

ILPs family signalling pathways are highly conserved in invertebrates, playing essential roles in regulating growth, body size, metabolism, stress resistance, life span and reproduction (Garofalo 2002, Gronke et al. 2010, Kaletsky and Murphy 2010, Murphy and Hu 2013). In most cases, invertebrates possess multiple ILPs genes, but

several or single INSR. For example, there are 40 ILPs in *Caenorhabditis elegans* (*C. elegans*) (Li and Kim 2008, Ritter et al. 2013) and 8 ILPs in *Drosophila melanogaster* (*D. melanogaster*) (Gronke et al. 2010, Colombani et al. 2012, Garelli et al. 2012), while only a single insulin like receptor (ILR) is found in each of two organisms, including Abnormal dauer formation protein 2 (DAF2) in *C. elegans* (Kimura et al. 1997) and *Drosophila* insulin like receptor (DIR) (Fernandez et al. 1995). Homolog of the relaxin GPCRs are identified in *D. melanogaster* (Van Hiel et al. 2015), moreover, in a basal metazoan animal, *Trichoplax adhaerens* (Jekely 2013). The downstream signalling network of ILPS signalling pathway is simpler in invertebrates than that in mammals. For example, *Drosophila* contains a single insulin receptor substrate (CHICO) and a single forkhead box O transcription factor (dFOXO), while human contains four kinds of IRS and FoxO transcription factors (Edgar 2006, Calnan and Brunet 2008). However, the overall principle of ILPs signalling remain conserved in invertebrates from ligands to the key mediator – Akt (Figure 1-2) (Garofalo 2002, Fielenbach and Antebi 2008). The relative simplicity of the downstream signalling network of ILPs signalling and the diversification of ILPs implicate that the diverse functions of ILPs signalling could be mediated by functional diversification of the ligands to a certain degree. Furthermore, experimentally tractable model organisms with rather simple ILPs family signalling cascades provide advantages to dissect the evolutionary conserved functions of ILPs family signalling.

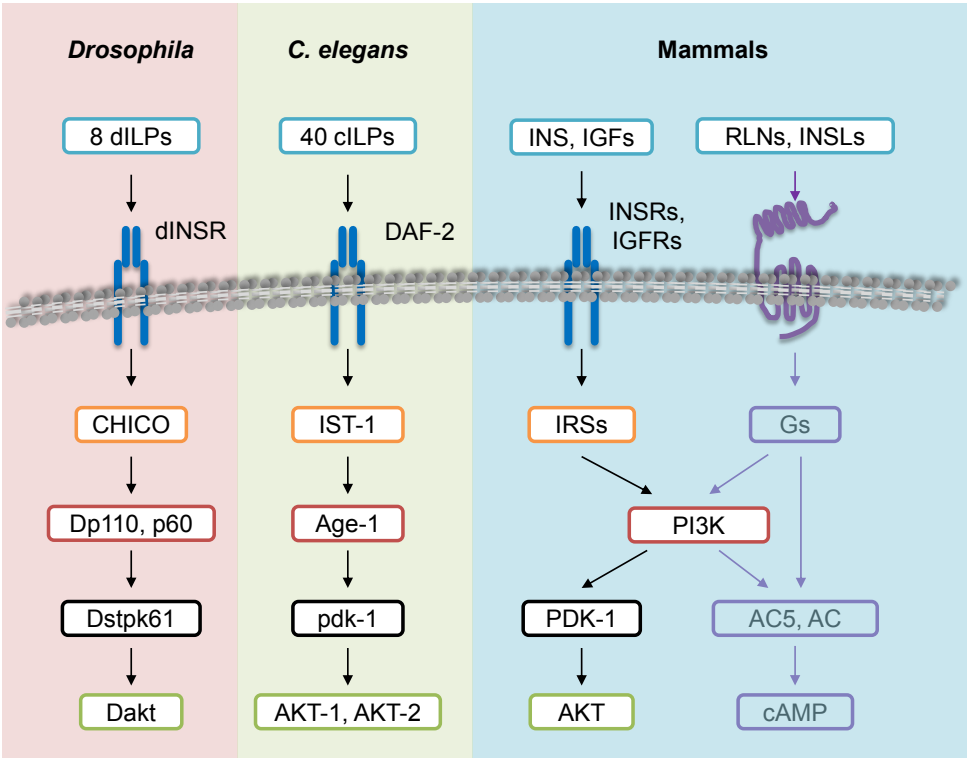

Figure 1-2 Evolutionary conservation of ILPs family signalling across species.

ILPs (in light blue) and homologous receptors (no colour) are present in *Drosophila*, *C. elegans* and mammals. An IRS homolog (in orange) is present in *Drosophila* (CHICO) and *C. elegans* (IST-1) (Wolkow et al. 2002). Homologs of PI3K, PDK-1 and AKT among *Drosophila*, *C. elegans* and mammals are indicated in red, black and green respectively. Cellular components of relaxin family signalling are indicated in purple. See Abbreviation.

1.2 ILPs as anchors to dissect functions of ILPs signalling.

ILPs family consists of more than 200 members across animal kingdom (Sanger 1959, PROSITE 2004). Proteins of ILPs family are synthesized as prepro-proteins containing 4 domains (pre, B, C, A) (Figure 1-3) (Pierre De Meyts et al. 2000-2013). Proteolytic removal of the pre-domain occurs in the rough endoplasmic reticulum. Fully folded pro-ILP molecules are transported to the Golgi apparatus in which they are packaged into storage granules together with the converting proteases or their precursors (Steiner et al. 1984, Steiner et al. 1985). During the formation and maturation of secretion granules, the C- domain of pro-ILP is typically cleaved off in order to form mature ILP, while the A and B domains are covalently linked by two invariant disulphide bridges (Steiner et al. 1985). Secondary structure analysis shows that the B-domain contains a single helix which lies across the 2 helices of the A-domain (Figure 1-3)(Pierre De Meyts et al. 2000-2013). Genome analysis reveals that the B- and A-domains are encoded by individual exons separated by an intron, which interrupts the C domain encoding sequence (Figure 1-3) (Steiner et al. 1985).

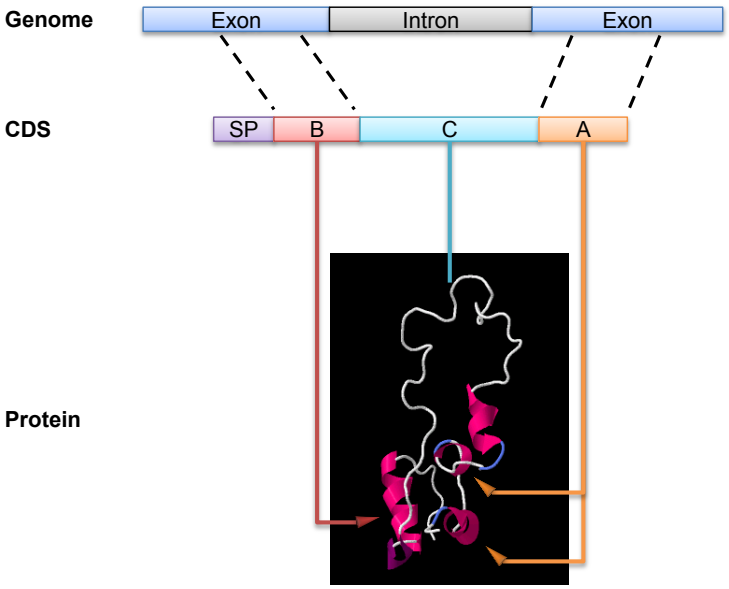

Figure 1-3 ILPs family features

CDS: coding DNA sequence; SP: signal peptide.

In vertebrates and invertebrates, most ILPs are produced in neuroendocrine cells located in the central neurous system and play a role of neuropeptides (Garofalo 2002, Fernandez and Torres-Aleman 2012). However, there are some *ilps* expressed in other organs, such as *insulin* produced in pancreas β cells in human and *dilp6* produced in fat cells in *Drosophila* (Bai et al. 2012). In general, ILPs have a number of functions, shared between ILPs or specialised in specific ILPs (Ritter et al. 2013). First, ILPs regulate glucose metabolism. Insulin in human is well known for its important role in regulation of metabolic activity, such as induction of glycogen synthesis, inhibition of gluconeogenesis and influence of lipid storage. ILPs with similar functions can also be found in invertebrates. In *Drosophila*, level of trehalose, which is the major hemolymph sugar in insects, increases in *dilp2* mutants, while *dilp6* mutants demonstrate slightly enhanced lipid storage (Gronke et al. 2010). Furthermore, release of bombyxin, a peptide of ILPs family in insects, is suppressed by starvation, stimulated by feeding, and influences the concentration of trehalose (Satake et al. 1997, Masumura et al. 2000). Second, ILPs are implicated in growth and size control of body or organ. IGFs are a key growth hormones in mammals influencing dramatically body and organ size, while *dilp2* not only delays the development time of egg-to-adult in *Drosophila* if mutated (Gronke et al. 2010), also increases organismal size through increasing cell size and cell number of individual organs if overexpressed (Brogiolo et al. 2001). Third, ILPs are involved in life span regulation. Reduction of insulin could increase longevity and delay the onset of protein-aggregation-mediated toxicity in mammals and *C. elegans* (Cohen and Dillin 2008, Taguchi and White 2008), While *dilp2* plays as a limit factor of *Drosophila* lifespan. Fourth, ILPs play a role in stress resistance. In *Drosophila*, *dilp1-4* mutant were resistant to paraquat and starvation, while *dilp2-3, 5* were highly resistant to oxidative stress (Gronke et al. 2010). Fifth, ILPs has been implicated in the reproduction. Relaxin, produced by the corpus luteum and/or placenta, is a major circulating hormone during pregnancy in all mammalian species (Bathgate et al. 2013). In *Drosophila*, mutants of *dilp2*, *dilp3*, *dilp5* and *dilp6* demonstrate significantly decreased fecundity (Gronke et al. 2010).

1.3 *Hydra* – a basal metazoan model organism

Hydra has been an important model organism for studies on regeneration, development, pattern formation and symbiosis since its first discovery (van Leeuwenhoek 1702) and use in experimental studies in the early 18th century (Trembley 1744). More recently, thanks to well established transgensis techniques (Wittlieb et al. 2006) as well as available transcriptomes of *Hydra vulgaris AEP* (Hemmrich et al. 2012) and genome of *Hydra magnipapillata* (Chapman et al. 2010), studies on *Hydra* have contributed significantly to our understanding of the origin and evolution of developmental genes and pathways, innate immunity, ancient nervous system, tumorigenesis, and the concept of the metaorganisms or holobionts (Bosch et al. 2009, Khalturin et al. 2009, Boehm et al. 2012, David 2012, Fujisawa and Hayakawa 2012, Meinhardt 2012, Bosch 2013, Franzenburg et al. 2013, Bosch 2014, Domazet-Loso et al. 2014, Grasis et al. 2014).

Phylogeny: The genus *Hydra* belongs to the phylum Cnidaria located at the base of Eumetazoan (Figure 1-4). The phylum Cnidaria, as a sister group of the Bilateria, is characterised by their phylotypic cell type – the cnidocytes or nematocytes (Tardent 1995). In contrast to the Porifera, Cnidaria contain following characters: true tissues connected by tight junctions, sensory, nerve and muscles cells and a gastric cavity (Nielsen et al. 1996). Cnidaria are divided into five classes: Anthozoa, Staurozoa, Scyphozoa, Cubozoa and Hydrozoa (Collins et al. 2006). Within *Hydra*zoans, the species *Hydra viridissima*, which contains an unicellular *Chlorella* algae as its symbiotic partner (Habetha et al. 2003), is located at the base of the phylogenetic tree followed by *Hydra oligactis*, *Hydra carnea* and the laboratory strain of *Hydra vulgaris AEP* (Martin et al. 1997), *Hydra vulgaris* and *Hydra magnipapillata* (Figure 1-4). Despite the species name, it is known that *Hydra vulgaris AEP* is rather closely related to *Hydra carnea* instead of *Hydra vulgaris*, while *Hydra magnipapillata* together with *Hydra vulgaris*, build the most derived group within the Hydrozoans (Figure 1-4) (Schwentner and Bosch 2015).

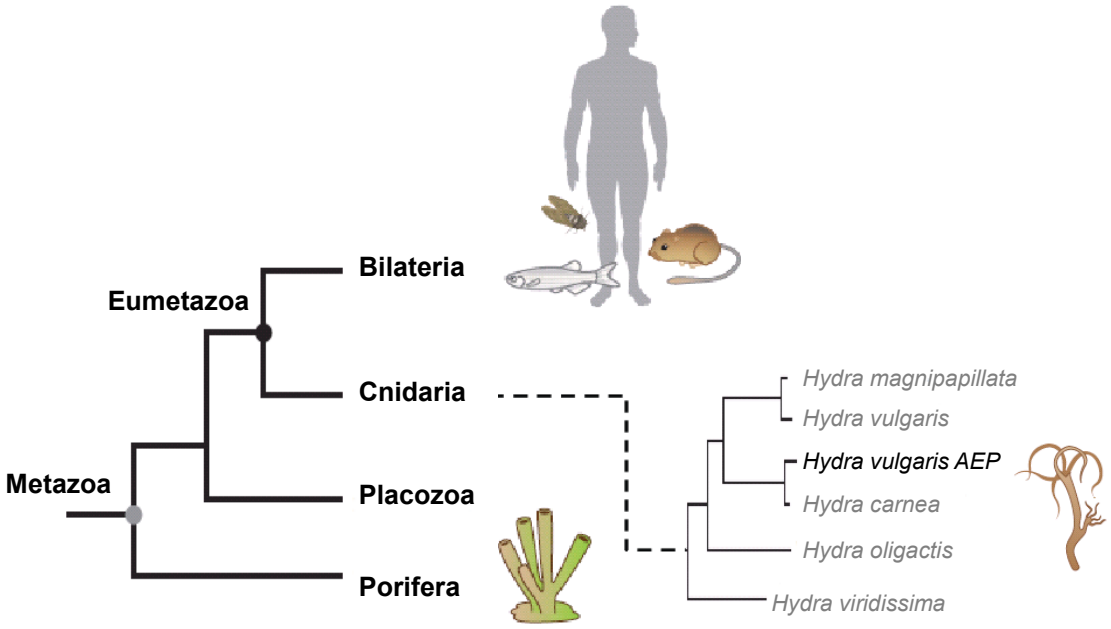

Figure 1-4 Schematic phylogenetic tree showing the main branches in metazoan evolution.
The Porifera are at base of the metazoan and Cnidaria represent a sister group to all Bilateria. Cnidaria are divided into five classes, one of which is *Hydra*zoa including the species of *Hydra viridissima*, *Hydra oligactis*, *Hydra carnea, Hydra vulgaris AEP*, *Hydra vulgaris* and *Hydra magnipapillata*. Figure modified from (Bosch 2013).

Morphology and Histology: *Hydra* polyp has a simple body with a single oral-aboral body axis. Its body consists of the head with hypostome and tentacles, the tube-like body column, bud region and the foot region with peduncle and basal disc for attachment to the substrate (Figure 1-5A). *Hydra*'s body is made of two monolayered epithelia - ectoderm and endoderm separated by an extracellular matrix (ECM) called mesoglea, which provides stability and elasticity to the polyp (Figure 1-5B). The ectoderm faces the outside of a polyp, while the endoderm surrounds the internal gastric cavity (Figure 1-5B). *Hydra* possesses around 20 different cell types originating from three independent stem cell linages: a unipotent ectodermal epithelial cell lineage, a unipotent endodermal epithelial cell lineage and a multipotent interstitial cell (i-cell) lineage (Bosch 2009, Bosch et al. 2010). I-cells are located in the ectoderm throughout the gastric region and give rise to a variety of specialized somatic cells, such as nerve cells, nematocytes, gland cells as well as germ cells (David and Murphy 1977, Koizumi and Bode 1991, Bosch 2007). Gland cells, located in the endoderm, secrete mucus and digestive enzymes to the gastric cavity. Nematocytes are formed by proliferating and differentiating nests of nematoblasts. They are later taken up by battery cells and

are used in the tentacles for prey catching and defence (Slautterback 1967, Wood and Novak 1982, Campbell 1987).

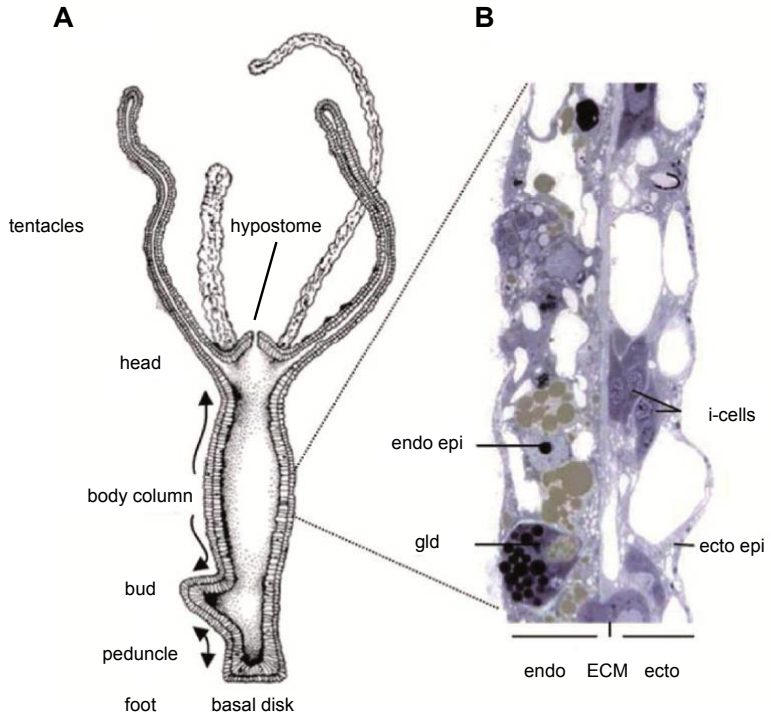

Figure 1-5 The body plan of *Hydra*

(A) Schematic longitudinal cross section of a *Hydra* polyp. (B) Cellular composition of the epithelial layers of the body column, indicating *Hydra*'s diploblastic organization. Endo, endoderm; ecto, ectoderm; ECM, extracellular matrix – mesoglea; endo epi, endodermal epithelial cells; gld, gland cell; i-cells, interstitial cells; ecto epi, ectodermal epithelial cells. Figure modified from (Bode 2009, Bosch 2013).

Reproduction: *Hydra* reproduce either asexually by budding or sexually (Figure 1-6A). Through budding in the lower gastric region (Figure 1-5A) (Campbell 1967), *Hydra* continuously lose tissue. However, new cells are constantly generated by an active stem cells community (Bosch et al. 2010). Budding frequency ranges from three to four days under optimal conditions, where feeding regime plays an essential role (Bosch and David 1984). Besides budding, *Hydra* is alter to reproduce sexually under environmental cues, such as temperature decrease or starvation (Littlefield 1985, Bosch and David 1986, Littlefield et al. 1991). When sexual maturation is triggered, gametes are formed from germ line precursors, which are maintained in sexually undifferentiated polyps (Bosch and David 1990). *Hydra* life span is remarkable long, exceeding 1000 years (Figure 1-6B) (Jones et al. 2014, Schaible et al. 2015).

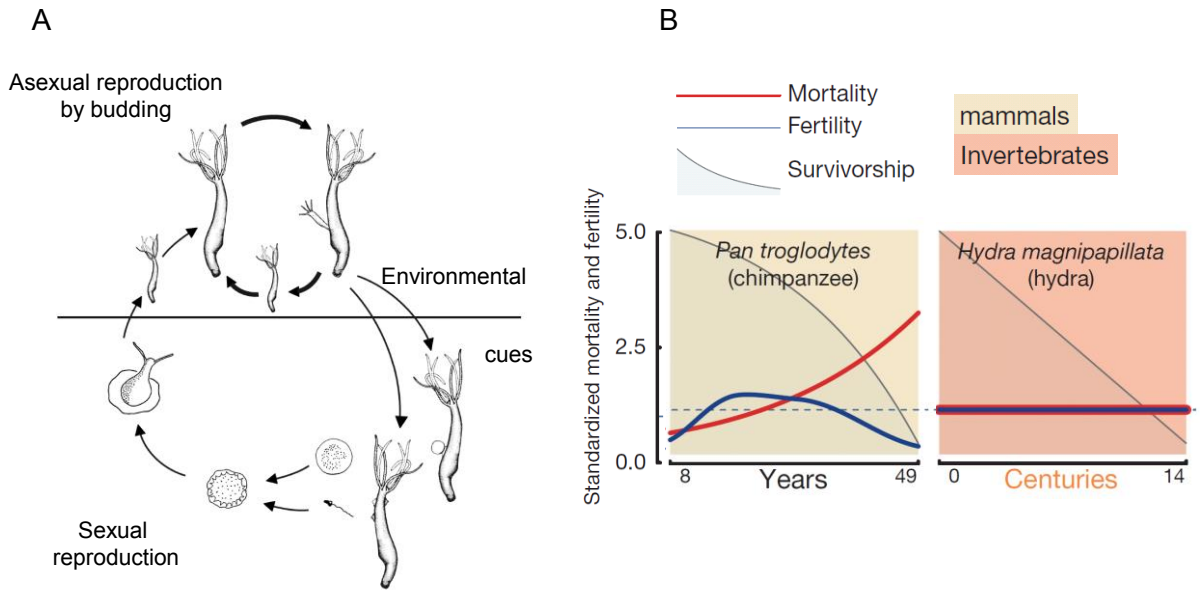

Figure 1-6 The life cycle of *Hydra*

(A) *Hydra* reproduces either asexually by budding or sexually by forming gametes induced by environmental cues. Figure modified from (Bosch 2009) (B) Relative mortality (red line), fertility (blue line) and survivorship (on a log scale) as functions of age. Figure modified from (Jones et al. 2014)

Nervous system: *Hydra* contains a diffuse nerve net throughout the body. Moreover, in some *Hydra* species, a nerve ring can be observed near the base of the hypostome (Koizumi 2007). The nerve net contains two types of neurons: ganglion cells and sensory cells (Davis et al. 1968, Koizumi et al. 1988, Koizumi 2007). There are distinct subsets of neurons, expressing different kinds of neuropeptides in specific spatial and temporal distributions along the development of *Hydra* (Matsuno and Kageyama 1984, Mitgutsch et al. 1999, Hansen et al. 2000, Hansen et al. 2002). For example, the RFamide-expressing neurons are more abundant in the *Hydra* head and lower peduncle region (Hansen et al. 2000) (Figure 1-7A). A similar express pattern is also found in developing buds, where RFamide is found first in the neurons at hypostome of the bud head and later in the neurons of the peduncle when the foot develops (Hansen et al. 2000) (Figure 1-7A). Some neuronal subpopulation can express more than one kind of neuropeptides at the same time (Figure 1-7B).

Hydra neurons possess phenotypic plasticity. Not only neurons in mature nerve net can change their neuropeptide phenotype in response to changes in their position (Koizumi and Bode 1986), but also ganglion cells can transform into sensory cells, indicating that the differentiated state of a neuron in *Hydra* is metastable (Koizumi et

al. 1988). A wide variety of neuropeptides from *Hydra magnipapillata* were identified by the *Hydra* peptide project (Fujisawa 2008), and further functionally analysed (Takahashi and Takeda 2015). Although neuropeptides appear as not essential for the basic pattern formation of *Hydra* (Mitgutsch et al. 1999), recent studies show that they play an important role in muscle contraction, bud detachment, body column elongation and neuronal homeostasis (Takahashi et al. 2003, Takahashi and Takeda 2015).

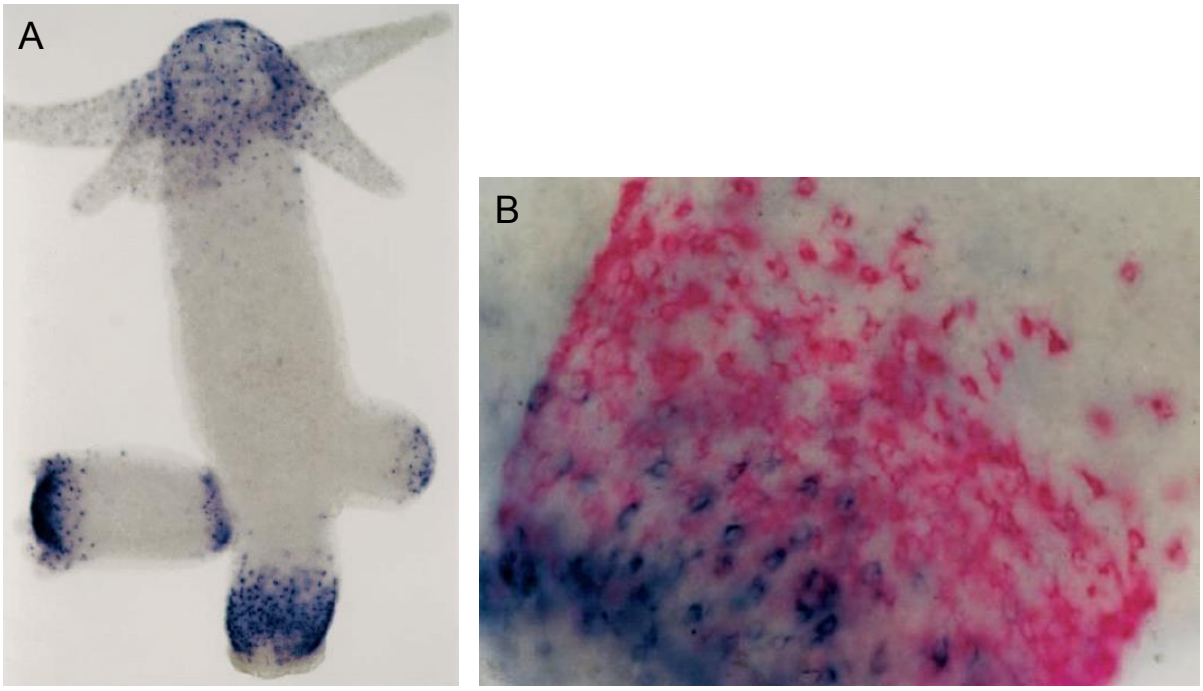

Figure 1-7 Whole amount in situ hybridization of *Hydra* with cRNA probes coding for the various *Hydra* preprohormones (Hansen et al. 2000).

(A) Hybridization with a preprohormone-A cRNA probe and subsequent staining in purple. Stained, distinct neurons located at the tentacles, hypostome (mouth region), upper gastric region (just below the head) and peduncle (a region just above the basal disk); furthermore, a similar pattern is found in developing buds. Figure from (Hansen et al. 2000). (B) Double-labeling whole-mount in situ hybridization with a cRNA probe coding for prepro-*Hydra*-KVamide (Red) and a cRNA probe coding for prepro-*Hydra*-LWamide (purple). Figure from (Hansen et al. 2000).

Immunity: *Hydra* lives in a variety of freshwater habitats that contain enormous amount of microbes of all sorts, including potential pathogens. Although *Hydra* possesses neither non-permeable barriers like exoskeletal or cuticular structures, nor mobile phagocytes (Bosch et al. 2009), it has developed epithelial cell based defence mechanisms and an effective innate immune system to regulate its species specific commensal microbiota (Fraune and Bosch 2007), as well as to defence pathogens. *Hydra* recognises bacteria through Toll-like receptor signalling (Franzenburg et al. 2012) and generates many kinds of antimicrobial peptides (AMPs) such as

*Hydra*macin (Jung et al. 2009) and members of the arminin and periculin peptide family (Augustin et al. 2009). For example, *Hydra*macin, regulated by its upstream gene FoxO (Boehm et al. 2012), is expressed exclusively in endodermal epithelium and is active against both gram-positive and gram-negative bacteria (Jung et al. 2009).

1.4 ILPs signalling in *Hydra* and lower metazoans

ILPs, ILR and downstream cascades are highly conserved among lower metazoans. Several ILPs have been reported in several flatworm species, potentially involved in reproduction control (Wang et al. 2014). In Cnidaria, a group of GPCRs is grouped together with receptors for the chordate insulin-like peptide relaxin (Jekely 2013). Moreover, two ILPs homologs, together with three ILR homologs were identified in *Nematostella vectensis* (*Nv*) (Anctil 2009). In *Trichoplax adhaerens*, there are orthologs of relaxin GPCRs as well as ILPs (Jekely 2013, Nikitin 2015). Among invertebrates, ILPs have less identical to each other (identity scores 15-23%), but their structured organizations are very similar to that in higher vertebrates (Smit et al. 1998).

Hydra magnipapillata possess an insulin/IGF-1 receptor gene (Steele et al. 1996) and three *Hydra* insulin like peptides (*hyilps*) genes; *ilp-A* (Genebank accession numbers GU219979.1), *ilp-B* (GU219980.1), and *ilp-C* (GU219981.1), as well as ILPs signalling downstream cascades (Herold et al. 2002, Bottger et al. 2006, Manuel et al. 2006, Boehm et al. 2012). Three HyILPs contain three intramolecular disulphide linkages and their expression are observed mainly in the head region and basal disc (Wenger et al. 2016). It is mentioned that one of ILPs is expressed in neurons and the other two are expressed in epithelial cells, moreover, two of ILPs can rescue the growth defects in *Drosophila* depleted of dILPs producing cells (Fujisawa 2008). However, both conclusions are not supported by evidences. One possible function could be that overexpression of ILP-A compensate the apoptosis induced by overexpression of *Hydra*-FoxO-eGFP protein (Lasi et al. 2010). Therefore, conservation of ILP features, the detailed expression patterns and functions of hyILPs still remain largely unknown.

1.5 Aims of the study

ILPs family and their signalling pathways are ubiquitous throughout Bilaterians, regulating metabolism, growth, life span, stress resistance and reproduction (Kimura et al. 1997, Saltiel and Kahn 2001, Ikeya et al. 2002). However, the conservation of ILPs family was not clear among the basal metazoans. *Hydra*, as an important basal model organism, possess 3 ILPs and rather simple ILPs family signalling cascades such as foxO (Boehm et al. 2012). To gain an insight of conserved roles of ILPs family within basal animals, the following issues should be addressed in this work using highly informative molecular techniques like qRT-PCR, *in situ* hybridization, immunochemistry, transgensis, and the available online databases.

I. Seeking the origin of ILPs family.

It is not known when ILPs family emerged during animal evolution. Therefore, this subject will be accomplished by *in silico* searching for ILPs in the available databases of basal animals from Cnidaria, Placozoa, Porifera, Ctenophora and Choanozoa.

II. Uncovering the expression pattern of ILPs in a basal animal - *Hydra*.

The expression pattern of HyILPs should be investigated at both mRNA and protein level.

III. Investigation the roles of HyILPs as well as its intercellular processing.

ILPs family signalling pathways play important roles in either responding to environmental stimuli or regulating animal development. Therefore, the expression of *hyilps* should be monitored under different environmental challenges. HyILPs gain- and loss-of-funciton experiments should be conducted in order to get further insights.

2. Results

2.1 Characterisation of ILPs family in *Hydra*

2.1.1 Summary of ILPs fingerprints in animal kingdom

In order to refine the ILPs family in *Hydra*, ILPs family key structural features (fingerprints) were summarised from literature (Steiner et al. 1985, Pierre De Meyts et al. 2000-2013, PROSITE 2004). ILPs fingerprints contain four invariant features and one alternative feature: First, ILPs are encoded in the genome as prepro-ILPs consisted of four basic domains: signal peptide (SP), B, C, A domains. A and B domain residues were translated from two exons of *ilps*, while an intron located in the middle of the coding sequence (CDS) for C domain residue (Figure 2-1A). Second, ILPs possess a conserved cysteine pattern. Two-disulphide bonds can be formed between cysteines located in A and B domains, helping to form correct ILPs' secondary structure (Figure 2-1B). Third, the B domain contains one helix which lies across the two helices of A domain (Figure 2-1C). Fourth, length of prepro-ILPs is less than 400 amino acids in general. Some prepro-ILPs have convertase cleavage sites - rich in Lysine or Arginine which are essential to remove the C domain and form mature ILPs (Figure 2-1D), this is considered an alternative ILP feature for ILPs family.

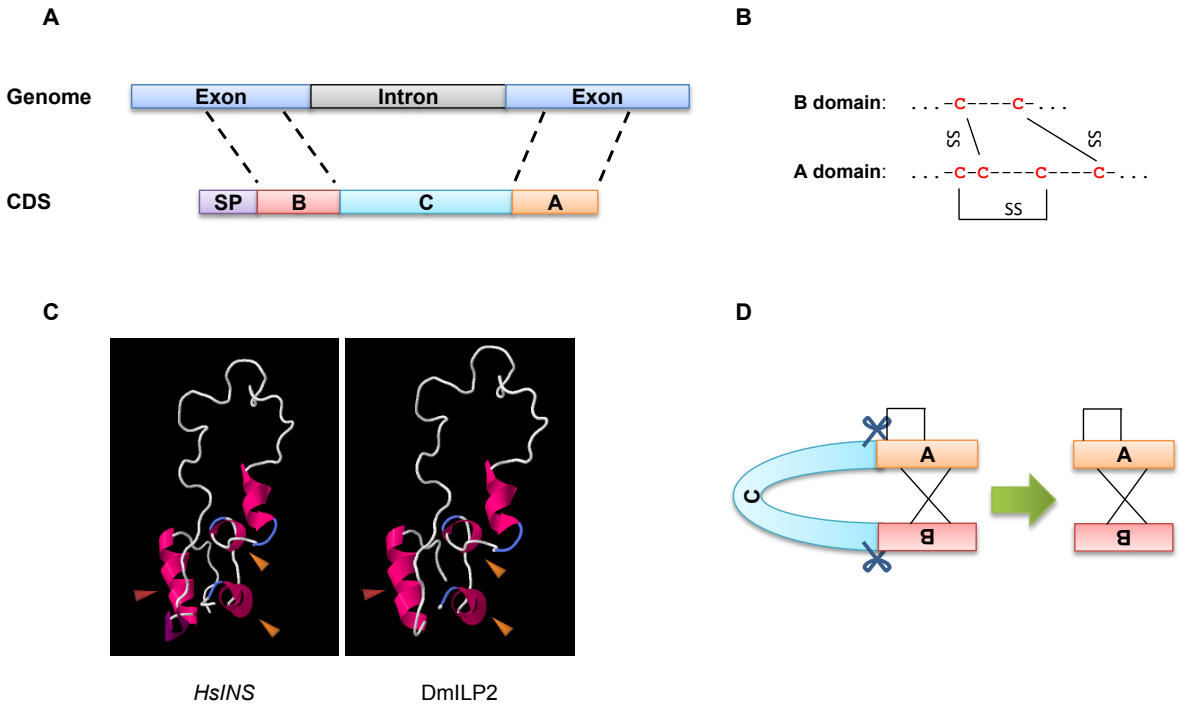

Figure 2-1 ILPs fingerprints summary

(A) pre-proILPs contain four basic domains: Signal Peptides (SP), B domain, C domain, A domain. B and A domains residues are coded in two exons, while an intron is located in the coding sequence of C domain residues (B) Conserved disulfide bonds. C: Cysteine; SS indicates disulfide bonds formed between B domain and A domain through cysteines. (C) *Homo sapiens* pre-insulin and D. melanogaster ILP2 secondary structure views created by Phyre2 using their original sequence. Red arrow points at one helix in B domain and yellow arrows point at two helices in A domain. (D) Some ILPs C chains are cleaved at convertase cleavage sites, markedly, in order to form mature ILP.

To search for ILPs in *Hydra*, a ILPs screening workflow was developed (Figure 2-2). First, 16 ILPs from both vertebrates and invertebrates were selected and submitted to online pattern search engine – PRATT (Li et al. 2015) (See Appendix Figure 8-1 for amino acid sequences of these 16 ILPs, and Figure 8-4 for phylogenetic analysis). The engine revealed an initial ILPs amino acid pattern, which contained a conserved cysteine pattern (Figure 2-1B) (Pierre De Meyts et al. 2000-2013, PROSITE 2004). This ILPs cysteine pattern was used as a seed for screening ILPs in SwissProt databank containing 550000 protein sequences on PATTINPROT using 100% similarity (Bairoch and Apweiler 1997, Combet et al. 2000). The screening resulted in 179 ILP candidates, which contained 106 known ILPs out of 234 known ILPs in the database. Therefore, the recovery rate is 45.3%, calculated from the 106 recovered ILPs/234 known ILPs ratio. In order to increase the recovery rate, partial ILPs cysteine pattern was selected as priority ILPs cysteine pattern. Since the priority ILPs cysteine pattern could help to recover 227 known ILPs, providing a high recovery rate - 97.0%, it can be treat as a significant amino acids sequence pattern of ILPs family. Thus it was used as the searching seed to refine ILPs family in *Hydra*. 4 *Hydra* species peptides transcriptome/genome databanks were used for prior ILP cysteine pattern screening: *Hydra vulgaris AEP* (Hemmrich and Bosch 2008), *Hydra magnipapillata* (Hm) (Chapman et al. 2010), *Hydra oligactis* (Internal Compagen) and *Hydra viridissima* (Hemmrich and Bosch 2008). Meanwhile, INS and three known HvILPs were used as seeds for tBLASTn in *Hydra* transcriptome data in Compagen (Hemmrich and Bosch 2008) and *Hydra* genome data in Metazome (Chapman et al. 2010). Finally a pool of HyILP candidates, generated by combining the results from PATTINPROT and tBLASTn, were sent to ILPs fingerprints test. *Hm* genome database was used for analysing the gene structure of HyILPs (Chapman et al. 2010).

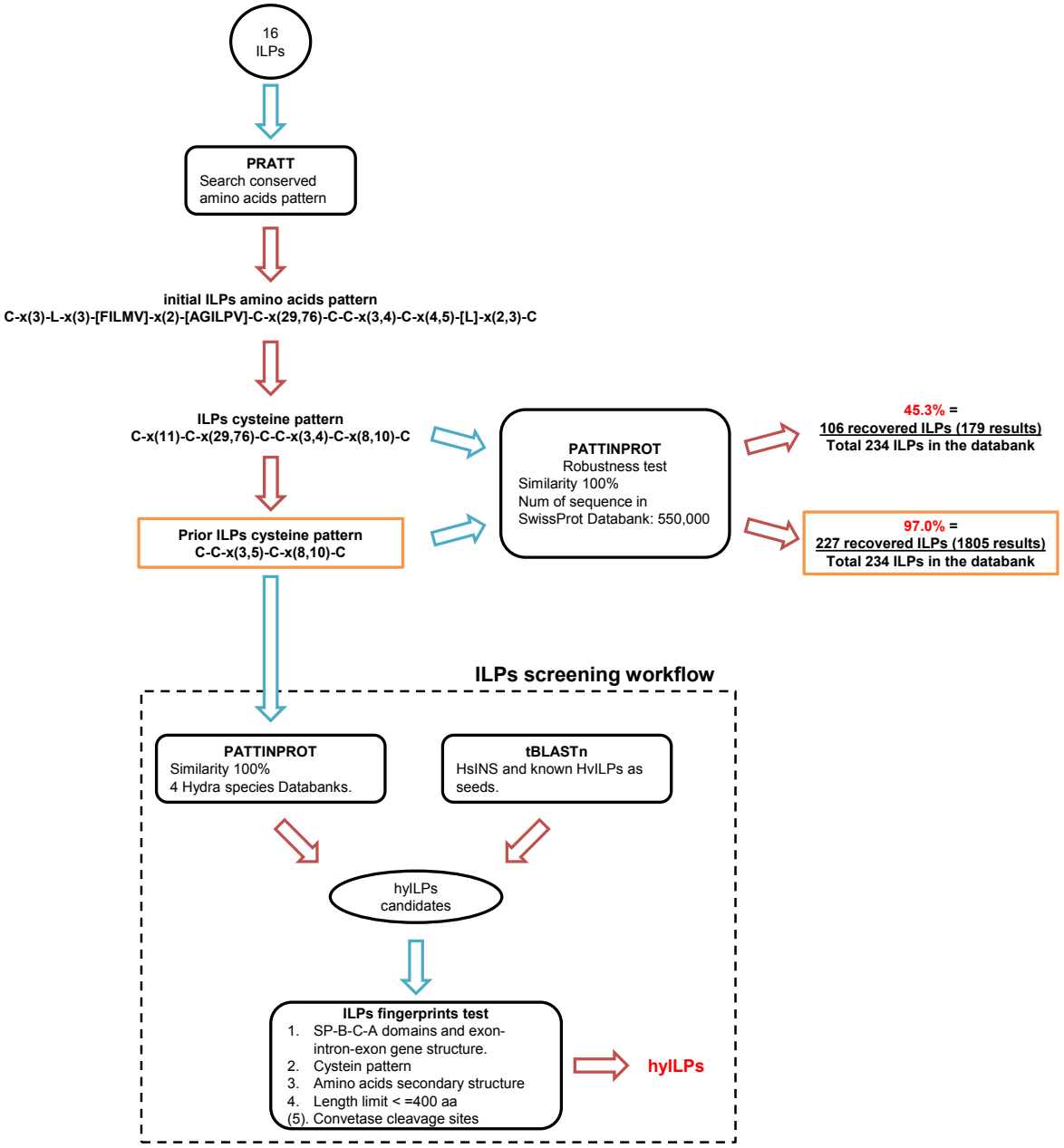

Figure 2-2 Development of insulin fingerprints and ILPs screen workflow

Criteria of PATTINPROT were set up to 100% similarity to template. Abbreviations: ILPs, Insulin like peptides; PRATT, an amino acids pattern online searching engine; PATTINPROT, an amino acid pattern online Blast engine; aa, amino acid; HsINS, *Homo sapiens* insulin; hyILPs, *Hydra* insulin like peptides; X (m,n), number of amino acid ranged from m to n; C, cysteine; L, leucine; F, Phenylalanine; I isoleucine; M, methionine; V, valine; A, alanine; G, glycine; P, proline. Light blue arrow indicated *in silico* process; Red arrow indicated processed results.

2.1.2 *Hydra* possesses 3 orthologues of ILPs (HyILPs)

Through the ILPs fingerprint test described above (Figure 2-2), total 12 HyILPs were found in 4 *Hydra* species, where each *Hydra* species possessed 3 HyILPs. HyILPs of *Hydra oligactis* (*Ho*) and *Hydra viridissima* (*Hv*) were newly identified through the ILPs screening workflow, while HyILPs of *Hydra vulgaris AEP* (*HvAEP*) and *Hydra magnipapillata* (*Hm*) were previously reported (unpublished information, Genebank accession numbers GU219979, GU219980, and GU219981). The mRNA sequences of 12 HyILPs were found in the transcriptome data in Compagen (Hemmrich and Bosch 2008) by tBLASTn, followed by verification via RT-PCR amplification and Sanger sequencing. The refined mRNA sequences of HyILPs were translated into peptides and sent for amino acid sequence alignment (See Appendix Figure 8-2 for amino acid sequences of these HyILPs). With help of Hm genome database, conserved exon-intron structure of ILPs was identified within all three Hm ILPs, which means A and B domains of Hm ILPs were translated from independent exons (Figure 2-3A). ILPs fingerprints of 12 HyILPs were summarised in a schematic diagram containing SP, B-C-A domains, cysteine pattern and potential convertase cleavage sites (Figure 2-3B). A phylogenetic tree of 12 HyILPs was built using an *Nv* ILP (Nv207484) as a outgroup (Anctil 2009). MEGA6.06 was used to find the best model to build the phylogenetic tree, which was the Jones-Thornoton-Taylor (JJT) matrix with Gamma Distributed (G). The HyILPs phylogenetic tree revealed that the distances between three HyILPs within each *Hydra* species were greater than the distances among the putative orthologues in the different *Hydra* species (Figure 2-3C). Thus, the three ancestral *ilps* gene were present before the divergence of the 4 *Hydra* species. Interestingly, *Hv* ILP-A tended to be distinctive from HyILP-A cluster, rooted as the base of HyILPs. HyILP-B cluster was more related to HyILP-C cluster indicating that HyILP-B and HyILP-C may be derived from an ancient *hyilp* gene.

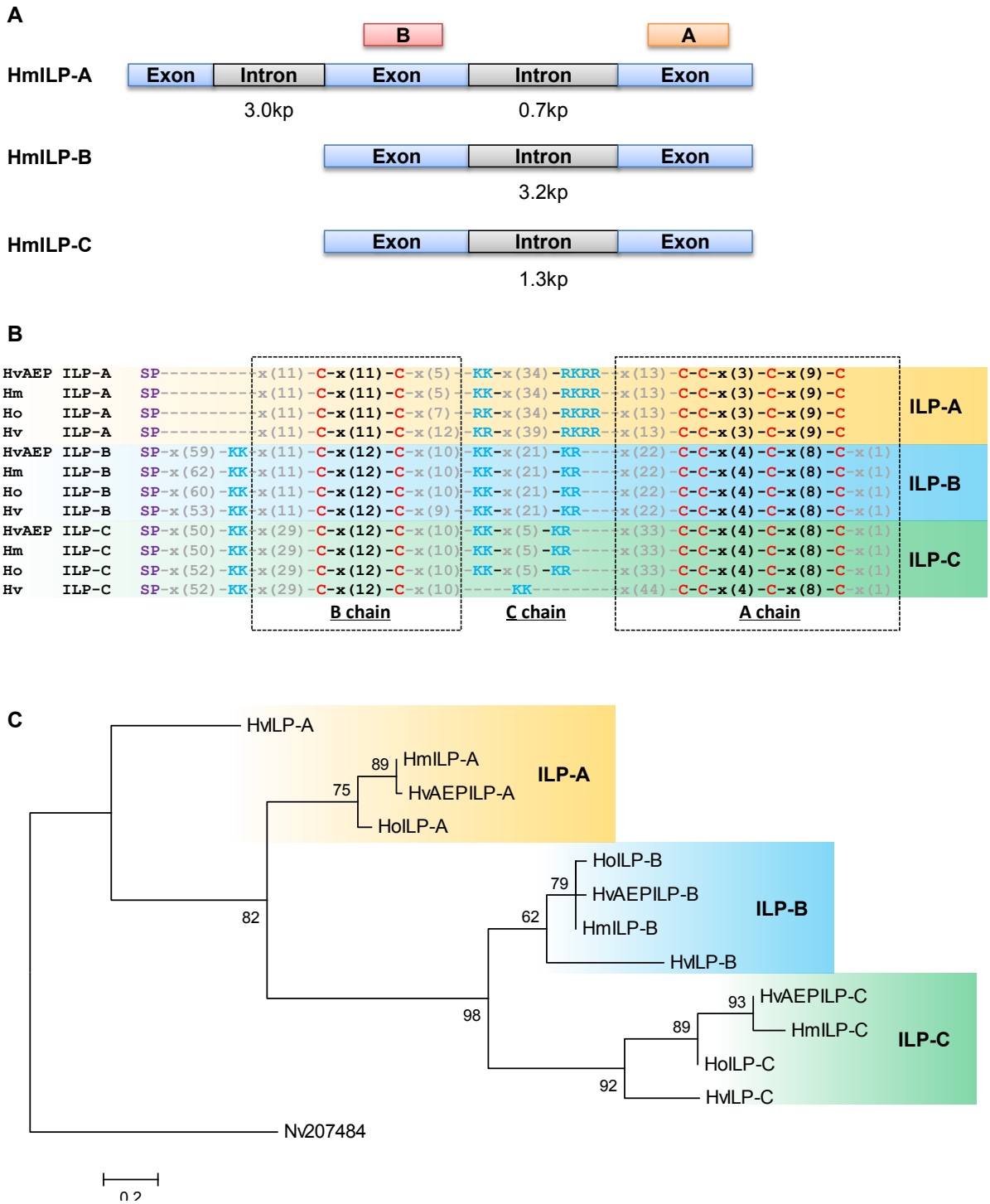

Figure 2-3 12 HylLP sequence and phylogenetic analysis

(A) Exon-intron structure of hyilps gene (pre-mRNA). (B) Major feather of hyILPs: B, C, A chains, cysteine pattern and convertase sites analysis (C) Phylogenetic tree of HyILPs build by maximum likelihood method. Numbers at nodes are bootstrap support values calculated by 1000 replicates using Jones-Thornoton-Taylor (JJT) model with a discrete Gamma distribution with 5 rate categories. Bootstrap values under 50 are not shown. HyILPS were subdivided into three clusters. Abbreviations: *HvAEP*, *Hydra vulgaris AEP*; Hm, *Hydra magnipapillata*; Ho, *Hydra oligactis*; Hv, *Hydra viridissima*; Nv: *Nematostella vectensis*; x(n), number of amino acid; **SP**: **Signal Peptide**; **Potential convertase cleavage sites**; **C: cysteine**.

To investigate the secondary structure of 12 HyILPs, Protein Homology/analogy Recognition Engine V2.0 (Phyre2) (Kelley et al. 2015) was used for predicting their secondary structure. Phyre2 sought suitable existing peptide models to construct secondary structure of HyILPs. The results included chosen model, confidence level, sequence identity and a 3D animation of peptide secondary structure. Chosen model indicated which model was used as the template for building peptide secondary structure. Confidence revealed how reliable the constructed secondary structure was. Sequence identity indicated how much was the similarity between a query sequence and the template sequence. Within HyILP-A cluster, HvILP-A predicted secondary structure possessed highest confidence of 93.7% when using NMR structure of human proinsulin as the template, although its identity was around 16% calculated from 79 aligned residues / HvILP-A sequence without SP. While two helixes could be found in HvILP-A predicted secondary structure, one helix predicted by ILP fingerprints in B domain was missing (Figure 2-4). The rest three HyILP-As demonstrated low confidence, low sequence identity as well as low number of aligned residues (around 20 aa) at the A domain with only one helix (Figure 2-4). Surprisingly, both HyILP-B cluster (Figure 2-5) and HyILP-C cluster (Figure 2-6) presented high confidence (>90%) using NMR structure of proinsulin as the template with around 30% sequence identity calculated from 20 amino acids at A domain. The A domain secondary structure of both HyILP-Bs and HyILP-Cs possessed two helices predicted by ILP fingerprints. In summary, predicted secondary structures of 12 HyILPs revealed relatively high degree of similarities to the NMR structure of proinsulin built from *Homo sapiens*.

Predicted 3D model **Alignment and basic information**

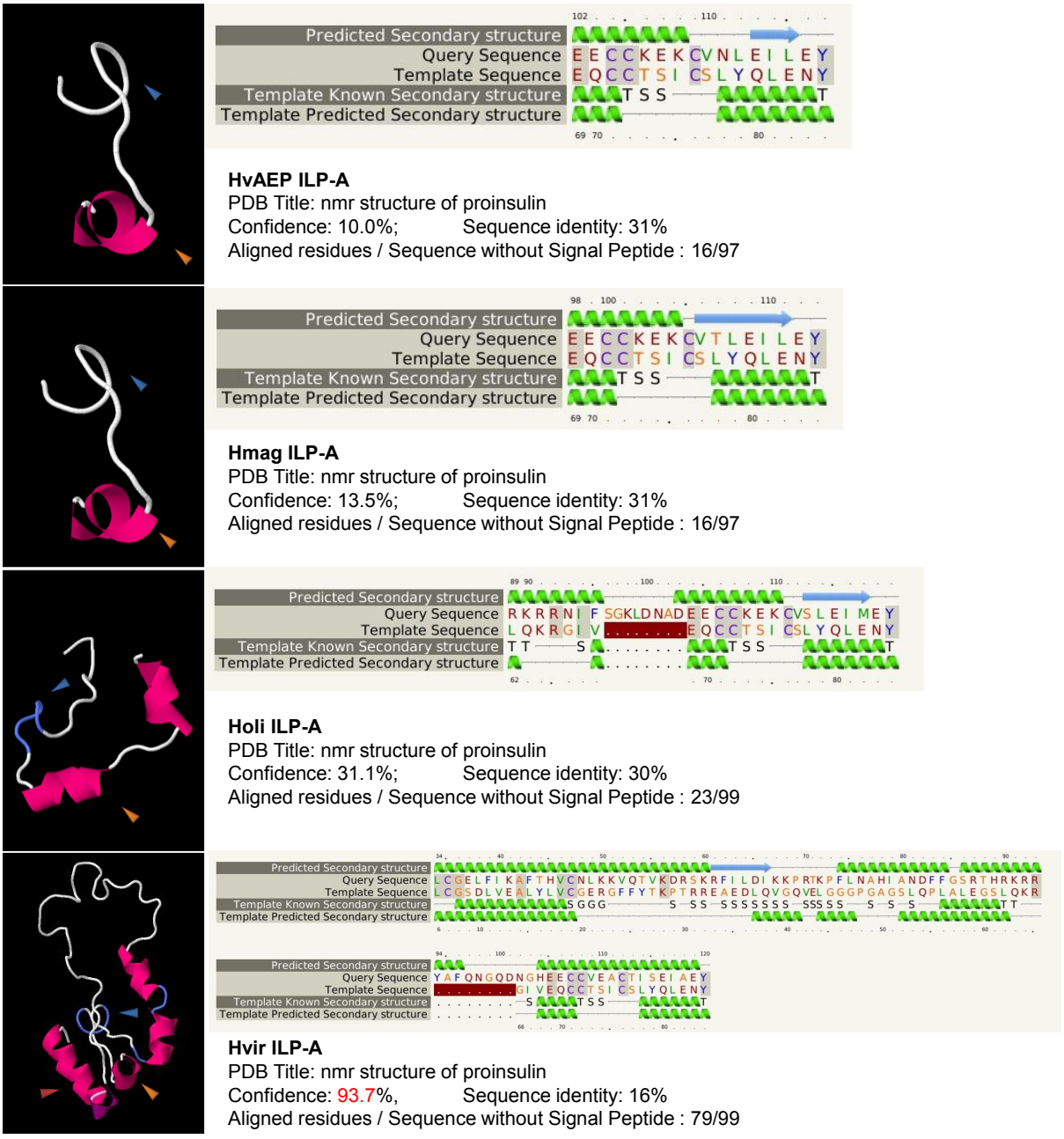

Figure 2-4 Secondary structure predictions of HyILP-A

Predicted 3D model (left): Red region indicate Alpha helix; Purple region indicates Beta strand; Blue region mark disordered region; Red arrows point at the helix in B domain, yellow arrows point at the helix in A domain, and blue arrows point at the missing helix. 3D model was built based on predicted secondary structure; Alignment and basic information (right): Green helices represent α-helices, blue arrows indicate β-strands and faint lines indicate coil; Identical residues in the alignment are highlighted with a grey background; Insertion or deletions are highlighted with red background; S = bend; G = 3-turn helix; T = hydrogen bonded turn; HvAEP, *Hydra vulgaris AEP*; Hmag, *Hydra magnipapillata*; Holi, *Hydra oligactis*; Hvir, *Hydra viridissima*; PDB: the Protein Data Bank; Confidence: represents the probability (from 0 to 100%) that the match between query sequence and its template is true homology; Sequence identity: represent the percentage of identical residues between query sequence and its template.

Predicted 3D model **Alignment and basic information**

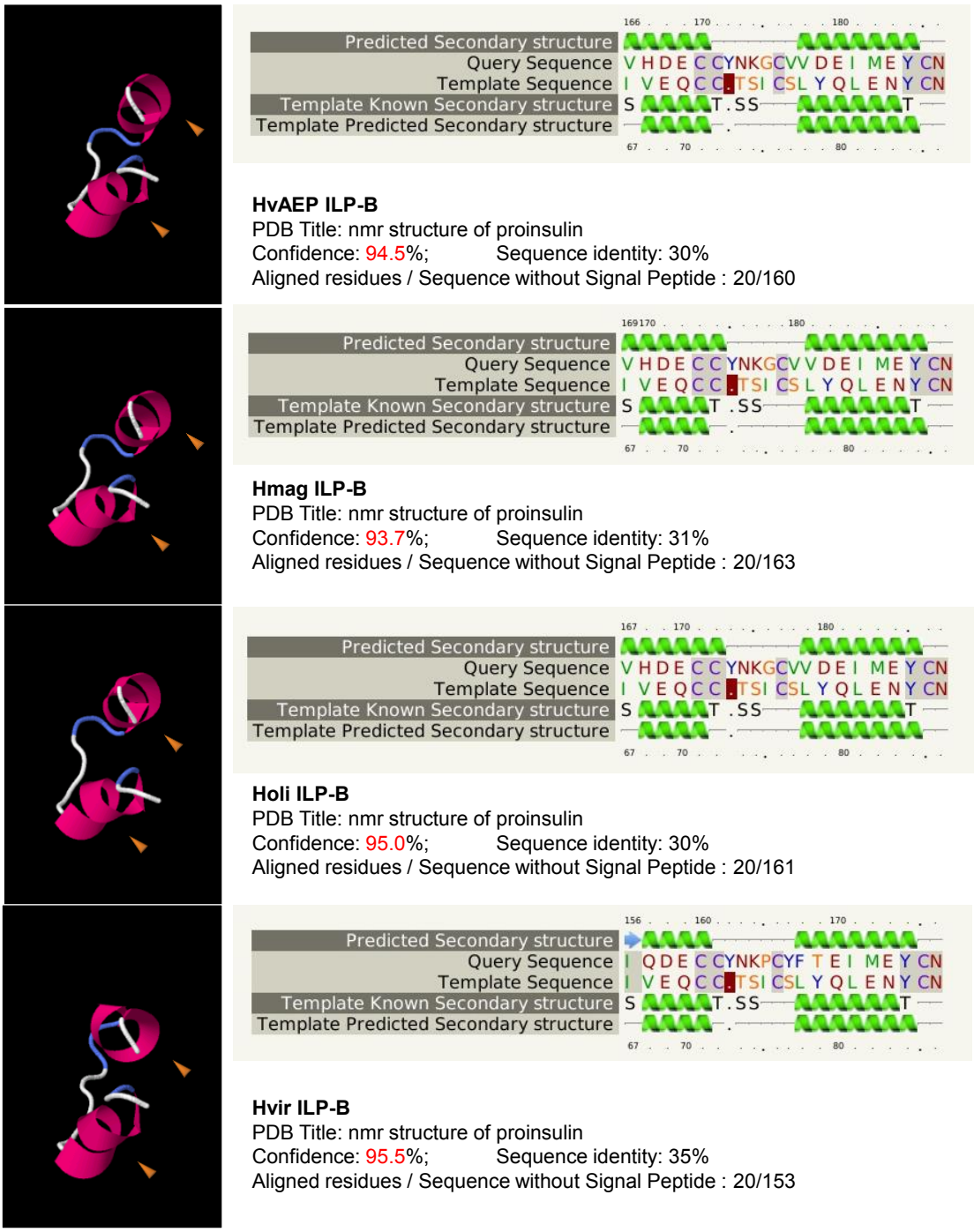

Figure 2-5 Secondary structure predictions of HyILP-B

Predicted 3D model (left): Red region indicate Alpha helix; Purple region indicate Beta strand; Blue region mark disordered region; Yellow arrows point at the helix in A domain. 3D model was built based on predicted secondary structure; Alignment and basic information (right): Green helices represent α-helices, blue arrows indicate β-strands and faint lines indicate coil; Identical residues in the alignment are highlighted with a grey background; Insertion or deletions are highlighted with red background; S = bend; G = 3-turn helix; T = hydrogen bonded turn; HvAEP, *Hydra vulgaris AEP*; Hmag, *Hydra magnipapillata*; Holi, *Hydra oligactis*; Hvir, *Hydra viridissima*; PDB: the Protein Data Bank; Confidence: represents the probability (from 0 to 100%) that the match between query sequence and its template is true homology; Sequence identity: represent the percentage of identical residues between query sequence and its template.

Predicted 3D model **Alignment and basic information**

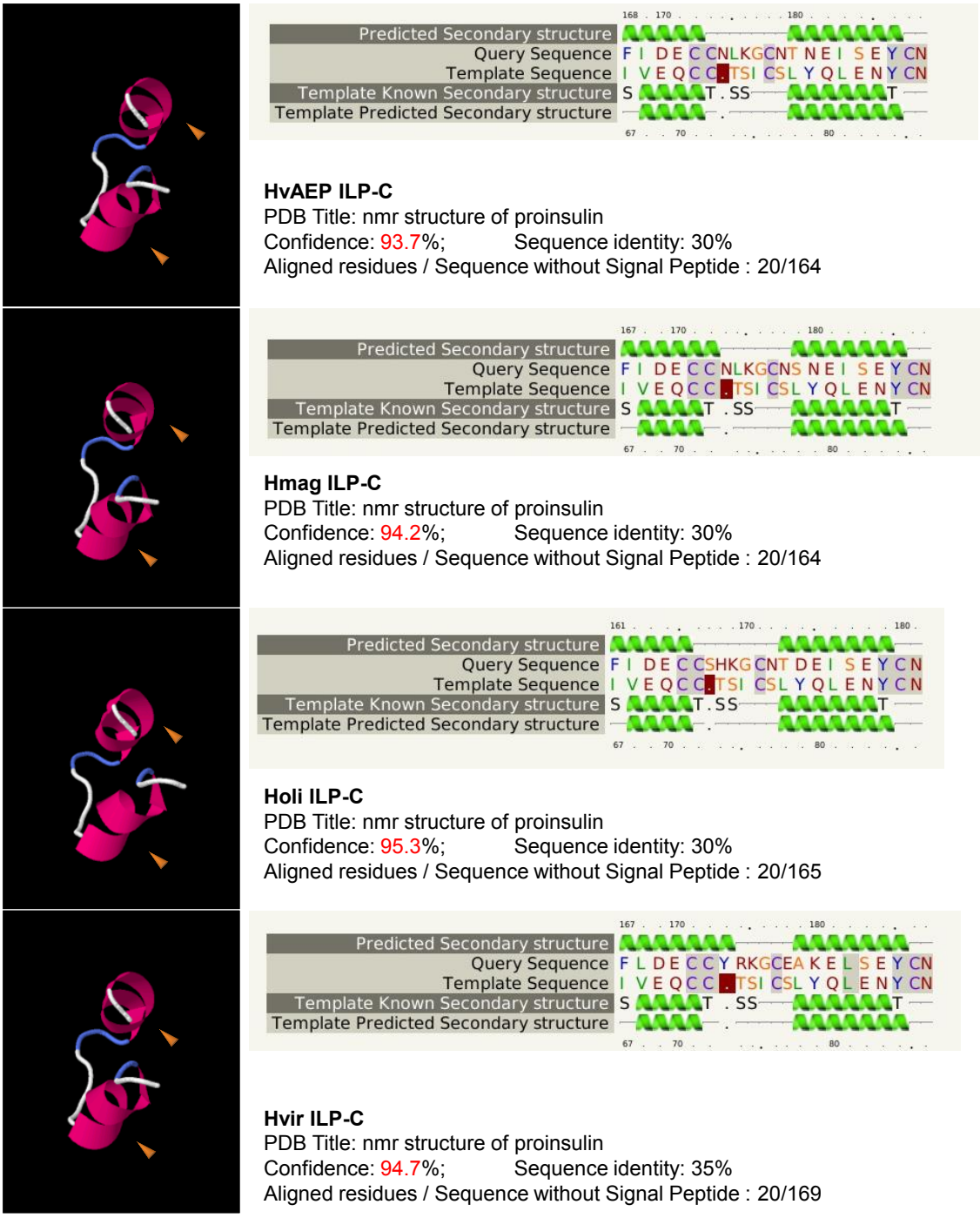

Figure 2-6 Secondary structure predictions of HylLP-C

Predicted 3D model (left): Red region indicate Alpha helix; Purple region indicate Beta strand; Blue region mark disordered region; Yellow arrows point at the helix in A domain. 3D model was built based on predicted secondary structure; Alignment and basic information (right): Green helices represent α-helices, blue arrows indicate β-strands and faint lines indicate coil; Identical residues in the alignment are highlighted with a grey background; Insertion or deletions are highlighted with red background; S = bend; G = 3-turn helix; T = hydrogen bonded turn; HvAEP, *Hydra vulgaris AEP*; Hmag, *Hydra magnipapillata*; Holi, *Hydra oligactis*; Hvir, *Hydra viridissima*; PDB: the Protein Data Bank; Confidence: represents the probability (from 0 to 100%) that the match between query sequence and its template is true homology; Sequence identity: represent the percentage of identical residues between query sequence and its template.

2.1.3 Evaluating the origin of ILPs.

To investigate the universality of ILPs among Cnidarians, the prior ILP cysteine pattern (Figure 2-2) was used for screening ILPs in 3 Cnidarian model organisms' predicted peptide-databanks: *Nematostella vectensis*, *Acropora digitfera* and *Aurelia aurita*. The ILPs screening workflow resulted in 7 ILPs in *Nematostella vectensis* including 2 known ILPs (Anctil 2009), 6 ILPs in *Acropora digitifera*, 4 ILPs in *Aurelia aurita* (amino acids sequences of ILPs provided in Appendix Figure 8-3). Interestingly, the numbers of ILPs in Cnidarians are different from each other. To further investigate the origin of ILPs, ILPs screening workflow was used to screen peptide-databanks of model animals from Porifera, Ctenophora and Choanozoa: *Amphimedon queenslandica* (Kersey et al. 2016), *Oscarella carmela* (Hemmrich and Bosch 2008), *Sycon ciliatum* (Hemmrich and Bosch 2008), *Mnemiopsis leidyi* (Ryan et al. 2013, Moreland et al. 2014) and *Monosiga brevicollis* (Lang et al. 2002, King et al. 2008). However, there was no ILP candidate identified among these species. These results indicated that ILPs might have emerged between Cnidaria and Ctenophora (Figure 2-7).

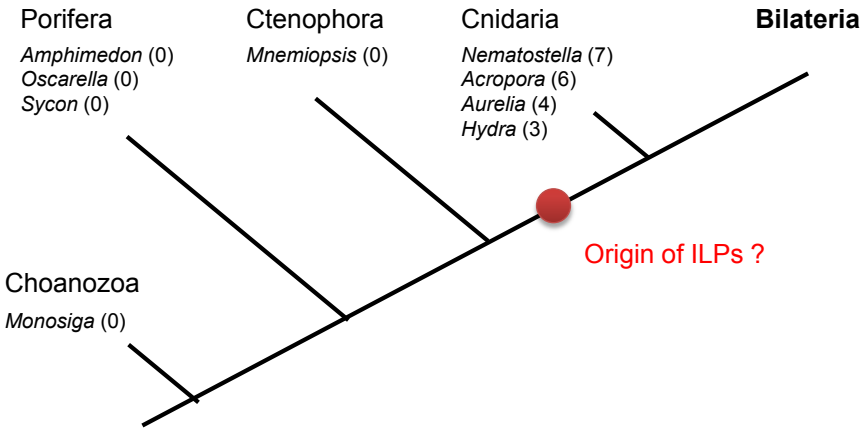

Figure 2-7 Predicted origin of ILPs

Cnidaria is a the sister group to Bilateria (Putnam et al. 2007). Together with Ctenophora and Porifera, Cnidaria form the earliest branches in the animal tree of life. *Nematostella*: *Nematostella vectensis*; *Acropora*: *Acropora digitfera*; *Aurelia*: *Aurelia aurita*. *Amphimedon*: *Amphimedon queenslandica*; *Oscarella*: *Oscarella carmela*; *Sycon*: *Sycon ciliatum*; *Mnemiopsis*: *Mnemiopsis leidyi*; *Monosiga*: *Monosiga brevicollis*. Number of found ILPs is indicated in brackets.

2.2 Investigation of ILPs gene expression pattern in *Hydra*

2.2.1 Expression pattern analysis of *hyilps* and *Hydra insr* (*Hyinsr*) genes

To understand the expression pattern of HyILPs and HyINSR, two sets of expression data (Microarray and RNA-seq unpublished data from the Bosch's lab) along the *Hydra* body column were used. All HyILPs in the following text refer to HyILPs in *HvAEP* species unless mentioned. Both datasets revealed that *hyinsr* and three *hyilps* genes are highly expressed in the head region as well as foot region, except *hyilp-A* which is expressed predominately in the head region (Figure 2-8A). Interestingly, the expression level of *hyilp-B* increases from Body-up towards the foot region while the expression level of *hyilp-C* decreases (Figure 2-8A). The transcriptome from 3 type of stem cells (unpublished data from the Bosch's lab) indicate that *hyinsr* and *hyilps* are almost exclusively expressed in the ectodermal stem cells (Figure 2-8B).

A

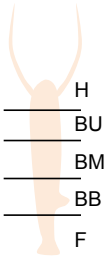

	Microarray				RNA-Seq			
Average reads	*hyinsr*	*hyilp-A*	*hyilp-B*	*hyilp-C*	*hyinsr*	*hyilp-A*	*hyilp-B*	*hyilp-C*
Head	622	178		1562		23		86
Body_Up								
Body_Mid								
Body_Bud								
Foot			4426		407		163	

B

454 sequencing reads			
Gene	Ecto	Endo	I-cell
hyilnsr	73	9	8
hyilp-A	31	2	2
hyilp-B	55	0	1
hyilp-C	20	0	1

Figure 2-8 Expression pattern of ILPs in *Hydra*

A: *HvAEP* ILPs and hyINSR gene expression levels along the *Hydra* body column were analysed by both Microarray and RNA-Seq techniques (unpublished data from the Bosch's lab). The length of the bar indicating the average reads of the genes and the maximum reads were indicated by number. ***hyinsr* gene**; ***hyilp-A***; ***hyilp-B***; ***hyilp-C***; (B): *HvAEP* ILPs and hyINSR expression levels were measured among three stem cell populations sorted by FACS (unpublished data).

The expression pattern of all three *hyilps* in a polyp was assessed by *in situ* hybridization. Only *hyilp-B* shows detectable signals (Figure 2-9A), revealing that HyILP-B mRNA is produced in putative neurons at the tip of the head region (Figure 2-9B), in the peduncle region (Figure 2-9C) and scattered in the head region of a bud

(Figure 2-9D). To further investigate the expression of *hyilps* and *hyinsr* in neurons, neuron population was enriched by centrifugation and then used in qRT-PCR test. Epithelial populations (Figure 2-10B) and Neuron populations (Figure 2-10C) were enriched from total animal samples (Figure 2-10A). Furthermore, qRT-PCR was also used for *Hydra* neurons samples sorted by Fluorescence-activated cell sorting (kindly provided by Andrea Murillo, Lab of Prof. Bosch), the transcripts level of target genes were indicated by Delta Ct value. Delta Ct describes the cycle difference between target gene and housekeeping genes through equation "Delta Ct = Ct_{target} – $Ct_{Housekeeping}$", where housekeeping genes expressed abundantly. Thus, the higher Delta Ct indicates lower expression level and lower Delta Ct reveals that the target gene has higher expression. Transcript of neuron derived antimicrobial peptide 1 (NDA-1) gene (unpublished data from the Bosch's lab) was used as internal control as it was strong expressed in neuron population. Thus, high expression level of *nda-1* in neuron population samples indicates high concentration of neuron cells, while epithelial cells samples with low expression level of *nda-1* indicates that the sample contains few neurons (Figure 2-10D). Highly expressed *hyilp-B* and lowly expressed *hyilp-C* were found in both amplified neuron samples (Figure 2-10E) and neurons sorted by FACS (Figure 2-10F). in contrast, the expression level of *hyinsr* and *hyilp-A* showed low expression levels in the amplified neuron samples (Figure 2-10E). In the amplified neuron samples, the expression levels of *hyinsr* and *hyilp-A* were two-fold downregulated compared to control (Figure 2-10E). Unexpectedly, their expression levels were upregulated in the neuron sample from FACS sorting (Figure 2-10F).

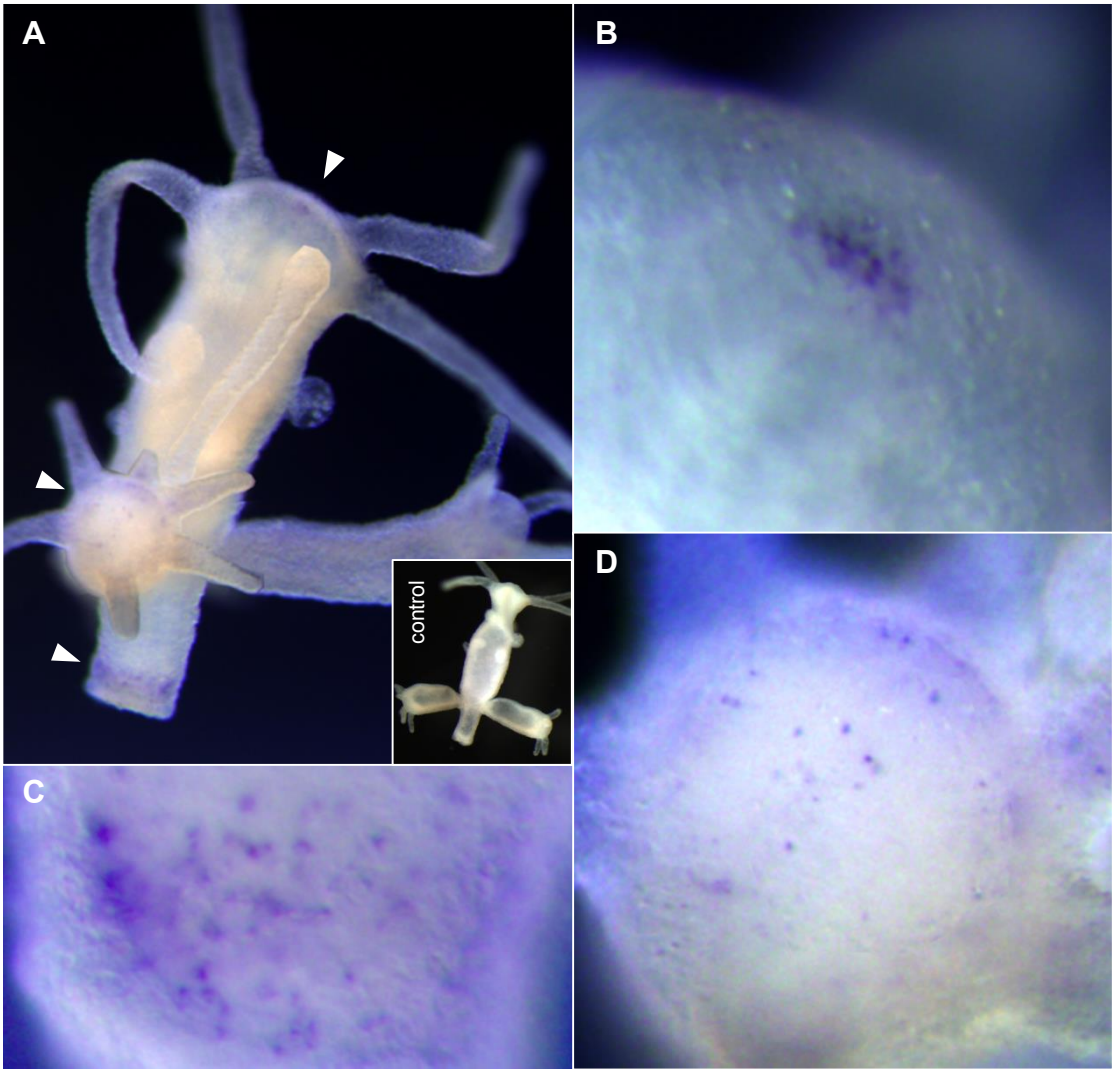

Figure 2-9 HylLPB expression observed in putative nerve cells by *in situ* hybridization.
(A) Total animal *in situ* hybridization. (B) Head region of adult polyp. (C) Foot region of adult polyp. (D) Head region of a developing bud. White arrows point to several stained regions. Control: no signal is detected.

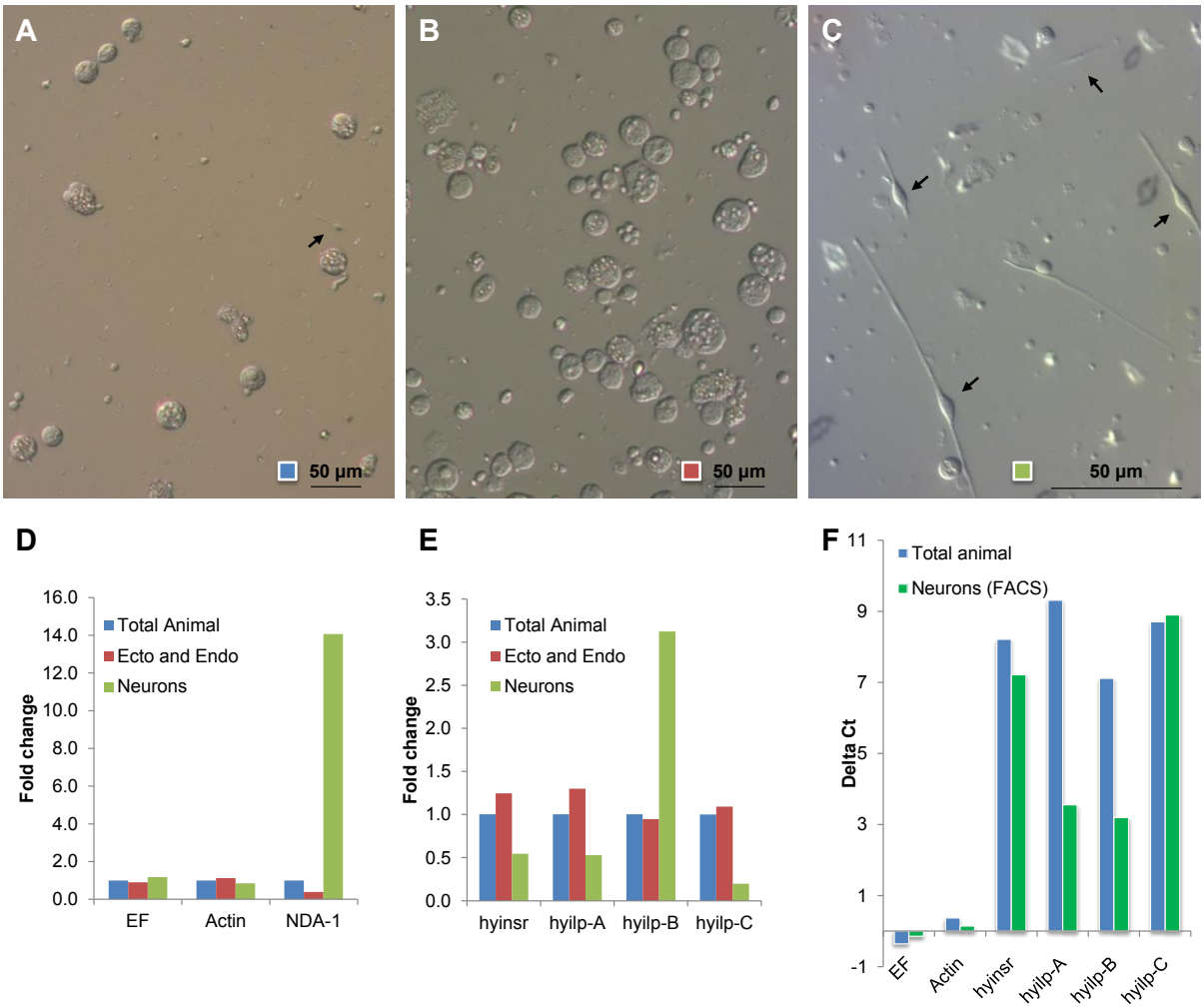

Figure 2-10 *hyilps* are expressed in neuron population

(A) Total animal cell suspension of *Hydra* under microscope. Arrow points to neurons. (B) Epithelial cell suspension of *Hydra* depleted from neurons. (C) Neuron enriched suspension. (D-E) Transcripts levels of HyILP genes in different cell suspensions. n = 2 replicates. (F) Comparison of the transcript levels of hyINSR and ILPs between total animal suspension samples and a neuron sample sorted by FACS by Delta Ct from qRT-PCR.

2.2.2 Detection of HyILPs by antibodies

To investigate the expression pattern of HyILPs on protein level, antibodies against HyILP-A and HyILP-B were designed. Confocal Laser Scanning Microscopy (CLSM) was used for the detection of ILPA and ILPB proteins at cellular level. HyILP-A was found in the ganglion cells along the body column. The antibody detected vesicle-like aggregations in the cytoplasm of ganglion cells (Figure 2-11). HyILP-B showed significant expression in both sensory neurons and ganglion cells in different body parts (Figure 2-12). Sensory neurons which expressed HyILP-B were found mainly in the head region (Figure 2-12A1 to A4), while ganglion cells with HyILP-B expression located in the head region, body region and extensively in the peduncle region (Figure

2-12B1 to B4 and Figure 2-12C1 to C4). The vesicle-like aggregations formed by HyILP-B accumulated at apical region of sensory cells, while they can be found everywhere in the cytoplasm of ganglion cells. An overview of HyILP-B expression cells in the head region is presented on Appendix Figure 8-9.

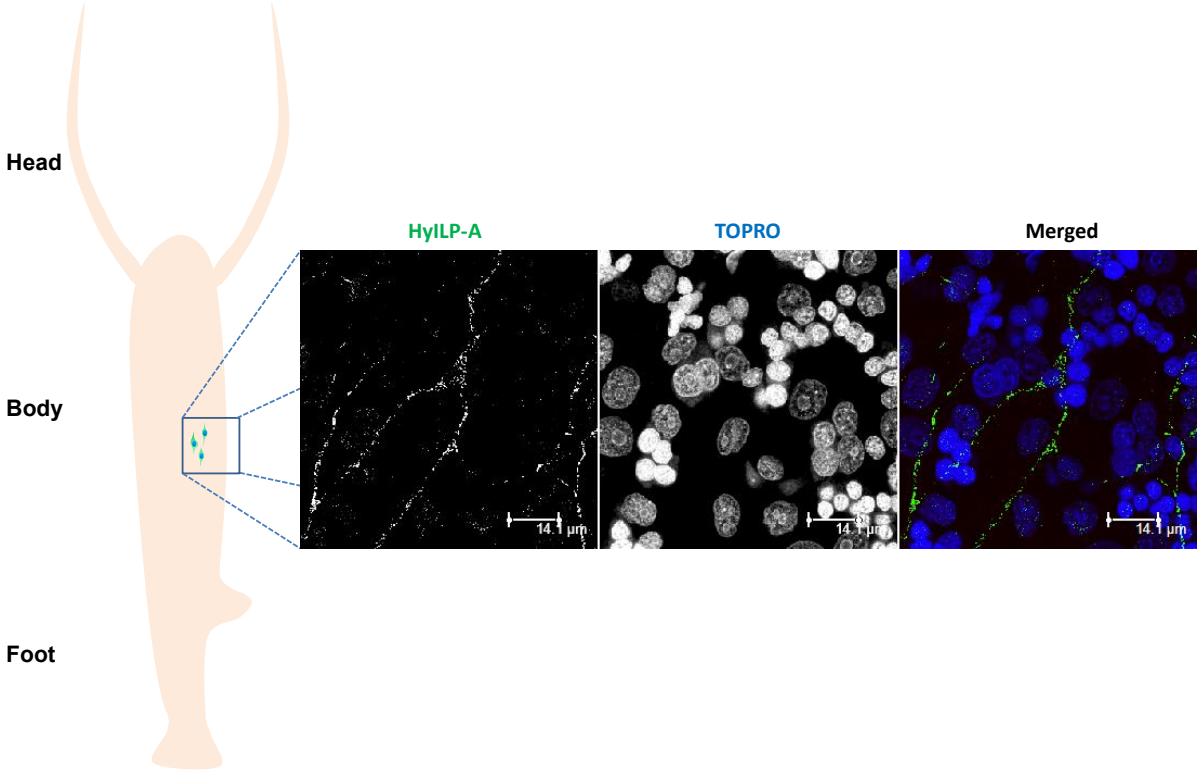

Figure 2-11 HyILP-A expression in ganglion cells along the body axis

HyILP-A expression accumulated in the vesicles of ganglion cells. **HyILP-A**; **Nuclei**.

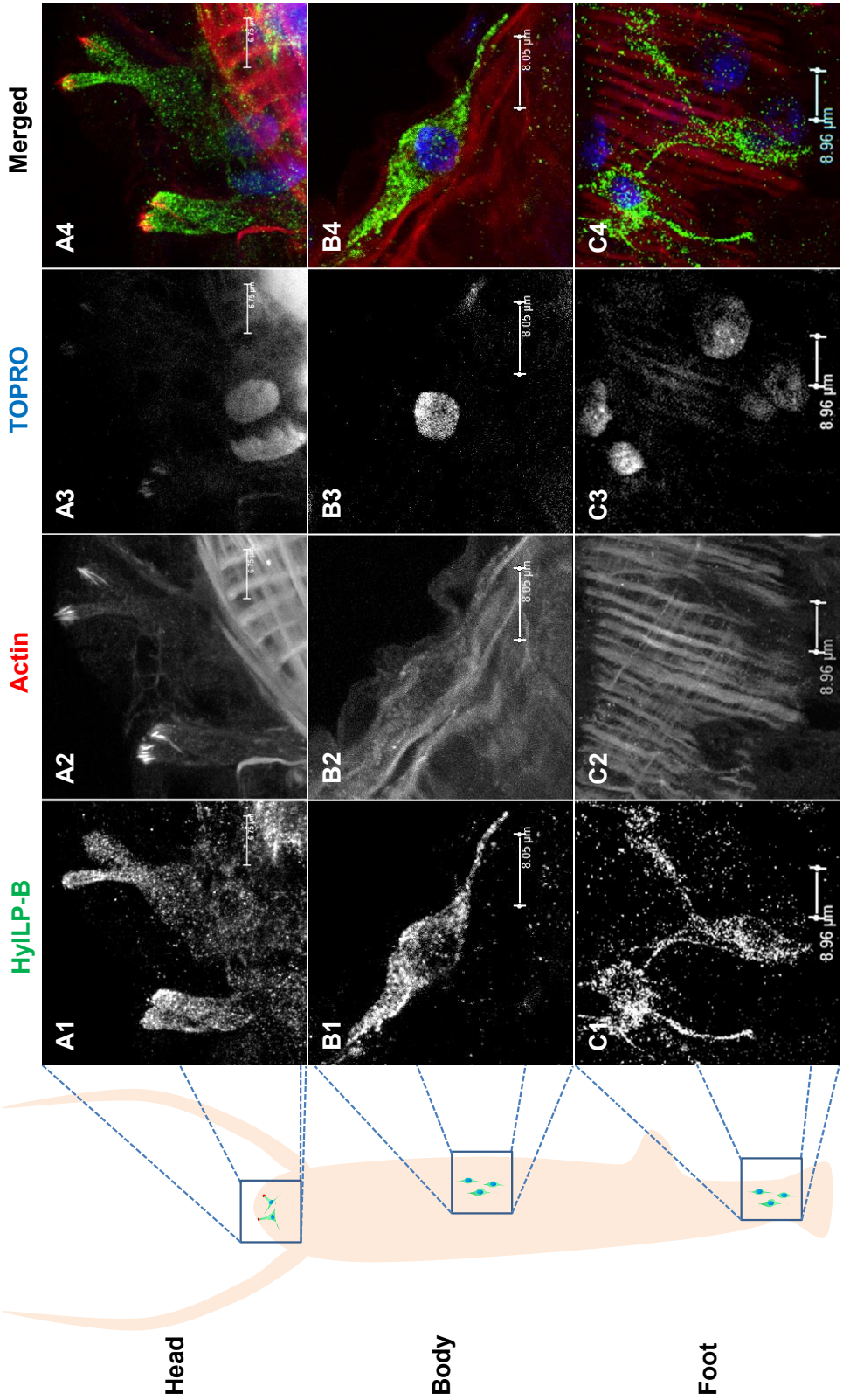

Figure 2-12 HylLP-B expression in different nervous cells

(A1-A4): Sensory neurons expressing HylLP-B. (B1-B4): ganglion cell expressing lLP-B in the body column. (C1-C4): ganglion cells in the peduncle region. **HylLP-B**; **Actin filament**; **Nuclei**.

2.3 Investigation of signalling pathways and functions where HyILPs are potentially involved

2.3.1 Starvation and loss of HyINSR enhances *hyilp-A* expression

To investigate whether nutrition limitation and reduced ILPs family signalling influence the expression of HyILPs, HyINSR knockdown transgenic *Hydra* line and its corresponding control line were used for a starvation challenge experiment prior to qRT-PCR test. *Hyinsr* was two-fold downregulated significantly in the HyINSR knockdown *Hydra* under feeding condition (Figure 2-13A). Interestingly, *hyilp-A* was upregulated significantly under starvation in both wild type and HyINSR knockdown *Hydras* (Figure 2-13B). There were no significant difference found on *hyilp-B* or *hyilp-C* expressions level under either starvation or HyINSR loss-of-function conditions (Figure 2-13B). *Hydramacin* is known as a downstream gene suppressed by *Hydra* FoxO (Boehm et al. 2012). Thus it was predicted as a potential downstream gene of *Hydra* ILPs family signalling. However, the expression of *hydra*macin was not affected by loss-of-function HyINSR, but reduced significantly under starvation in both wild type and HyINSR knockdown *Hydras* (Figure 2-13B). It suggests that starvation might suppress the expression of *hydramacin* through FoxO pathway. The putative interaction between nutrient level and ILPs signalling in *Hydra* are summarised in Figure 2-13C.

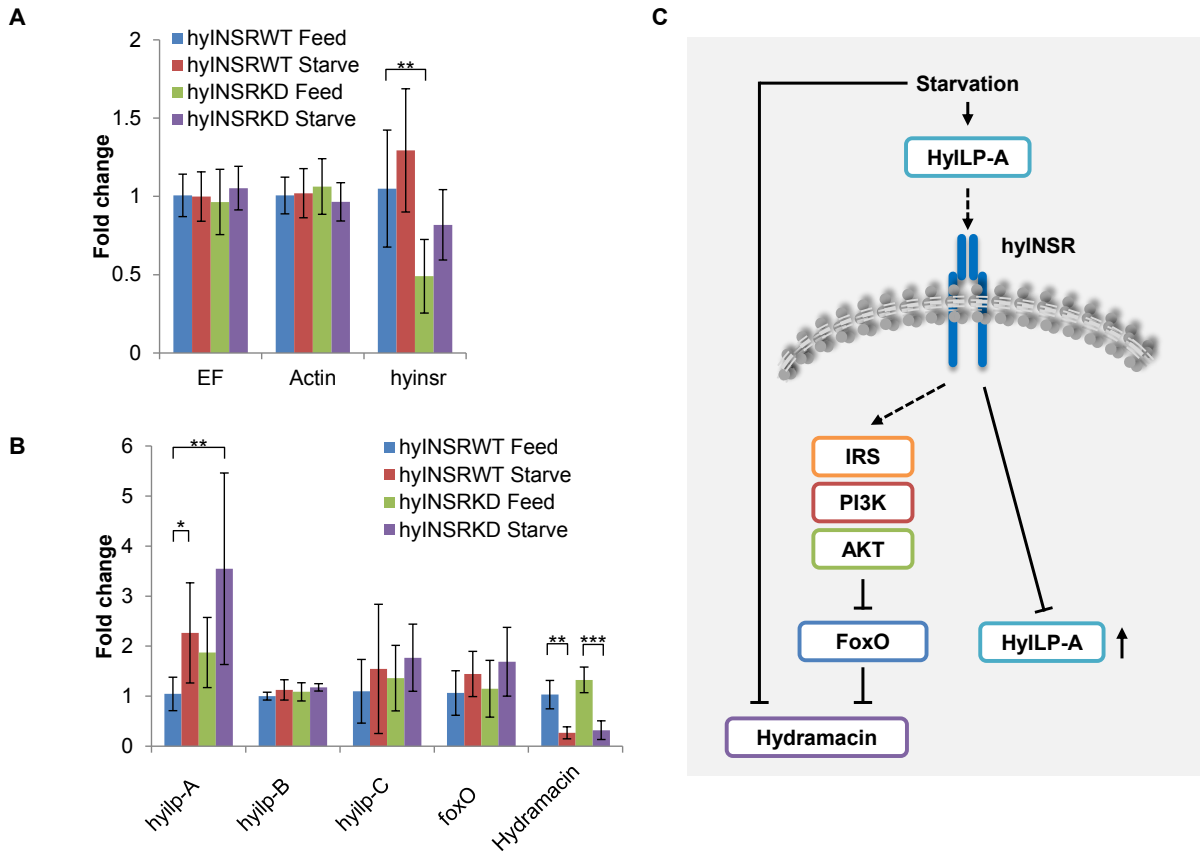

Figure 2-13 Starvation and HyINSR loss-of-function influence the expression of *hyilps*

(A-B) Illustration the levels of *hyinsr*, *Hydra*macin and *Hydra ilps* transcripts through qRT-PCR. n = 5 replicates except n=3 for *hyilp-B* and n=2 for *hyilp-C*. Wild Type: WT; Feed: regular *ad libitum* feed 3 times a week; starve: starved for 10 days. Error bar indicated standard deviation. (C) Putative relationships between nutrient and ILPs family signalling in *Hydra*. Solid line: known relationships between genes or data supported; Dotted line: putative interaction between genes.

2.3.2 Dynamic expression pattern of HylLP-B during the budding process

In situ hybridization revealed that *hyilp-B* is not only expressed in head, peduncle and neurons (Figure 2-9), but also expressed dynamically during the budding process. First, asymmetric expression of *hyilp-B* can be found at budding region before any visible morphological change (Figure 2-14A). Second, the expression of *hyilp-B* spreads around the area where a bud is going to develop (Figure 2-14B and Figure 2-14D). Third, *hyilp-B* is expressed at the boundary base of a bud when the bud was developing (Figure 2-14C). Fourth, the expression of *hyilp-B* can be found at the bud head and initiated bud tentacles (Figure 2-9D and Figure 2-14E); Finally, an intensive ring-like expression pattern of *hyilp-B* could be observed at the peduncle region of new bud (Figure 2-14E), which is the same as the one in an adult *Hydra* (Figure 2-9C). The dynamic expression pattern is summarised in Figure 2-14F.

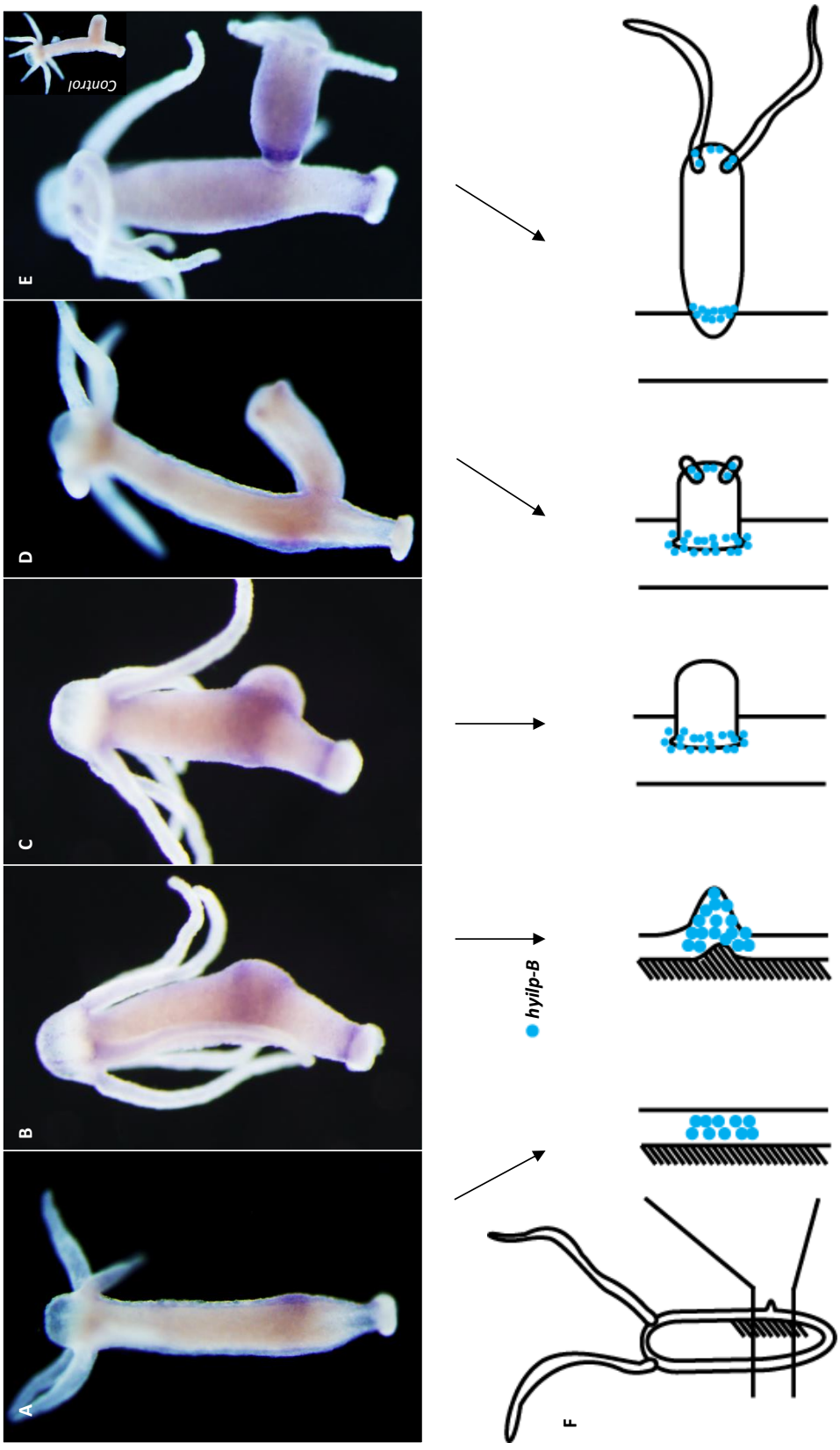

Figure 2-14 *hyilp-B* dynamic expression pattern during budding.

(A) A summarised model of *hyilp-B* dynamic expression during budding process. (B-F) expression pattern of *hyilp-B* at different stages of budding through *in situ* hybridization.

2.3.3 Potential downstream genes of HyILPs signalling

To investigate possible downstream genes of ILPs signalling in *Hydra*, Wnt signalling was targeted and analysed. To test whethe *hyilps* are downstream genes of GSK3, alsterpaullone (ALP) was used for inhibiting the activity of GSK3 (Broun et al. 2005). Glycogen synthase kinase-3 (GSK3) is a serine/threonine kinase known as a downstream cascade of both INS/IGFs and Wnt signalling pathways in mammals. HyINSR knockdown line and its corresponding control were used for this experiment in order to induce a second stimulus on GSK3. It was found that the expression of *hyinsr*, *hyilp-A* and *hyilp-C* were suppressed under ALP treatment in both HyINSR knockdown polyps and control polyps (Figure 2-15A). Interestingly, upregulation of *hyilp-B* can only be found in the INSR knockdown animals under ALP treatment (Figure 2-15B). Therefore, *hyinsr*, *hyilp-A* and *hyilp-C* were negatively regulated by GSK3, while *hyilp-B* might be co-regulated by both HyINSR and GSK3.

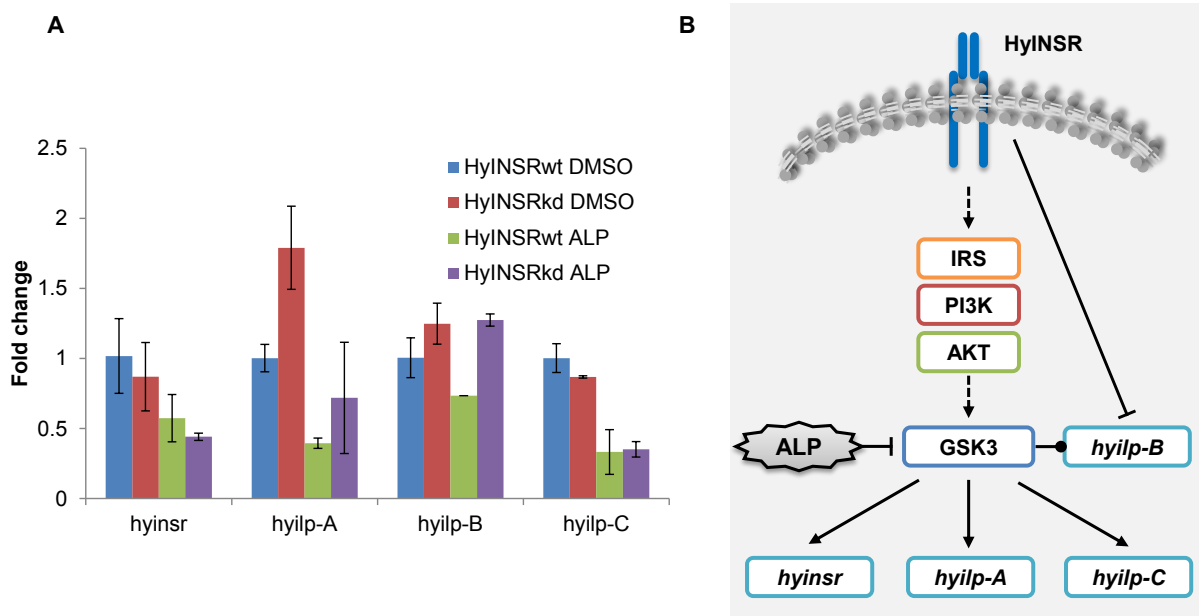

Figure 2-15 HyINSR knockdown under the ALP challenge in *Hydra*

(A) Expression levels of *hyinsr* and *hyilps* transcripts. n = 2 replicates. Error bar indicated standard deviation. Wild Type: WT; Dimethyl sulfoxide: DMSO; ALP: Alsterpaullone. (B) Putative interaction between hyILPs and GSK3 in *Hydra*. Solid line: known relationship between genes or supported by evident; Dotted line: putative relationship between genes.

β-catenin is an important downstream cascade of Wnt signalling pathway through GSK3 in *Hydra* (Broun et al. 2005, Gee et al. 2010). In this study, two independent transgenic lines (B4 and B9) which contain constantly active β-catenin were used for testing the interaction between β-catenin and HyILPs signalling (Figure 2-16A and B).

High expression level of GFP indicated enormous amount of β-catenin in both transgenic lines (Figure 2-16 C and E). However, neither *hyinsr* nor three *hyilps* are influenced at transcript level in both transgenic lines (Figure 2-16 D and F). Therefore, Wnt signalling does not regulate the expression of *hyilps* through β-catenin in *Hydra*.

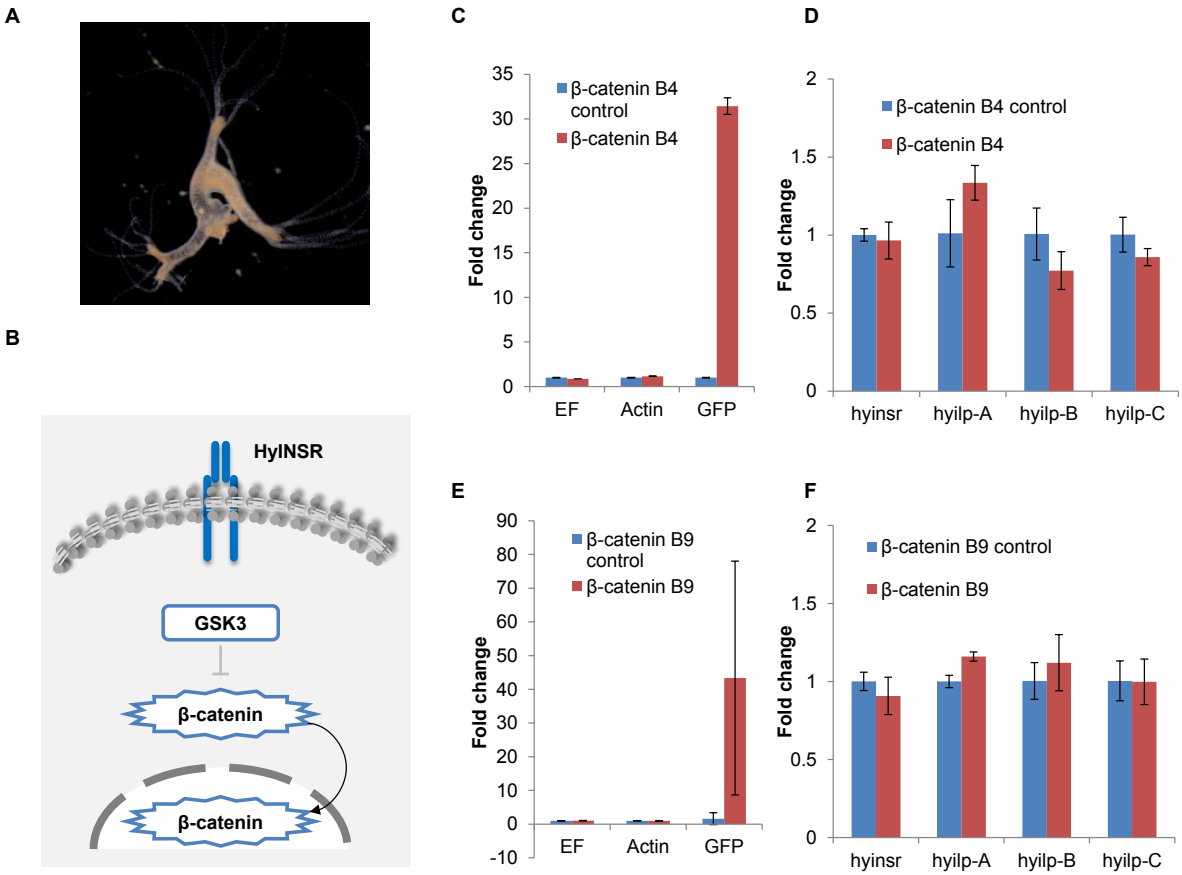

Figure 2-16 ILPs were not affected by constantly active β-catenin

(A) Muti-headed transgenic *Hydra* with constantly active β-catenin fused with GFP. (B) Active β-catenin translocated into nucleus and activated downstream genes. Grey line: not function regulation; Solid arrow: translocation of protein. (C-F) Expression levels of hyINSR and *Hydra* ILPs transcripts in two *Hydra* lines with constant active β-catenin revealed by qRT-PCR. n = 2 replicates. EF and Actin are housekeeping genes and GFP an internal control gene. B4 and B9 are two independent transgenic lines; β-catenin B4 control and β-catenin B9 control are their corresponding control lines, respectively. Error bar indicate standard deviation.

2.4 Investigation of HylLP-B function through transgensis.

2.4.1 Overexpression of HylLP-B-GFP in epithelial tissues

To further investigate function of ILP-B in *Hydra*, ILP-B overexpression construct was designed (Figure 2-17A), where ILP-B was fused with GFP under actin promoter. DsRED was used for the trace cell lineage where transgenic construct was expressed. A set of primers was designed to reveal the expression level of ILP-B from different sources. Total ILP-B was used for detecting the amount of total ILP-B in *Hydra*; ILP-B-GFP was used for detecting the amount of ILP-B expressed from transgenic construct; Endogenous ILP-B was used for detecting the amount of endogenous ILP-B (Figure 2-17A). Two independent transgenic lines were established based on both GFP and DsRED signals: ILP-B-GFP B6 and B9, that contained the overexpression construct in both ectodermal and endodermal tissues. QRT-PCR revealed that both transgenic lines contained large amount of *ilp-B*, expression level was 50 fold elevated in ILP-B-GFP6 in transgenic line, and 10 fold in ILP-B-GFP9 transgenic line. (Figure 2-17B and C). On protein level, GFP antibody was used for detecting the ILP-B-GFP under CLSM (Figure 2-17D and E). The results indicated that ILP-B-GFP in ectodermal cells accumulated in the vesicles at apical surface and bottom region towards extracellular matrix (mesoglea), while ILP-B-GFP in the endodermal cells was accumulated at vesicles towards mesoglea as well as defused within the cytoplasm (Figure 2-17F).

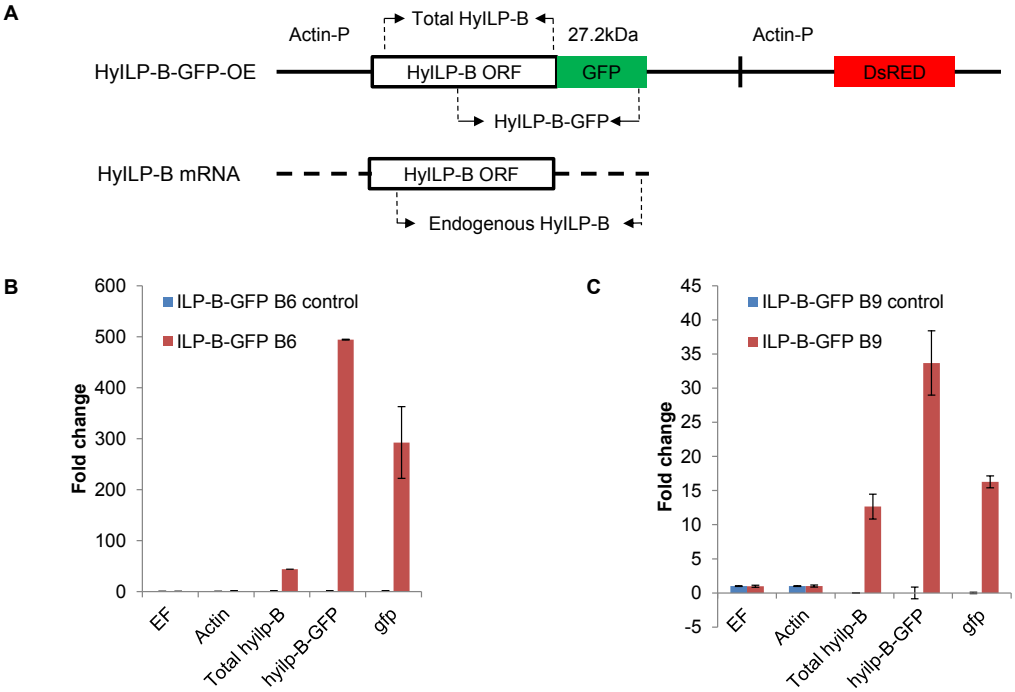

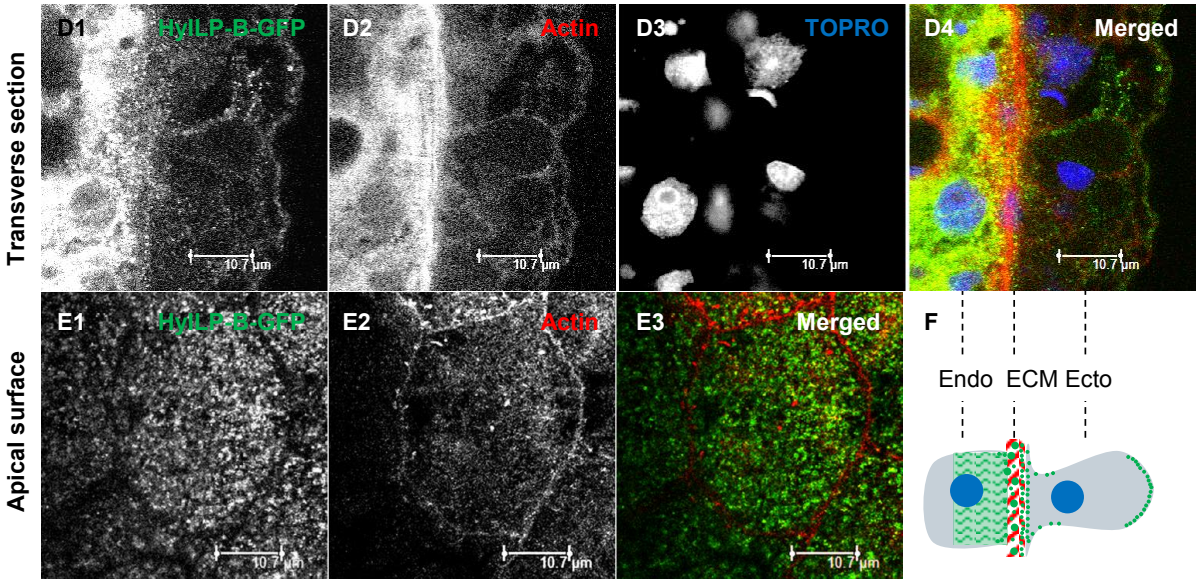

Figure 2-17 Overexpression of HyILP-B by HyILP-B-GFP in epithelial cells

(A) HyILP-B-GFP overexpression construct and HyILP-B open reading frame (ORF). Arrow indicated qRT-PCR primers targeted region. (B-C) Transcripts level of control genes in two HyILP-B-GFP transgenic *Hydra* lines. n = 2 replicates. Error bar indicated standard deviation. (D1-D4) Transverse section of epithelial tissue from HyILP-B-GFP B9 transgenic *Hydra* under CLSM using GFP antibodies. (E1-E3) Apical surface of ectodermal tissue from HyILP-B-GFP B9 transgenic Hydra under CLSM using GFP antibodies. (F) ILP-B-GFP intracellular distribution model. Endo: endodermal tissue; Ecto: ectodermal tissue; ECM: extracellular matrix.

2.4.2 Phenotype analysis of HyILP-B-GFP overexpression

To analyse whether overexpression of HyILP-B would suppress the expression of other putative components of ILP signalling, *hyinsr* and three endogenous *hyilps* genes were tested by qRT-PCR. However, none of their expression was affected (Figure 2-18A and B). To further analyse possible phenotypes caused by overexpression HyILP-B-GFP, population growth rate analysis was carried out on both HyILP-B-GFP transgenic lines and corresponding control lines. Experimental data were used to approximate the exponential growth formula $x_t = x_0(1+r)^t$. In order to extract the growth rate *r*, the formula was transformed into $r = (\frac{x_t}{x_0})^{\frac{1}{t}} - 1$ or $r = \sqrt[t]{\frac{x_t}{x_0}} - 1$, where *t* was the time ($0 < t \leq t_{end}$); x_t is the number of Polyp at time *t*; t_0 was the time when the first bud dropped from initial mother polyp. thus, x_0=2. Dataset was normalised to the day when the first bud dropped. Only the dataset from middle of the experiment to the end of experiment was used for further analysis. R and *lme4* were used to perform a linear mixed effects analysis of the relationship between growth rate r and genetic background (Winter 2013). As fixed effects, genetic background and

date (No interaction term) were entered into the full model. As random effects, intercepts were used for samples or independent populations, as well as by sample random slopes for the effect of date. Visual inspection of residual plots did not reveal any obvious deviation from homoscedasticity or normality. P-values were obtained by likelihood ratio tests of the full model with the effect of genetic background against the null model without this effect though "anova ()" function. Full model and Null model designed in R were listed below:

$$Full\ model = lmer(Growth\ rate \sim Genetic\ background + (1|Date) + (1|Sample))$$

$$Null\ model = lmer(Growth\ rate \sim (1|Date) + (1|Sample))$$

In HyILP-B-GFP B6 comparison group, HyILP-B-GFP B6 control sample possessed average growth rate of 0.1219, while ILP-B overexpression affected significantly the growth rate ($\chi^2(1)=7.4077$, p=0.0065), lowering it by about 0.0216 ± 0.0032 (standard errors) (Figure 2-18C). In HyILP-B-GFP B9 comparison group, HyILP-B-GFP B9 control sample demonstrated average growth rate of 0.1083. However, there was no significant difference between HyILP-B-GFP B9 overexpression line and its corresponding control line (Figure 2-18D).

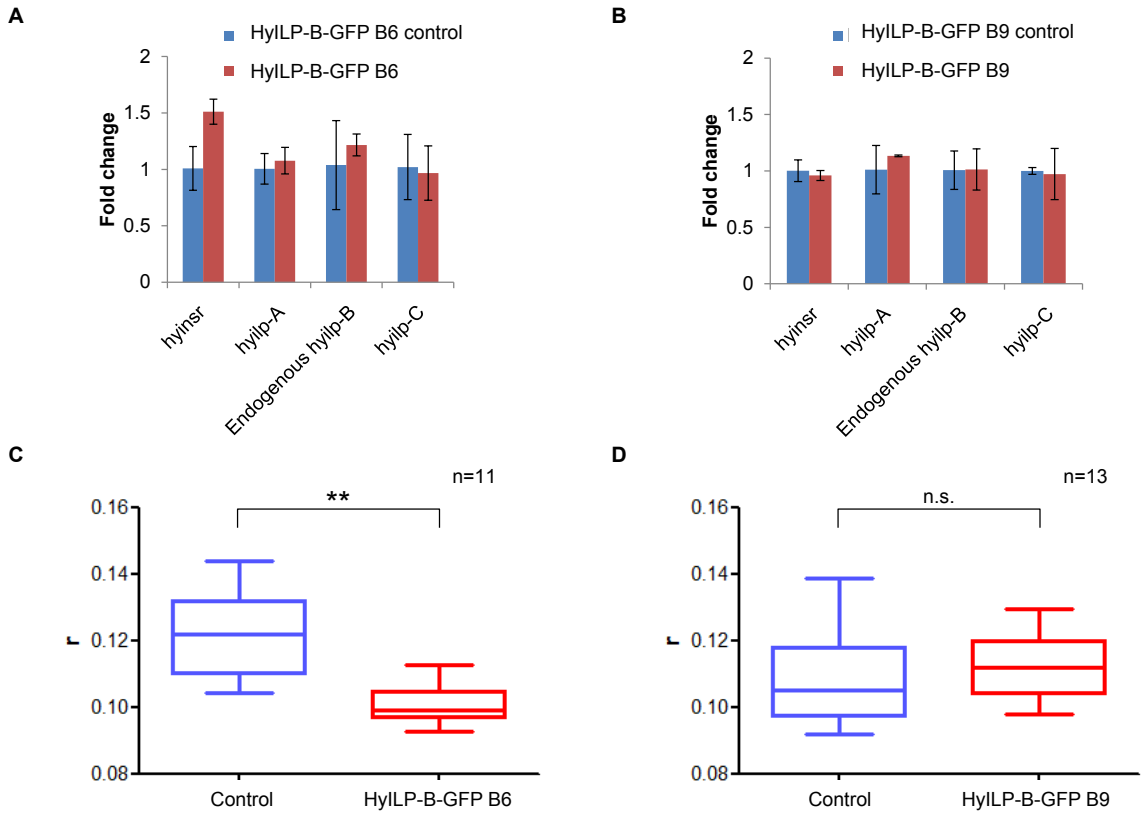

Figure 2-18 Growth rate analysis on HyILP-B-GFP overexpression.
(A-B) Transcript level of *hyinsr* and *hyilps* genes in HyILP-B-GFP B6 and B9 transgenic and control lines. n = 2 replicates. Error bar indicated standard deviation. (C-D) comparison of growth rate *r* in HyILP-B-GFP B6 and B9 transgenic and control lines. $x_t = x_0(1+r)^t$; x_t is the number of polyps at date *t*; x_0=2; **<0.01; n.s.: nonsignificant.

2.4.3 Overexpression of HyILP-B-cMyc

To eliminate the possible influence from relatively large protein GFP fused to HyILP-B and validate the effect of HyILP-B overexpression through another independent transgenic line, transgenic construct of HyILP-B fused with a cMyc-tag under actin promoter was designed and used for building transgenic *Hydra* (Figure 2-19A). cMyc-tag is a small tag peptide (1.5kDa) and can be detected by commercial antibody. DsRED was used for the labelling cell linages where transgenic construct was intergrated. Primers against HyILP-B-cMyc are used for detecting the amount of HyILP-B expressed from transgenic construct (Figure 2-19A). Two independent transgenic lines were generated, as evidenced by permanent DsRED signal: ILP-B-cMyc 1 and 4, which contain the overexpression construct in ectodermal tissues. QRT-PCR revealed that HyILP-B-cMyc 1 transgenic line contained massive amount of *ilp-B*, more than 150 fold elevated, while only two fold upregulation was found in HyILP-B-cMyc 4 transgenic line (Figure 2-19B and C). Antibody to cMyc was used for detecting the HyILP-B-cMyc under CLSM (Figure 2-19D and E). The results indicated that HyILP-B-cMyc accumulated in the vesicles at apical surface of ectodermal cells only in HyILP-B-cMyc 1 transgenic line (Figure 2-19F). Unfortunately, no signal was detected in HyILP-B-cMyc 4 transgenic lines. Therefore, HyILP-B-cMyc 1 was used for further analysis.

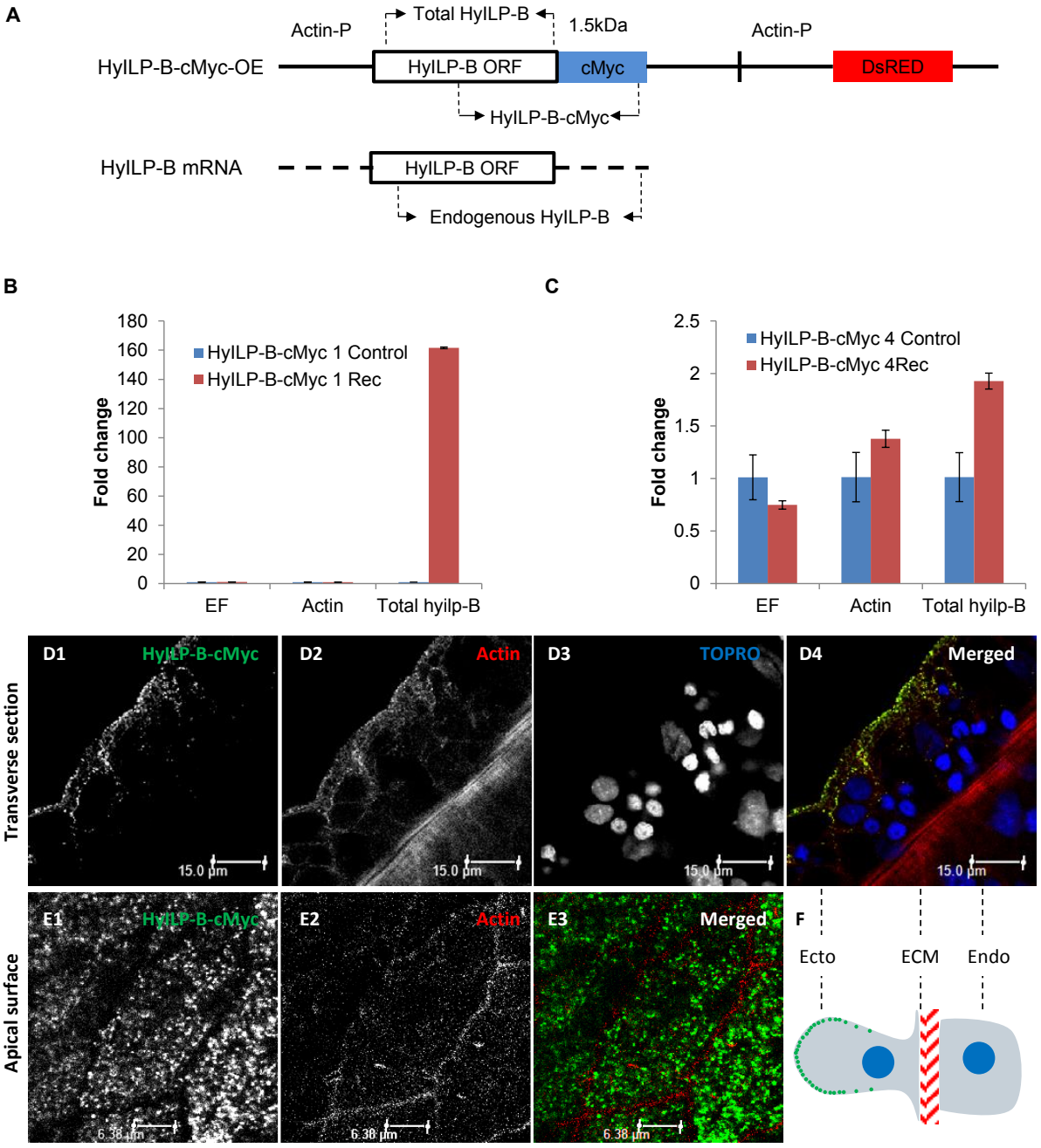

Figure 2-19 Overexpression of HyILP-B by HyILP-B-cMyc contruct.

(A) HyILP-B-cMyc overexpression construct and HyILP-B open reading frame (ORF). Arrow indicates qRT-PCR primers targeted region. (B-C) Transcripts level of control genes in two HyILP-B-cMyc transgenic *Hydras* lines. n = 2 replicates. Error bar indicates standard deviation. (D1-D4) Transverse section of epithelial tissue from HyILP-B-cMyc 1 transgenic *Hydra* under CLSM using cMyc antibodies. (E1-E3) Apical surface of ectodermal tissue from HyILP-B-cMyc 1 transgenic *Hydra* under CLSM using cMyc anitibodies. (F) HyILP-B-cMyc intracellular distribution model. Endo: endodermal tissue; Ecto: ectodermal tissue; ECM: extracellular matrix.

2.4.4 Phenotype analysis of *Hydra* with HyILP-B-cMyc overexpression in ectodermal tissues

To analyse whether there exists compensation mechanism among HyILPs, hyinsr and three endogenous *hyilps* genes were tested in ILP-B-cMyc 1 transgenic lines by qRT-PCR. However, all tested genes were not influenced by overexpression of HyILP-B-cMyc (Figure 2-20 A). To analyse possible phenotypes caused by overexpression, population growth experiment was carried out in HyILP-B-cMyc 1 transgenic line and its corresponding control line. Their population growth curves were followed (Figure 2-20 B). Moreover, full model and null model (see chapter 2.4.1) of growth rate analysis were adjusted by adding random slope:

$$Full\ model = lmer(Growth\ rate \sim Genetic\ background + (1 + Genetic\ background|Date) + (1 + Genetic\ background|Sample))$$

$$Null\ model = lmer(Growth\ rate \sim (1 + Genetic\ background|Date) + (1 + Genetic\ background|Sample))$$

The model revealed that HyILP-B control samples had demonstrated average growth rate of 0.1015, while HyILP-B overexpression affected significantly the growth rate ($\chi^2(1)=7.236$, $p=0.00715$), lowering it by about 0.0184 ± 0.0031 (standard errors) (Figure 2-20 C). To investigate whether cell cycle was influenced by HyILP-B overexpression, BrDU pulse labelling experiment was induced. However, there was no significant cell cycle difference found in ectodermal cells between HyILP-B-cMyc overexpression lines and corresponding control lines (Figure 2-20 D). Therefore, it was unlikely HyILP-B overexpression slow down the population growth through reducing cell proliferation.

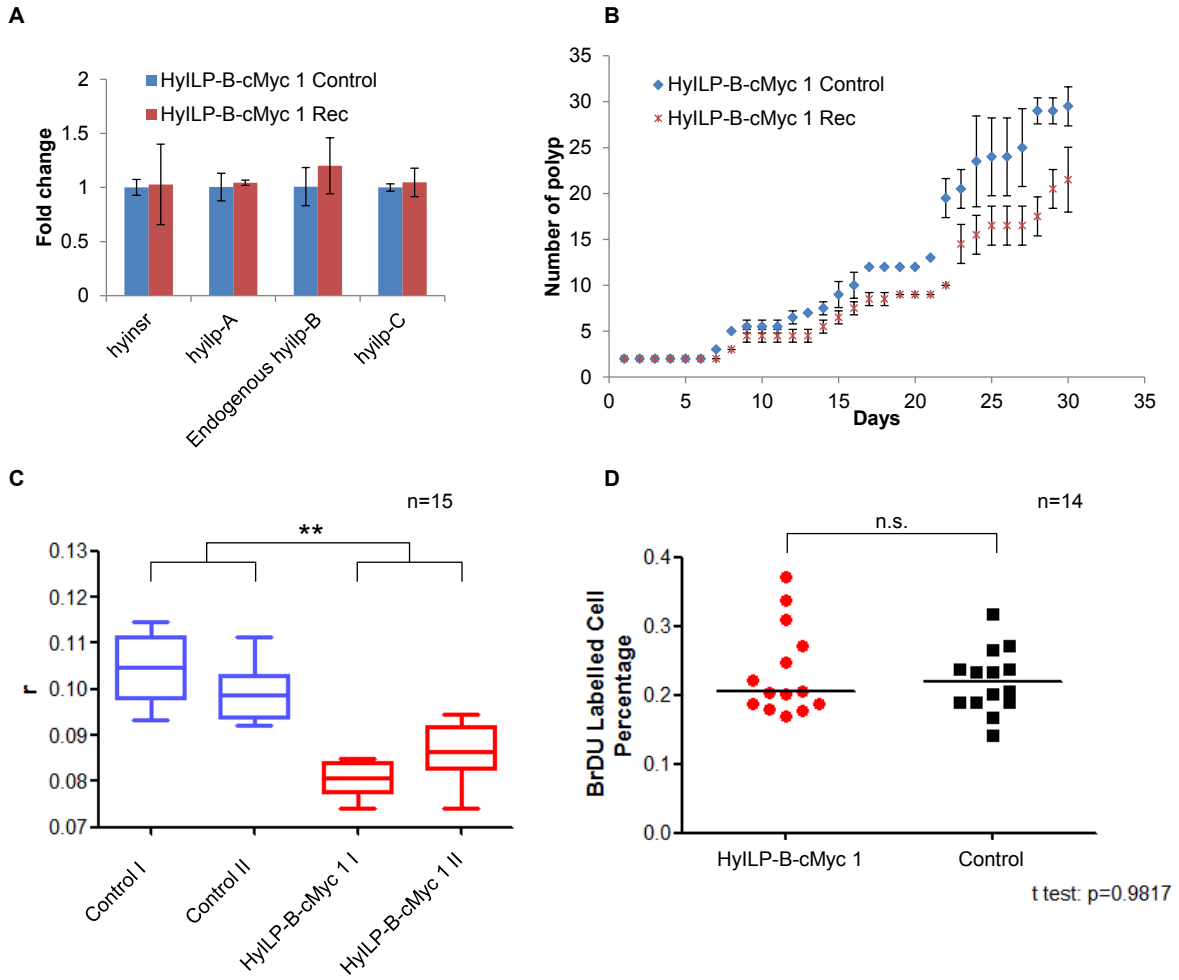

Figure 2-20 Overexpression of HyILP-B by HyILP-B-cMyc leads to growth retardation

(A) Transcript level of *hyinsr* and *hyilps* genes in HyILP-B-cMyc 1 transgenic and control lines. n = 2 replicates. Error bar indicates standard deviation. (B) Growth curve of HyILP-B-cMyc 1 transgenic and control lines. n = 2 replicates. Error bar indicates standard deviation. (C) Comparison of growth rate r in HyILP-B-cMyc 1 transgenic and control lines. $x_t = x_0(1+r)^t$; x_t is the number of Polyp at date t; x_0=2; **: P<0.01; (D) BrDU pulse labelling blind test on ectodermal cells from HyILP-B-cMyc 1 transgenic and control lines. P=0.9817 (Student t test). n = 14 replicates. n.s.: nonsignificant.

2.4.5 Knockdown of HyILP-B in ectodermal tissue

To investigate influence of HyILP-B knockdown in *Hydra*, HyILP-B hairpin construct was built (Figure 2-21 A). HyILP-B-hairpin was fused to GFP protein under actin promoter. Two independent transgenic lines were established: HyILP-B Hairpin 12 and 14. QRT-PCR revealed that expression level of HyILP-B decreased significantly in both transgenic lines (Figure 2-21 B and C).

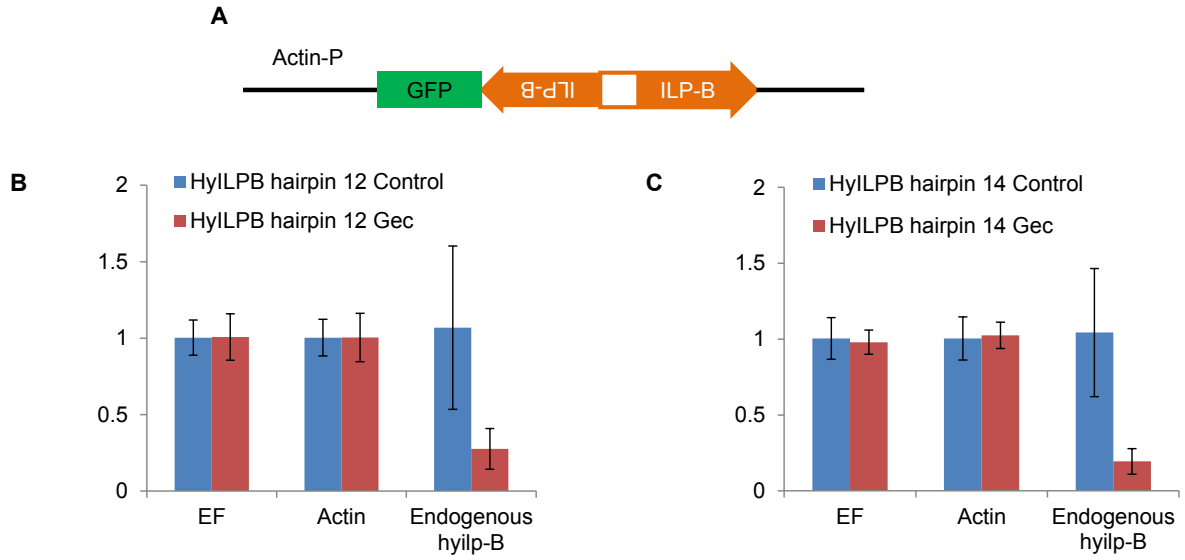

Figure 2-21 HyILP-B-hairpin transgenic *Hydra*

(A) HyILP-B-Hairpin overexpression construct. (B-C) Transcripts level of control genes in two HyILP-B-Hairpin transgenic *Hydras*. n = 2 replicates. Error bar indicated standard deviation.

2.4.6 Phenotype analysis of *Hydra* with HyILP-B knockdown in ectodermal tissue

To analyse whether there exists a feedback controlling hyilp-B expression mechanism, *hyinsr* and the other two endogenous *hyilps* genes were tested by qRT-PCR. However, none of their expression was affected (Figure 2-22 A and B). Growth rate analysis (refer to chapter 2.4.4) was carried out on both HyILP-B-Hairpin (HyILP-B-HB) transgenic lines. However, there was no significant difference between HyILP-B-Hairpin transgenic lines and their corresponding control lines, respectively (Figure 2-22 C and D).

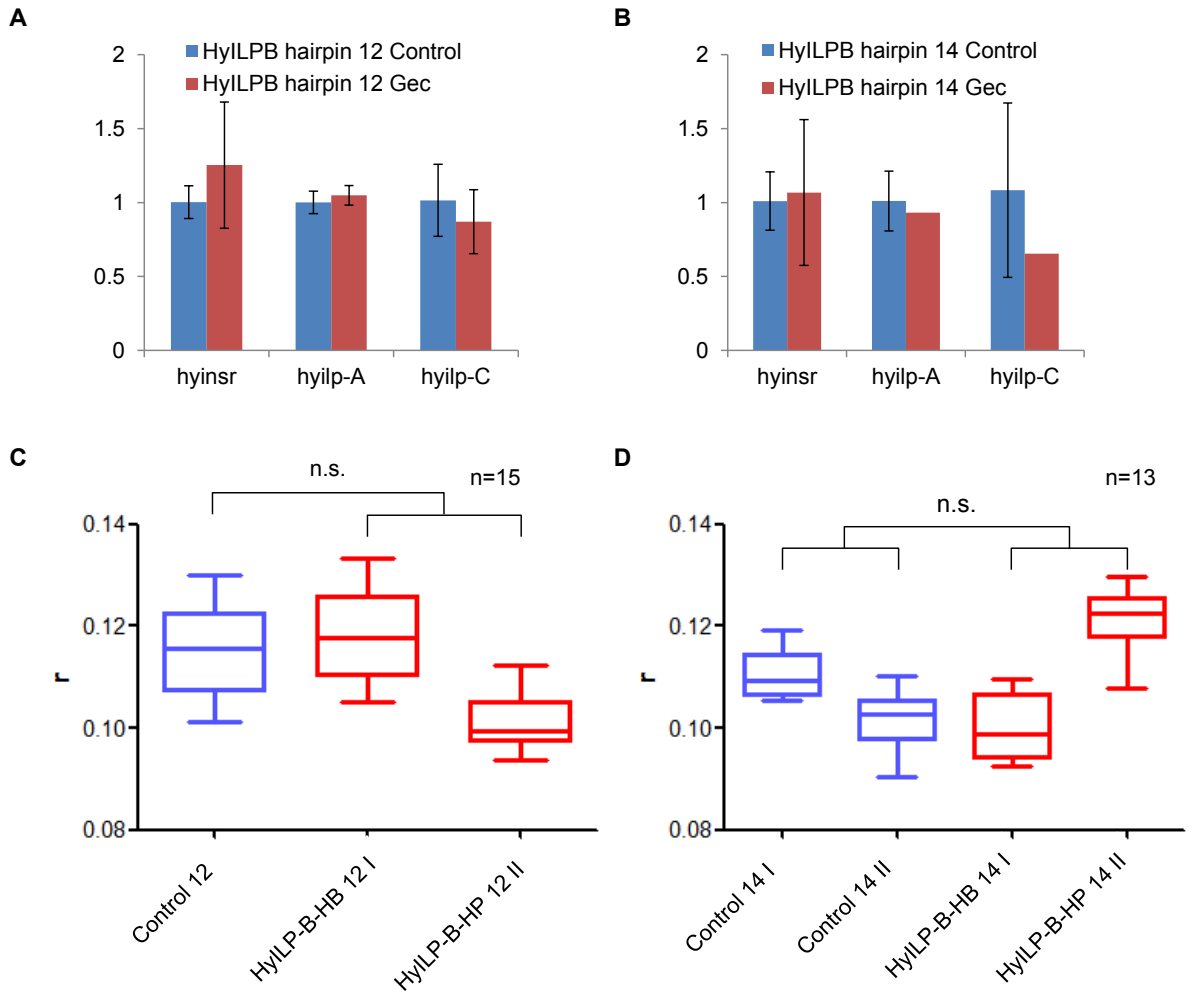

Figure 2-22 Growth rate analysis of HyILP-B-Hairpin transgenic lines

(A-B) Transcript level of *hyinsr* and two *hyilps* genes in ILP-B-Hairpin transgenic and control lines. n = 2 replicates. Error bar indicates standard deviation. (C-D) Comparison of growth rate r in both HyILP-B-HB transgenic and control lines. $x_t = x_0(1+r)^t$; x_t is the number of polyp at date t; x_0=2; n.s.: nonsignificant.

2.4.7 HyILP-B is not cleaved as ILPs in mammals

To investigate whether the predicted C domain of HyILP-B is cleaved out, Western blot experiment was carried out on 3 samples: Wild Type (wt) *HvAEP*, HyILP-B-cMyc and HyILP-B-GFP transgenic lines using both HyILP-B and GFP antibodies. HyILP-B antibody targeted a short amino acids sequence within HyILP-B A domain, named HyILP-B antigen peptide (Figure 2-23A). Therefore, under assumption that C domain is not cleaved off, HyILP-B antibody would detect an 18.9 kDa band in all 3 samples (Figure 2-23A). Moreover, HyILP-B-cMyc sample would contain a 20.1 kDa band, while HyILP-B-GFP sample would possess a 46.1 kDa band (Figure 2-23A). Under cleavage C domain assumption, HyILP-B antibody would detect a 4.7 kDa band in all

3 samples (Figure 2-23A). Additionally, a 5.9 kDa band as well as a 31.9 kDa band would be found in HyILP-B-cMyc and HyILP-B-GFP samples, respectively (Figure 2-23A). The head and foot (H+F) parts from Wild Type (wt) *HvAEP* were used for Western blot because of their highly concentrated HyILP-B protein. GFP antibody is used as a positive control to detect the HyILP-B-GFP peptide. HyILP-A antigen peptide was used as a blocking control, which was used to produce HyILP-A antibody.

The Western blot results revealed that the C domain of HyILP-B was not cleaved out. A band of size around 19 kDa was found in sample from wt *HvAEP*, HyILP-B-cMyc and ILP-B-GFP samples (Figure 2-23B). Moreover, a band at size of around 21 kDa was detected in HyILP-B-cMyc sample, which could be HyILP-B-cMyc peptide (Figure 2-23B). At the same time, a band at size of around 50 kDa band was detected in ILP-B-GFP sample by either HyILP-B or GFP antibody, indicating it was HyILP-B-GFP peptide (Figure 2-23B). In addition, the function of HyILP-B antibody could be blocked almost completedly by synthesized ILP-B antigen peptide, but not HyILP-A antigen peptide, indicating HyILP-B antibody was able to work specifically in western blot (Figure 2-23B). This experiment revealed that the C domain of HyILP-B was not cleaved out and, HyILP-B antibody could detect the endogenous HyILP-B as well as ectopic HyILP-B.

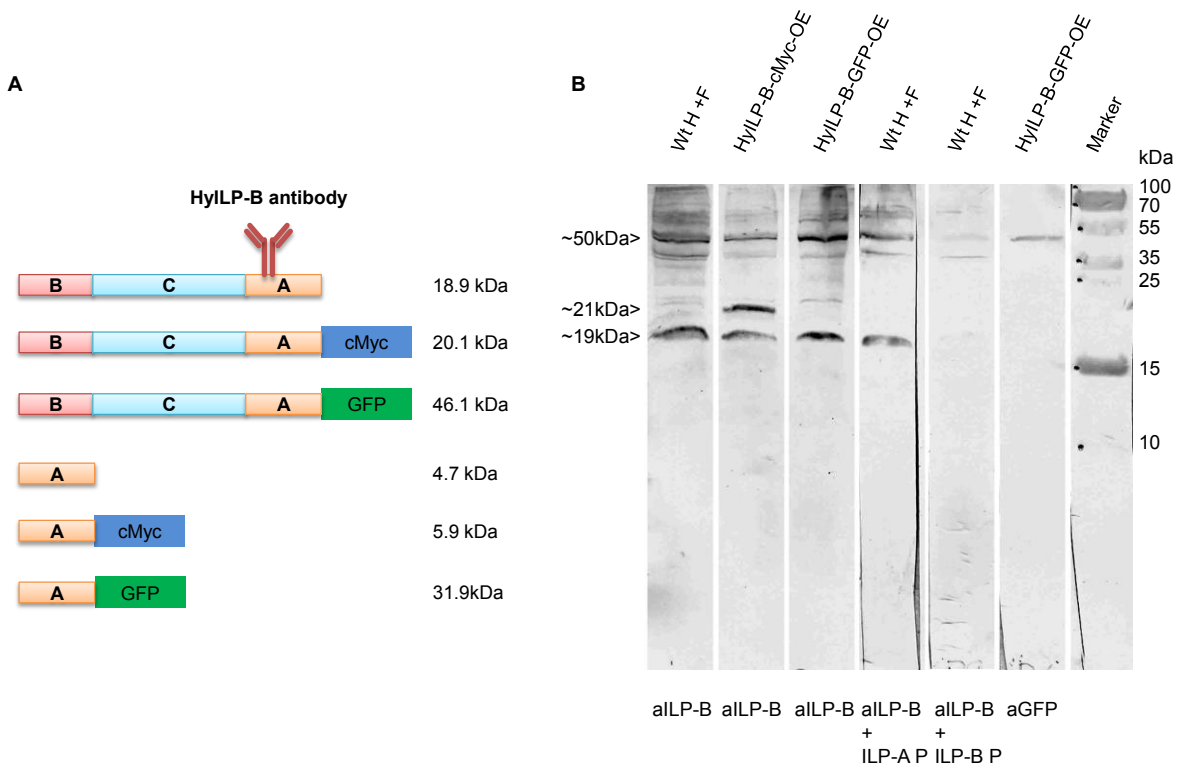

Figure 2-23 Western blot of HyILP-B results

(A) Predicted size of HyILP-B, HyILP-B-GFP and HyILP-B-cMyc peptides under assumptions of non-cleavage and cleavage. (B) Western blot on wild type, HyILP-B-GFP and HyILP-B-cMyc samples using HyILP-B and GFP antibodies. Wild type: wt; Head and Foot: H+F; HyILP-B antibody: aILP-B; GFP antibody: aGFP; HyILP-A antigen peptide: ILP-A P; HyILP-B antigen peptide: ILP-B P; HyILP-B-cMyc overexpression transgenic line: HyILP-B-cMyc-OE; HyILP-B-GFP overexpression transgenic line: HyILP-B-GFP-OE.

3. Discussion

The aim of this thesis was to understand the evolutionary conserved roles of ILPs family using *Hydra* as a model animal. A workflow of *in silico* search for ILPs was developed, called ILPs screening workflow. It revealed the present of *ilp* genes in Placozoa, Cnidaria and Bilateria phyla, while no *ilp* gene was detected in Choanozoa, Porifera and Ctenophora. In every case, an organism's genome contained multiple *ilp* genes, including 7 *ilps* in *Nematostella vectensis*, 6 *ilps* in *Acropora digitfera*, 4 *ilps* in *Aurelia aurita* and 3 *ilps* in *Hydra*. At transcriptome level, all 3 *ilps* from *Hydra vulgaris AEP* were expressed in the head region, while *hyilp-B* and *hyilp-C* were also expressed in the foot region. Furthermore, *hyilp-B* revealed a dynamic expression pattern at the budding region during bud development. Interestingly, both *hyilp-A* and *hyilp-B* turned out to be expressed in neurons where no *hyilp-C* was found. Environmental stimuli on *Hydra* indicated starvation and knockdown of *hyinsr* gene promoted high expression of *hyilp-A*. Meanwhile, inhibition of GSK-3 by ALP suppressed the expression of *hyilp-A* and *hyilp-C*. With the help of transgensis technique, *Hydra* polyps with HyILP-B overexpression construct were generated and revealed a phenotype of population growth delay with constant cell proliferation rate in ectodermal cells. In contrast, no obvious phenotype was observed on *Hydra* polyps with HyILP-B knockdown construct. In addition, the proteolysis analysis indicated that the C domain of ILP-B was retained. In the following, I will discuss the origin of ILPs family and its relationship with emergence of nervous system, detailed characterised hyILPs as well as their associate signalling pathways and putative functions in *Hydra*.

3.1 ILPs family emerged before the radiation of eumetazoans

ILPs fingerprints do not only apply to ILPs from deuterostomes and protostomes, but are conserved in the ILPs from basal metazoans. For example, *Hydra* is a basal metazoan model organism belonging to Cnidaria, containing 3 ILPs genes which possessed ILPs fingerprints of signal peptide, cysteine pattern and moreover, the exon-intron-exon gene structure (Figure 2-3A). Recently, 4 ILPs and 5 INSR genes were discovered in *Trichoplax adhaerens* (Nikitin 2015), whose ILPs also retain the major ILPs fingerprints. One ILP contains additional adjacent cysteine residues complicating the prediction of disulphide bridges. However, it is known that not every ILP contains all four essential ILPs fingerprints. For example, a few ILPs contain

different cysteine pattern with either more cysteines or less cysteines (Pierce et al. 2001, Colombani et al. 2012) and couples of ILPs miss the exon-intron-exon structures (Iwami 2000).

Taking into account results of the ILPs screening workflow and results from Nikitin (Nikitin 2015), it is likely that ILPs family was invented before Placozoa along with some essential neuroendocrine function related genes (Srivastava et al. 2008), even though *Trichoplax adhaerens* does not have definitive nervous system. On the other hand, regardless the controversial evolutionary position of Ctenophora (Pisani et al. 2015, Whelan et al. 2015), *Mnemiopsis leidyi* contained no ILP gene, however, possessed a non-canonical nervous system (Moroz and Kohn 2016). Therefore, the identification of origin of ILPs family is consistent with that the nervous system evolved more than once along the evolution. Furthermore, instead of being a fundamental requirement for the origin of nervous system, ILPs family are more likely to be the regulatory peptides integrated into the nervous systems invented in Eumetazoa (Figure 3-1), matching the hypothesis that nervous system arose through secretory cells producing regulatory peptides (Veenstra 2011).

Although the identification of ILPs reveals the potential connection between regulatory cells and targeted cells, the investigation of receptors for ILPs are not straightforward. Besides interacting with INSR, ILPs may also interact with GPCR in the basal animals, where GPCR are also proposed to facilitate the evolution of nervous system (Krishnan and Schioth 2015). It is known that GPCR are molecular targets for neurotransmitters and neuropeptides in higher animals, such as RXFPs and Frizzled (Huang and Klein 2004, Bathgate et al. 2013). Therefore, to further dissect the ancestral role of ILPs family in *Hydra*, it would be interesting to investigate whether HyILPs interact with specific *Hydra* GPCRs (Fernandez and Torres-Aleman 2012) besides HyINSR (Steele et al. 1996). On the other hand, there exist several putative IIS components were identified in sponges, including an ILP (later proved to be a contaminated ILP from a rodent (UniProtKB - P21563))(Robitzki et al. 1989), several insulin receptor-like tyrosine kinases (RTKs) (Skorokhod et al. 1999) as well as insulin receptor substrate (Srivastava et al. 2010).

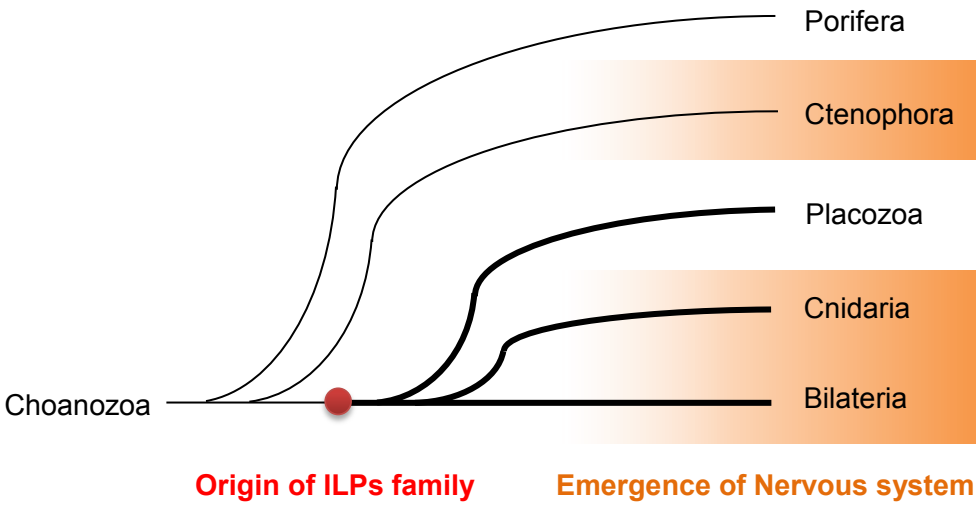

Figure 3-1 Origin of ILPs family along with emergence of nervous system.
Origin of ILPs family before Placozoa, Cnidaria and Bilateria as well as emergence of nervous system in Ctenophora and Eumetazoa.

3.2 Neuron-derived HyILP-A possibly involved in nutrient sensing and lipid regulation.

HyILP-A, which was the only *Hydra ilp* upregulated its expression level under HyINSR knockdown and starvation, appears to play a putative role of maintaining the nutrient status in *Hydra* (Figure 3-2A). It is known that one important canonical role of the ILPs family signalling pathways is monitoring and regulating energy metabolism. Human insulin, for example, reduces blood sugar concentration and promotes fat storage in fat cells and muscle. On contrast, the expression of *hyilp-A* increased after starvation, revealing that HyILP-A possessed a different role rather than suppressing the glucose concentration in *Hydra*. Meanwhile, upregulation of *hyilp-A* under HyINSR knockdown indicated that *hyilp-A* may be regulated by HyINSR signalling. Previously, Dr. Anna-Marei Böhm (Phd Thesis) found accumulated fat droplets in endodermal cells upon HyINSR knockdown as well as starvation, revealing the role of HyINSR signalling in lipid storage. The finding of *hyilp-A* expressed neurons along the *Hydra* body column may suggest that lipid storage was regulated by *Hydra* nervous system through HyILP-A (Figure 3-2B). On the other hand, the starvation challenge may influence stem cells homeostasis along the body column. Therefore, HyILP-A may also played a role in maintaining the stem cell cycle. However, it would require further investigations, such as analysing the fluctuation of stem cell genes expression level under HyILP-A

overexpression or knockdown conditions. Interestingly, expression of *dilp6* also increases in *Drosophila* during starvation and pupal stage (Slaidina et al. 2009) and its mutants shows the biggest reduction in body weight of all *dilp* single mutants (Gronke et al. 2010), which suggests that DILP6 is an IGF-like peptide secreted by the fat body that promoting growth during larval-pupal development (Okamoto et al. 2009, Slaidina et al. 2009, Gronke et al. 2010). It is not clear why the expression of *hyilp-A* was suppressed during the ALP treatment but not regulated by β-catenin. One explanation could be lipid synthesis was inhibited in order to prepare for secondary axis development induced by ALP (Broun et al. 2005), thus leading to suppression of *hyilp-A* through a non-canonical GSK3 pathway (Figure 3-2A). The potential cooperation between GSK3 and HyILP-A hinted there was a synergy between Wnt and Insulin signalling conserved in early metazoan.

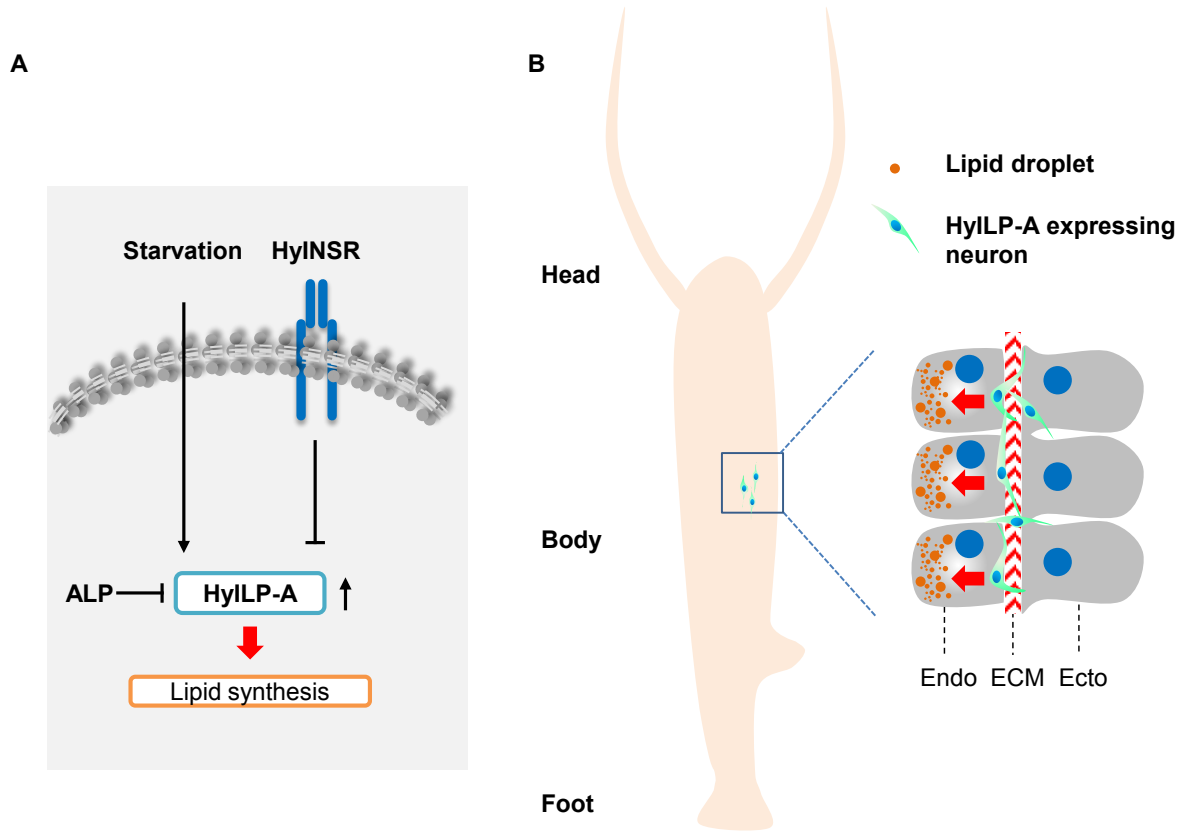

Figure 3-2 Putative role of HyILP-A in lipid regulation

(A) Model of HyILP-A regulation. (B) Hypothesis of HyILP-A working scheme. Alsterpallone: ALP; Endodermal tissue: Endo; Ectodermal tissue: Ecto; Extracellular matrix: ECM.

3.3 Neuron-derived HyILP-B plays a role in *Hydra* development

When INS/IGFs signalling pathway is promoting cellular or organismal growth (Nakae et al. 2001), most of its ligands possess specific spatio-temporal expression pattern

(Gorczyca et al. 1993, Fernandez and Torres-Aleman 2012, Chen et al. 2013), even though some of them have overlapping expression domains. For example, in *Drosophila*, DILP2, DILP3 and DILP5 are co-expressed in brain median neuron secretory cells (MNCs) controlling larval growth and development (Brogiolo et al. 2001, Rulifson et al. 2002). However, DILP2 is activated in the first instar, DILP5 in the second instar and DILP3 in mid-late third instar (Gronke et al. 2010). This can also be found in nematode (Ritter et al. 2013).

HyILP-B most likely is an upstream gene of HyINSR. In *Hydra*, *hyilp-B* expression level was quite robust against HyINSR knockdown, starvation and ALP/β-catenin manipulation. However, it has complex spatio-temporal expression patterns during bud development (Figure 2-9, Figure 2-12 and Figure 2-14), which are roughly corresponding to the expression pattern of HyINSR (Steele et al. 1996) (Figure 3-3). Both *hyinsr* and *hyilp*-B were co-expressed at the bud initiation, at the base of the tentacles and in the peduncle region during the bud development. The different expression patterns between *hyinsr* and *hyilp*-B were found at the middle stage of bud development, where *hyilp*-B was expressed at the boundary base of a bud and *hyinsr* was expressed at the apexes of bud head. Further analysis revealed that *hyilp-B* showed a scattered expression pattern at the head region of a bud at the middle stage (Figure 3-3), whose expression latter was concentrated at the apexes of head where *hyinsr* was expressed constantly. Therefore, HyILP-B could be a development process mediator, monitoring and promoting bud development.

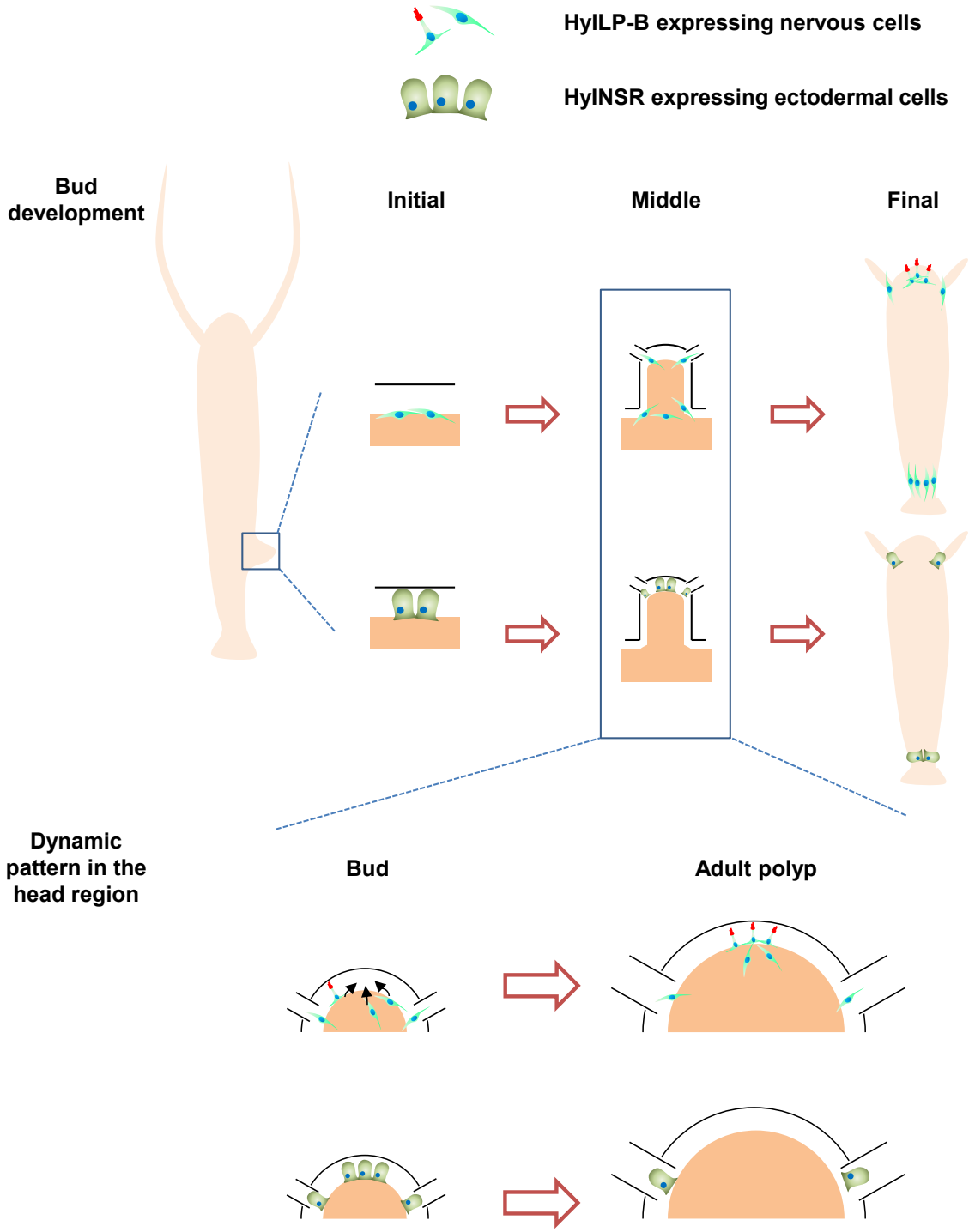

Figure 3-3 HyILP-B cooexpressed with HyINSR during bud development.
Summarise the expression pattern of HyILP-B and HyINSR (Steele et al. 1996)

Hydra nervous net consists of many different subsets of neurons possessing specific expression profiles, where the phenotype of a neuron is determined by its positional cue (Bode 1992). Because *Hydra* cells are constantly displaced towards extremities including neurons, nervous cells are maintained by adding new differentiated neurons or by phenotype conversion of displaced neurons (Koizumi et al. 1988, Bode 1992).

Surprisingly, expression of *hyilp-B* was found in both sensory neurons and ganglion cell. Meanwhile, the mobility of neurons expressing *hyilp-B* was so high that they seemed not to lose their phenotype when they were not located at apexes of head or peduncle region (Figure 3-3). Three possible functions of HyILP-B were summarised based on the expression pattern of HyILP-B (Figure 3-4). First, it is secreted within interstitial tissue space and promotes differentiation and proliferation of surrounded cells including epithelial cells and interstitial cells. Second, it may induce downstream genes of HyINSR signalling in ectodermal cells where HyINSR is exclusively expressed (Steele et al. 1996). Third, it may work like neurotransmitter connecting nervous cells.

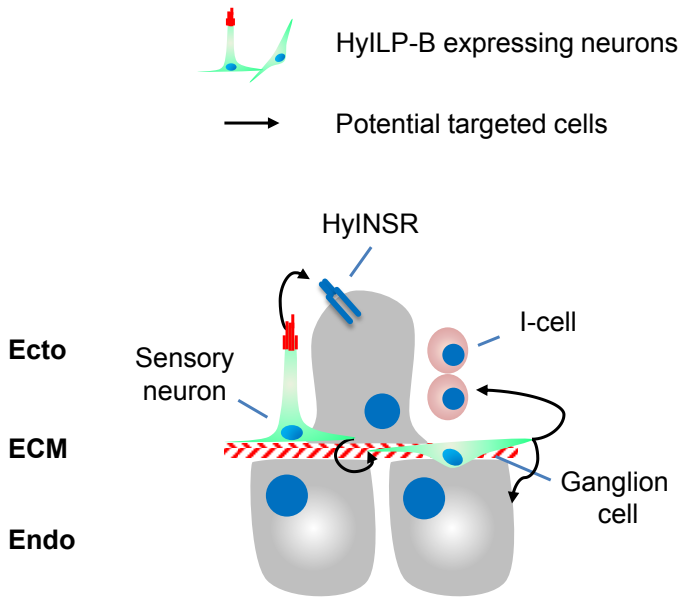

Figure 3-4 Potential target cells of HyILP-B

Endo: endodermal tissue; Ecto: ectodermal tissue; ECM: extracellular matrix: I-cell: interstitial cells.

The growth control through IIS/IGFs signalling is achieved mostly by mediating the concentration of ligands or ligand binding proteins such as IGFs and IGF binding proteins in higher vertebrates (Clemmons et al. 1998, Laron 2001), as well as ILPs in invertebrates (Gronke et al. 2010). Reducing or increasing concentration of these ligands or ligand binding proteins influences dramatically the time required for animal development and leads to smaller or bigger body, organ, or cell size (Claeys et al. 2002, Gronke et al. 2010). For example, ubiquitous expression of DILP2 leads to bigger flies with an increase in both cell size and cell number (Brogiolo et al. 2001). Unfortunately, the total developmental time of DILP2 overexpressing fly is not clear. The total development time is controlled by ILP signalling pathway through its effects

on the rate of cell growth and proliferation in different organs (Shingleton et al. 2005) as well as apoptosis (Kooijman 2006). In *Hydra*, the population growth rate decreased when *hyilp-B* was expressed ubiquitously. The robust cell proliferation rate of ectodermal cell hinted transgenic polyps might possess bigger cell size and body size requiring longer developmental time, which in return slowed down the population growth rate. At the same time, it could be possible that overexpressed *hyilp-B* triggered apoptosis, thus leading to longer body developmental time. Another possibility might be that ubiquitous expression *hyilp-B* confused polyp with the ending point of bud development, thus leading to longer bud development time. Therefore, further analysis need to be carried out on measuring bud and body size, development time of bud and polyp, as well as bud initiation frequency which is an important factor influencing population growth rate (discovered by Jan Taubenheim in the Bosch lab). Mutation of ILPs usually caused smaller size, growth retard and expended life-span in invertebrates (Gronke et al. 2010, Ritter et al. 2013). However, there is no significant population growth difference caused by *hyilp-B* knockdown. It is possible that partially knockdown of *hyilp*-B was not sufficient to cause detectable phenotype through population growth rate analysis. Meanwhile, *hyilp-B* expressed in neurons was still available for developmental processes such as bud development.

Hydra is able to produce and release numerous neuropeptides by proneuropeptide cleavage (Grimmelikhuijzen et al. 2002, Fujisawa 2008, Jekely 2013). Therefore, HyILP-B could be functional active with C domain residue. It is known that C domain increases the binding affinity of ILP dramatically in other animals (Bayne et al. 1989). HyILP-B and HyILP-C possess similar ILP family fingerprints and close evolutionary relationship (Figure 2-3). However, HyILP-C is regulated by ALP while HyILP-B is not, revealing that HyILP-C and HyILP-B may be regulated through different signalling pathways. Moreover, HyILP-C does not compensate lost expression of HyILP-B (Figure 2-22) indicating that it may not possess the same function as HyILP-B.

3.4 Conclusions and perspectives

This thesis was set out to explore the origin of ILPs family and has screened organisms from Choanozoa and basal metazoan groups (Cnidaria, Placozoa, Ctenphora and Porifera) by an *in silico* method searching for ILPs. This thesis has also sought to reveal the ancestral roles of ILPs family using a cnidarian model organism - *Hydra*. The general literature on these subjects is lacking. This thesis sought to answer two questions: 1. When did ILPs family emerged? 2. What is the ancestral role of ILPs family in *Hydra*?

To answer the first question, a filter with ILPs family fingerprints was built. Meanwhile, a universal ILP cysteine pattern were extracted and used as a seed searching for ILPs in available online databases. Unexpectedly, ILPs were only detected in the animals from Placozoa and Cnidaria. This observation provides three important messages: first, instead of being cause of emergence of multi-cellular organisms, ILPs family is a multi-cellular organism invention during its evolution. Second, almost every ILP is secreted by nervous system in the animal kingdom. Therefore, the observation that ILPs are not present in Ctenophora is consistent with the theory that different nervous systems are invented by Ctenophora and Eumetazoa, respectively. Furthermore, it also suggests general nervous system is most likely an inevitable invention along multi-cellular organism evolution with or without ILPs family. Third, ILPs were invented in the neuron-free animal *Trichoplax adhaerens* and presumably to be secreted and functional (Nikitin 2015) through connection between ILPs producing cells and targeted cells. Taking the known hypothesis that nervous system arose through secretory cells producing regulatory peptides into consideration, it is possible that some cells producing ILPs are not transformed into nervous cells during the animal evolution, such as human insulin produced in pancreas beta cells as well as *Drosophila* ILP6 produced in fat cells (Bai et al. 2012). On the other hand, different number of ILPs found in detected animals revealed that ILPs family keep expanding within the same phylum along time. For example, it is known in *Drosophila* genus that different species contained different number of ILPs (Gronke et al. 2010). In addition, the method of *in silico* search for ILPs is valid and able to screen ILPs quickly in other species.

To answer the second question, besides the exploration of *hyilps* expression pattern, monitoring *hyilps* expression was carried out under different environmental stimuli, HyINSR mutation and HyILP-B gain- and loss-of function challenges. Potential phenotype of HyILP-B gain- and loss-of function transgenic *Hydra* was analysed. Function analysis revealed HyILP-A plays a role in nutrients sensing, and most likely is regulated by *Hydra* Wnt signalling, which is crucial for pattern formation. HyILP-B is more likely to be involved in animal development regulation and potentially being upstream of HyINSR, because on one hand, *hyilp-B* expression level is quite robust against HyINSR knockdown, starvation and Wnt signalling pathway manipulations. Moreover, HyILP-B presents a spatio-temporal expression pattern which corresponds to the expression pattern of HyINSR during bud development (Figure 2-14 and Figure 3-3). Meanwhile, HyILP-B delays *Hydra* population growth rate when it is overexpressed (Figure 2-20). These results suggest that the ancestral roles of ILPs in *Hydra* are similar as ILPs in other high animals - nutrient regulation and growth control (Gronke et al. 2010, Ritter et al. 2013). Further research needs to be carried out in order to fully understand the role of HyILPs. First, gain- and loss-of-function of HyILP-A transgenic *Hydra* need to be generated and used for functional analysis. Second, transgenic *Hydra* with knockdown or even knock-out of HyILP-B in both ectodermal cells and nervous cells needs to be conducted in order to eliminate the influence of potential existing compensation in current ectodermal cell HyILP-B knockdown transgenic *Hydra*. Third, both expression pattern and function of HyILP-C are still not clear. Exploring the above subjects as future research strategies can gain further understanding of ancestral roles of ILPs in *Hydra*.

As a consequence of the methodology being used and the databases available, the study encountered a number of limitations, which need to be considered. First, the quality of peptide or predicted peptide databases would influence the accuracy of *in silico* search. In particular, some ILP with irregular cysteine pattern could not be detected, such as DILP8 (Colombani et al. 2012) and some ILPs in *C. elegans* (Pierce et al. 2001). One solution would be using EST database as an alternative database for ILPs searching. Second, it is known that RNA interference technology is not able to achieve completely knockdown and can also be prone to off-target effects in transgenic animals such as *Drosophila* (Ma et al. 2006). Therefore, new gene editing methods may be considered such as CRISPR/Cas9 technique (Hwang et al. 2013).

4. Material

4.1 Organisms and cell lines

Hydra species:	*Hydra vulgaris AEP*
	Hydra viridissima A99
	Hydra oligactis
	Hydra magnipapillata 105
Transgenic *Hydra vulgaris AEP*	INSR knockdown A6 (Dr. Anna-Marei Böhm)
	Constantly active β-catenin B4 (Gee et al. 2010)
	Constantly active β-catenin B9 (Gee et al. 2010)
Electro-competent bacteria:	*Escherichia coli* (*E. coli*) DH5α (invitrogen)
Feeding strain:	*Artemia salina*

4.2 Chemicals

Acetic acid	Roth
Acetic anhydride	Roth
Agar agar	Roth
Agarose	Roth
Ampicillin	Merck
Boric acid	Roth
Bovine serum albumine (BSA) fraction V	Roth
Bromophenol blue	Sigma
Calcium chloride (CaCl2)	Roth
CHAPS	Roth
Chloroform	Roth
Dextran sulfate	Roth
Dipotassium phosphate (K2HPO4)	Merck
dNTP mix (10 mM)	Fermentas
EDTA	Roth
Ethanol	Roth
Ethidium bromide	Roth
Euparal	Roth
Formamide	Roth
Gelatine	Sigma
Glucose	Roth
Glycerol	Roth
Glycine	Roth
Heparin	Roth
Hydrochloric acid (HCl)	Roth

Isopropanol	Roth
Levamisole	Roth
Magnesium chloride (MgCl2)	Merck
Magnesium sulfate (MgSO4)	Merck
Maleic acid	Roth
Methanol	Roth
Methylene blue	Merck
Monopotassium phosphate (KH2PO4)	Merck
Mowiol 4-88	Calbiochem
TES	Sigma
NBT/BCIP	Roche
Paraformaldehyde	Sigma
Peptone	Roth
Phalloidin-Tetramethylrhodamine	Sigma
Phenol	Roth
Potassium chloride (KCl)	Roth
Procaine hydrochloride	Sigma
Rhodamine B Isothiocyanate-Dextran R9379	Sigma
Rotiphorese® Gel 40	Roth
Sea salt (Reef crystalsTM)	Aquarium Systems
Sheep serum	Sigma
Sodium acetate	Roth
Sodium cacodylate	Sigma
Sodium chloride (NaCl)	Roth
Sodium citrate (Na3(C6H5O7))	Roth
Sodium deoxycholate	Sigma
Sodium hydroxide (NaOH)	Roth
Sodium pyruvate	Sigma
Tetramethylethylenediamine (TEMED)	Serva
Triethanolamine	Sigma
TRIS base	Roth
TRIS-HCl	Roth
TritonX100	Merck
tRNA yeast	Sigma
Tween20	Roth
Urea	Roth
Urethane	Sigma
Yeast extract	Roth

4.3 Media

Artemia medium	31.8 g sea salt / 1 L Millipore H_2O
Hydra medium	0.29 mM CaCl x $2H_2O$, 0.33 mM $MgSO_4$ x 7 H_2O, 0.5 mM $NaHCO_3$, 0.08 mM K_2CO_3
LB medium	10 g peptone, 5 g yeast extract, 5 g NaCl, Millipore H_2O up to 1 L, autoclaved
LB agar	LB medium, add 15 g agar agar, Millipore H_2O up to 1 L, autoclaved
LB medium with ampicillin	LB medium 1 L, autoclaved, add ampicillin reaching to 50 µg/ml when cool down to 60 °C
SOB medium	20 g peptone, 5 g yeast extract, 0.55 g NaCl, 1.86 g KCl, Millipore H_2O up to 1 L, autoclaved, add 10 ml 1M $MgSO_4$ und 10 ml 1M $MgCl_2$ (both sterile)
SOC medium	1 L SOB medium, add 0.02 M glucose (sterile)

4.4 Buffers and solutions

4.4.1 General

APS stock solution	25g Ammoniumpersulfate in Millipore H_2O
Denhardt´s (50x)	1% Polyvinylpyrrolidone, 1% Ficoll, 1% BSA fraction V in Millipore H_2O (sterile)
DNA loading buffer	50% glycerol, 10 mM EDTA (pH 8.0), 0.1% SDS, 0.1% Bromophenol blue, 0.1% Xylene cyanol
EDTA solution	0.5 M EDTA (pH 8.0)
Hoechst stock solution	1 mg/ml in Millipore H_2O
Mowiol	5 g Mowiol in 20 ml 100 mM TRIS (pH 8.0), stir for 16 h at room temperature, then add 10 ml glycerol, stir for 16 h at room temperature. Clarification of the solution by centrifugation (5000 rpm, 20 min). Stored at -20 °C in aliquots (500 µl). Prewarm to room temperature before use.

NTM buffer	100 mM NaCl, 100 mM TRIS-HCl, 50 mM $MgCl_2$, pH 9.5
NTMT buffer	NTM, add 0.1% Tween20
Paraformaldehyde stock	8% paraformaldehyde in Millipore H2O, heat in water bath at 50 °C, add droplets of NaOH until the powder lyses, pH 7.4
PBS buffer	150 mM NaCl, 80 mM K_2HPO_4, pH 7.34
PBS/glycerol	9:1 of PBS and glycerol
PBT buffer	PBS, add 0.1% Tween20
Phalloidin stock solution	0.1 mg/ml in Millipore H_2O
Sheep serum	Inactivation at 56 °C for 30 min
SSC buffer (20x)	3 M NaCl, 0.3 M sodium citrate (pH 7.0)
TAE buffer (50x)	242 g TRIS base, 57.1 ml 100% acetic acid, 100 ml 0.5 M EDTA, Millipore H_2O up to 1 L
TBE (10x)	0.89 M TRIS base, 0.89 M boric acid, 0.02 M EDTA
Urethane solution	2% urethane in Hydra medium
Dissociation solution	3.6mM KCl, 6.0mM $CaCl_2$, 1.2mM $MgSO_4$, 6.0mM Na citrate, 6.0mM Na pyruvate, 12.54 mM TES, 6mM Glucose, total PH 6.9 and store at -20 °C.
Pronase E solution	35mg Pronase E (8U / mg) was add into 5 ml dissociation solution before use.

4.4.2 *In situ* hybridization

Blocking solution	80% MAB-B, 20% heat-inactivated sheep serum
Glycine working solution	4 mg glycine per ml PBT

Hybridization solution	50% formamide, 5x SSC, 0.1% Tween20, 0.1% CHAPS, 1x Denhardt's, 100 µg / ml Heparin in Millipore H_2O
MAB	100 mM maleic acid, 150 mM NaCl, pH 7.5
MAB-B	MAB-T plus 1% BSA fraction V
MAB-T	MAB plus 0.1% Tween20
Triethanolamine	100 mM triethanolamine (pH 7.8)

4.4.2 *Western blot*

PI-water	1 tablet Complete Mini, protease inhibitors EDTA-free up to 5ml
3x Gel Buffer	36.4 g Tris-HCl in Millipore H2O, pH 8.45, 0.3 g SDS, up to 100 ml
1x Cathode Buffer, internal chamber	12.11 g Tris, 17.92 g Tricine, 1.0 g SDS in Millipore H_2O, up to 1L, store at 4 °C
5x Anode Buffer, outer chamber	121.1 g Tris, add 500 ml Millipore H_2O, adjust pH to 8.9, adjust the volume to 1L, store at 4 °C
2x Sample Buffer	1.0 ml Tris-HCl 1M buffer pH 6.8, 2.4 ml Glycerol, 0.8 g SDS, 2.0 mg Coomassie Blue G-250, up to 10 ml, Add DTT 0,031g per 1 Ml before use.
Transfer Buffer	2.8 g Tris, 1.45 g Glycin, 50 ml MetOH, 0.1ml 10% SDS in Millipore H2O, up to 500 ml.
TBS	2.4 g Tris, 9.0 g NaCl, adjust pH to 7.5 in Millipore H2O, up to 1 L, add 0.05% Tween20
Coomassie brilliant blue destaining solution	50 % (v/v) Methanol, 10 % (v/v) Acetic acid in Millipore H2O
Coomassie brilliant blue staining solution	0.05 % (w/v) Coomassie brilliant blue R250 in Coomassie brilliant blue destaining solution

5x SDS-PAGE loading buffer	200 mM Tris-HCl (pH 6.8), 20 %(v/v) Glycerol, 10 % (w/v) SDS, 0.05 %(w/v) Bromphenol blue in Millipore H2O; when use it add 10 % (v/v) β-Mercaptoethanol

4.4.3 Maceration

Maceration solution	1:1:13 of acetic acid, glycerol and Millipore H_2O

4.4.4 DNA sequencing

Sequencing gel for LI-COR (41 cm)	10.5 g urea, 14 ml Millipore H_2O, 3.75 ml Rotiphorese® Gel 40, 2.5 ml 10x TBE, 38 µl TEMED, 175 µl 10% APS

4.5 Kits

Amnicon® Ultra Centrifugal Filters	Millipore
DIG RNA Labeling Kit (SP6/T7)	Roche
First Strand cDNA Synthesis Kit	Fermentas
NucleoSpin® Extract II	Macherey Nagel
NucleoSpin® Plasmid QuickPure	Macherey Nagel
pGEM®-T Kit	Promega
QIAfilterTM Plasmid Midi Kit	Qiagen
QuantiTect Probe RT-PCR Kit	Qiagen
PureLink™ RNA Mini Kit	Life Technologies
Sequencing Kit	Applied biosystems
SequiTherm EXCELTM II DNA Sequencing Kit	Epicentre
SMARTTM PCR cDNA Synthesis Kit	Clontech

4.6 Enzymes

DNase I	Fermentas
Go Taq DNA polymerase	Promega
Platinum® Taq Polymerase High Fidelity	Invitrogen
Proteinase K	Sigma
Pronase E	Sigma
RNase A	Fermentas
T4 ligase	Fermentas
AsiSI	New England Biolabs
EcoRI	New England Biolabs
PacI	New England Biolabs
SbfI	New England Biolabs

PvuI	New England Biolabs
SpeI	New England Biolabs

4.7 Vectors

pGEM®-T	Promega
LigAF	Provided by Dr . Alexander Klimovich
ConsJL-13	Provided by Dr . Alexander Klimovich

4.8 Antibodies

Alexa Fluor® 488 donkey anti-mouse IgG (H+L)	Invitrogen
Anti-Digoxigenin-alkaline phosphatase linked Fab fragments	Roche
Polyclonal rabbit anti-GFP antibody	Roche
Mouse anti-Myc Tag #05-724	Millipore
Mouse-anti-GFP	Roche
Goat anti-rabbit_AF488	Life technology
Rabbit anti-HyILP-A (0.730mg/ml)	GenScript
Rabbit anti-HyILP-B (0.635mg/ml)	GenScript

4.9 DNA size standards

GeneRuler™ DNA Ladder Mix	Fermentas

4.10 Oligonucleotides (primers)

A list of the used oligonucleotides can be found in the Appendix 8.3.

4.11 Devices

4.11.1 PCR - thermocyclers

Primus 25	MWG-Biotech
Primus 96 advanced	peqLab
Primus 96 plus	MWG-Biotech
Real-Time Cycler 7300	Applied Biosystems

4.11.2 Gel electrophoresis chambers

MINI SUB-CELL®	Bio-Rad
Novex Mini-Cell	Invitrogen
PerfectBlue™ Twin L	Peqlab
SUB-CELL® GT	Bio-Rad

4.11.3 Incubators/shakers

C/R5 (waterbath)	Julabo
HIS25 Grant	BOEKEL
KS10 (rotation shaker)	Edmund Bühler
Thermoincubator	Heraeus Instruments
Thermomixer Compact	Eppendorf
ThermoStat plus	Eppendorf
Oven/ incubator	Memmert
Rotation incubator RM5	Assistant

4.11.4 Electroporation devices

Gene Pulser II	Bio-Rad
Pulse Controller II	Bio-Rad

4.11.5 UV devices

UV lamp Chroma 43	Vetter GmbH
ImaGo Compact Imaging System	B&L Systems
UV - Stratalinker® 1800	Stratagene

4.11.6 Centrifuges

Centrifuge 5415 D	Eppendorf
Centrifuge 5417 R	Eppendorf
MiniSpin	Eppendorf
Multifuge 3 S-R	Heraeus

4.11.7 Microscopies

AxioCam (digital camera)	Zeiss
Axioskop 2	Zeiss
Axiovert 100	Zeiss
CLSM TCS SP/UV	Leica
DC300F (digital camera)	Leica
DP71 (digital camera)	Olympus
KL1500 LCD	Schott
SZX16	Olympus
Wild M3C binocular	Heerbrugg

4.11.8 Photometer

BioPhotometer	Eppendorf

Nanodrop ND1000 photometer	Thermo Scientific

4.11.9 Sequencer

4300 DNA Analyzer	LI-COR
454 GS-FLX Titanium	Roche

4.11.10 Other devices

AF-10 (ice machine)	Scotsman
Freezer -20 °C	Liebherr
Freezer -80 °C	Forma Scientific
Microwave	Moulinex
Milli-Q Academic System	Millipore
pH211 Microprocessor pH Meter	Hanna Instruments
Refrigerator	Liebherr
Roche 454 FLX sequencer	Roche
UV-Stratalinker 1800	Stratagene
Vortex - Genie2®	Scientific Industries
Weighing machine	Sartorius

4.12 URLs

AG Bosch internal BLAST server	http://134.245.171.51/blast/
BLAST searches	http://blast.ncbi.nlm.nih.gov/Blast.cgi
Compagen	http://compagen.zoologie.uni-kiel.de/
Genome Browser *Hydra* (metazome)	https://metazome.jgi.doe.gov/pz/portal.html
NCBI	http://www.ncbi.nlm.nih.gov/
SMART	http://smart.embl-heidelberg.de/smart/
UniProt	http://www.uniprot.org
PRATT-Pattern Matching	http://www.ebi.ac.uk/Tools/pfa/pratt/
SignalP 4.1 Server	http://www.cbs.dtu.dk/services/SignalP/

PATTINPROT
https://npsa-prabi.ibcp.fr/cgi-bin/npsa_automat.pl?page=/NPSA/npsa_pattinprot.html
PRABI-working with uploaded database
https://npsa-prabi.ibcp.fr/cgi-bin/npsa_automat.pl?page=/NPSA/npsa_uploadfile.html
Phyre2-Protein Homology / analogY Recognition Engine V2.0
http://www.sbg.bio.ic.ac.uk/phyre2/html/page.cgi?id=index
Amphimedon queenslandica proteins database
http://metazoa.ensembl.org/Amphimedon_queenslandica/Info/Index

Mnemiopsis leidyi Protein models	http://research.nhgri.nih.gov/mnemiopsis/

Monosiga brevicollis (Choanoflagellate) Proteins
http://www.uniprot.org/proteomes/UP000001357

4.13 Software

Image editing	Photoshop CS3
Figure preparation	Illustrator CS3
Microscopy	Axio Vision 3.1; Leica IM 50 4.0
Sequence analysis	MEGA 6.0; DNAMAN 4.15; QIIME; BioEdit

5. Methods

5.1 Cultivation of organisms

5.1.1 Cultivation of *Artemia salina*

First instar nauplius larvae of Artemia salina served as prey for all used Hydra species. For hatching, eggs were incubated overnight at 32 °C in Artemia medium under permanent air supply. For feeding of Hydra polyps, nauplii were collected, washed with water to remove salts and re-suspended in *Hydra* medium.

5.1.2 Cultivation of *Hydra*

Experiments were carried out using *Hydra vulgaris AEP* (Hemmrich et al. 2007), *Hydra* oligactis, *Hydra* viridissima A99, *Hydra* magnipapillata 105. All laboratory cultured strains are available at the University of Kiel. All animals were cultured under constant, identical environmental conditions including culture medium, food (3 times per week) and temperature according to standard procedures (Lenhoff and Brown 1970).

5.2 Standard laboratory methods

5.2.1 RNA Isolation

Total RNA was extracted using PureLink™ RNA Mini Kit according to the manufacturer's protocol. At the end of extraction procedure Total RNA was precipitated with 70% ethanol for 20 min at 4 °C with maximum g, and re-dissolved in 10 µl Millipore H_2O.

5.2.2 Quantification of nucleic acids

The quantity and quality of isolated nucleic acids were determined at the absorbance at 260 nm using the Nanodrop spectrophotometer.

5.2.3 First strand cDNA synthesis

The synthesis of cDNA was performed using the First Strand cDNA Synthesis Kit according to the manufacturers protocol using Oligo(dT)18 primer. For subsequent comparative analyses of gene expression levels by real-time PCR, equal amounts of mRNA were added to the reactions.

5.2.4 Polymerase chain reactions (PCRs)

5.2.4.1 Standard PCR

A standard PCR reaction was set up in a final volume of 20 µl. Table 1 contains the pipetting scheme for the reaction. The used general PCR program is shown in Table 2. The PCR products were analysed via agarose gel electrophoresis.

Component	Volume [µl]
cDNA(1:20) + Millipore H_2O	14.1
Buffer containing $MgCl_2$ (5x)	4
dNTP mix (10 mM)	0.2
Taq polymerase (5 U/µl)	0.1
Forward primer	0.8
Reverse primer	0.8
Total volume	**20**

Table 1 Pipetting scheme for standard PCR.

Steps	Temperature	Duration	
Initial denaturation	95°C	3 min	
Denaturation	95°C	30 sec	30-40 cycles
Hybridization	*	30 sec	
Elongation	72°C	**	
Terminal elongation	72°C	3 min	

Table 2 Standard PCR program.

* Hybridization temperature was depending on the melting temperature of the used primer pairs.

** Elongation time was depending on the length of the amplified PCR fragment. A synthesis rate of the Taq polymerase of 1kb per minute was used to estimate elongation time.

5.2.4.2 Colony check

A colony check PCR was performed to analyse plasmids for insertion of DNA. A standard PCR reaction (see paragraph 5.2.4.1) of a final volume of 10 µl was set up without template DNA. Single bacterial colonies were served as templates. These were picked from agar plates and transferred directly to the reaction mix. For products ligated into pGEM®-T vector, plasmid specific SP6 and T7 primers were used. For products ligated into LigAF vector in front of GFP, actin promoter- and GFP-specific primers were used. In case of ligation behind the GFP, GFP- and actin terminator-specific primers were used. In any case, the PCR was run for 35 cycles.

5.2.4.3 High Fidelity PCR

For the amplification of DNA fragments for expression constructs, Platinum® Taq Polymerase High Fidelity with proof reading ability was used. Table 3 contains the pipetting scheme for the reaction. The used PCR program is shown in Table 4. The PCR products were analysed via agarose gel electrophoresis.

Component	Volume [µl]
cDNA(1:20) + Millipore H_2O	15.2
Buffer (10x)	2
$MgSO_4$ (50mM)	0.8
dNTP mix (10 mM)	0.2
Platinum® Taq Polymerase High Fidelity (5 U/µl)	0.2
Forward primer (10µM)	0.8
Reverse primer (10µM)	0.8
Total volume	**20**

Table 3 Pipetting scheme for High Fidelity PCR.

Steps	Temperature	Duration	
Initial denaturation	95°C	3 min	
Denaturation	95°C	30 sec	30-40 cycles
Hybridization	*	30 sec	
Elongation	68°C	**	
Terminal elongation	68°C	**	

Table 4 High Fidelity PCR program.

* Hybridization temperature was depending on the melting temperature of the used primer pairs.

** Elongation time was depending on the length of the amplified PCR fragment. A synthesis rate of the Taq polymerase of 1kb per minute was used to estimate elongation time.

5.2.4.4 Quantitative real-time PCR (qRT-PCR)

Gene expression levels were analysed by qRT-PCR using the QuantiTect Probe RT-PCR Kit and the 7300 real-time PCR system according to the manufacturer's protocols. Both EF-1 alpha and Actin were used for as references gene for determination of gene expression level in this thesis except the ALP treatment experiment, where only EF-1 alpha was used as reference gene. Gene expression levels were calculated relative to a single reference gene or double reference genes based on the standard-curve method (Livak and Schmittgen 2001) or method of geometric averaging of multiple internal control genes (Vandesompele et al. 2002), respectively. Table 5 contains the pipetting scheme for the reaction. The used PCR program is shown in Table 6

Component	Volume [µl]
cDNA(1:20) + Millipore H_2O	7.5
SYBR Green Reaction Mix	12.5
Forward primer (10µM)	2.5
Reverse primer (10µM)	2.5
Total volume	**25**

Table 5 Pipetting scheme for qRT-PCRs.

Steps	Temperature	Duration	
Initial denaturation	95°C	5 min	
Denaturation	95°C	15 sec	
Hybridization	57°C	30 sec	40 cycles
Elongation (detection step)	60°C	35 sec	
Dissociation step			

Table 6 qRT-PCR program.

5.2.5 Electrophoretic separation of DNA samples

DNA samples were separated using horizontal 1-2% agarose gel electrophoresis in 1x TAE buffer. To visualize DNA-bands ethidiumbromide was included into the gels (0.03%). After adding DNA loading buffer to the samples, DNA fragments were separated at 75-100 V, depending on the fragment size. The size of DNA fragments was estimated under UV-illumination using the GeneRulerTM DNA Ladder Mix as size marker.

5.2.6 Extraction of DNA fragments from agarose gel fragments

The desired PCR products were cut out on a UV illumination table and transferred into 1.5 ml reaction tubes. Afterwards, DNA was extracted using the NucleoSpin® Extract II Kit. The same kit was used for direct purification of PCR products. Both were performed according to the manufacturer's protocol. DNA was eluted by adding 20 µl NE buffer to the silica column.

5.2.7 Restriction digestion of DNA

The digestion was performed overnight at 37 °C and subsequently stopped by 20 min incubation at 70 °C. The digested fragments were separated using agarose gel electrophoresis and purified from the gel. The pipetting scheme for the reaction is shown in Table 7.

Component	Volume [µl]
Enzyme (2U / µl)	1
Buffer (10x)	5
BSA	0.5
DNA (3 µg) + Millipore H_2O	43.5
Total volume	**50**

Table 7 Pipetting scheme for digestion of DNA.

5.2.8 Ligation of PCR-products

5.2.8.1 Ligation of PCR products into the pGEM®-T vector

PCR products were ligated into the pGEM®-T vector via TA cloning. The Taq-polymerase generates adenosine (A) overhangs on the synthesized DNA strands. These "sticky ends" are used for the ligation into the vector carrying thymidin (T) overhangs. The pipetting scheme for the reaction is shown in Table 8. Ligations were carried out overnight at 4 °C and subsequently stopped by 20 min incubation at 70 °C.

Component	Volume [µl]
pGEM®-T (50 ng / µl)	0.5
Buffer (2x)	2.5
T4-Ligase (3 U / µl)	0.5
DNA (4-70 µg) + Millipore H_2O	1.5
Total volume	**5**

Table 8 Pipetting scheme for ligation of DNA fragments into the pGEM® -T vector.

5.2.8.1 Ligation of PCR products into LigAF vector

For generation of an expression construct PCR products were ligated into the LigAF vector via restriction sites. The pipetting scheme for the reaction is shown in Table 9. Ligations were carried out overnight at 4 °C and subsequently stopped by 20 min incubation at 70 °C.

Component	Volume [µl]
LiAF vector (100ng) + Millipore H_2O	8.5
Buffer (10x)	2
T4-Ligase (3 U / µl)	1
DNA (100 µg) + Millipore H_2O	8.5
Total volume	**20**

Table 9 Pipetting scheme for the ligation of DNA fragments into the LigAF vector.

5.2.9 Transformation of *E. coli* DH5α

50 µl of the *E. coli* DH5α E. coli cell suspension containing 1-15 µl ligation sample were electroporated with the Gene Pulser II using the following conditions: 1.8 kV, 25 µF. Immediately after electroporation, the cells were rinsed with 500 µl SOC medium and incubated at 37 °C and 220 rpm for 1 h. 100 to 1000 µl were plated on ampicillin-containing LB-agar. Only cells containing the plasmid providing resistance against the antibiotics were able to grow overnight at 37 °C.

5.2.10 Preparation of plasmids

Mini-preparations to isolate plasmids from clones propagated in LB liquid cultures were performed using the NucleoSpin® Plasmid QuickPure Kit according to the manufacturer's instructions. Followed by a midi-preparation of plasmids from clones propagated in LB liquid cultures was performed using the Plasmid Midi Kit according to the manufacturer's instructions. Afterwards an additional precipitation step was performed by the addition of 1/10 volume 3 M Sodium Acetate and 2 volumes of ethanol. The tubes were inverted and centrifuged for 15 min at 20000g at 4 °C. The pellet was washed in 300 µl of 75% ethanol, the centrifugation step was repeated and the pellet was dried on air and dissolved in 50 µl Millipore H2O for 1 h at 37 °C for subsequent injection of expression constructs into Hydra embryos.

5.2.11 Sanger DNA sequencing

DNA sequencing was carried out using the SequiTherm EXCEL II DNA Sequencing Kit-LC (Epicentre Technologies). This technique is based on the Sanger dideoximediated chain-termination method

(Sanger et al. 1977). Vector specific primers, IRD-800 or IRD-700 labeled at the 5' end, were used to generate sequence amplicons. Reactions were set up according to the manufacturer's protocol. Sequencing reaction products were separated and detected in a LI-COR Gene ReadIR 4200 automated sequencing machine and analysed with the manufacturer's software. Table 10 contains the pipetting scheme for the reaction.

Component	Volume [µl]
DNA (150ng) + Millipore H_2O	4
Buffer (3.5 x)	3.6
SequiTherm EXCEL II DNA Polymerase (5 U / µl)	0.4
IRO-labeled primer (5 µM)	0.5
Total volume	**8.5**

Table 10 Pipetting scheme for the LI-COR sequencing reaction.

A total of 2 µl of this mixture were added to 1 µl of nucleotide mix containing ddATP, ddCTP, ddGTP or ddTTP, respectively. The samples were subjected to the PCR program shown in Table 11. The reaction was stopped by the addition of 3 µl loading buffer. Prior to loading 0.7 µl of the samples on a 41 cm sequencing gel in the 4300 DNA Analyser, they were denaturated for 10 min at 95 °C. The sequencing was analyzed using the e-Seq 3.0 program.

Steps	Temperature	Duration	
Initial denaturation	95°C	5 min	
Denaturation	95°C	30 sec	
Hybridization	52°C	15 sec	30 cycles
Elongation (detection step)	70°C	1 min	

Table 11 PCR program for the LI-COR sequencing reaction.

DNA and protein sequences were analyzed using DNASIS v2.6 program together with BLASTN, BLASTP and BLASTX algorithms were used, which are a part of BLAST (Basic Local Alignment Search Tool) at the National Center for Biotechnology Information (NCBI) home page.

5.3 ILP screening workflow

5.3.1 Uncovering ILP cysteine pattern

Amino acid sequences of 16 ILPs of 11 model animals from both vertebrates and invertebrates were used for PRATT online programme using following parameters: MIN PERCENTATGE,100.0; PATTERN POSITION, off; MAX PATTERN LENGTH, 80; MAX NUM PATTERN SYMBOLS, 50; MAX NUM WILDCARD, 5; MAX NUM FLEX SPACES, 2; MAX FLEXIBILITY, 2; MAX FLEX PRODUCT, 10; PATTERN SYMBOL FILE, off; NUM PATTERN SYMBOLS, 20; PATTERN SCORING, info; PATTERN GRAPH, seq; SEARCH GREEDINESS, 3; PATTERN REFINEMENT, on; GEN AMBIG SYMBOLS, on; PATTERN FORMAT, on; MAX NUM PATTERNS, 50; MAX NUM ALIGNMENTS, 50; PRINT

PATTERNS, on; PRINT RATIO, 10; PRINT VERTICALLY, off. The first three best pattern were used in conjunction with each other in generating the initial ILPs amino acids pattern.

5.3.2 Searching for ILPs using ILP cysteine pattern

ILP cysteine patterns was used for PATTINPROT by following settings: similarity level, No Mismatch = 100% similarity; Extra residues at N and C-terminal extremities of pattern: 10; database: Swiss-Prot (UniProtKB / Swiss-Prot). When working with database of cadidate animals, Priority cysteine pattern was used for PRABI by following settings: Search pattern with similarity level, No Mismatch = 100% similarity; Extra residues at N and C-terminal extremities of pattern: 10; Extraction with removal identical sequences in created database and generate a pool of ILP candidates. ILP candidates with more than 400 amino acids were discard.

5.3.3 Signal peptide identification

ILP candidates was used for signal peptide detection by SignalP 4.1 server using following settings: Organism group, Eukaryotes; D-cutoff values, Sensitive; Graphics output, PNG; Output format, Standard; Method: Input sequence may include TM region.

5.3.4 Prediction of ILP secondary structure

Amino acid sequences of ILP candidates was used for PHYRE2 for secondary structure prediction using normal mode.

5.3.5 Convertase cleavage site checking

ProP 1.0 online tool was used to detect the cleavage sites of ILPs (Duckert et al. 2004) by following settings: Generate graphic; include signal peptide prediction.

5.4 Starvation challenge on INSR knockdown *Hydra* strains

INSR knockdown transgenic *Hydra* was divided into two groups: one was fed and washed 3-4 times a week for 10 days, while the other group was not fed for 10 days, however, got washed at the same time when the first group *Hydra* got washed. Same setup was applied to the control strain corresponding to INSR knockdown transgenic *Hydra*. All experimental groups were kept at 18 °C. Finally, the gene expression profiles of *Hydra* from above four conditions were analysed by qRT-PCR.

5.5 *Wnt* signalling interfering

5.5.1 Alsterpaullone treatment on INSR knockdown *Hydra* strains

All animals was not fed for 2 days before the experiment. INSR knockdown transgenic *Hydra* was divided into two groups: one group was exposed to 5 µmol/l alsterpaullone in 0.025% DMSO in hydra medium, while the other control group was exposed to in 0.025% DMSO in hydra medium (Broun et al.

2005). Same setup was applied to the control strain corresponding to INSR knockdown transgenic *Hydra*. All experimental groups were kept at 18 °C in dark. Samples were taken at 12 hours and 24 hours. The gene expression profiles of *Hydra* from above four conditions were analysed by qRT-PCR.

5.5.2 Constantly active β-catenin

Both β-catenin B4 and B9 strains and their corresponding control strains were kept at 18 °C and fed 3-4 times a week. The gene expression profiles of above four *Hydra* strains were analysed by qRT-PCR.

5.5 Neuron populations enrichment

5.5.1 Dissociation of Hydra

1ml Pronase E solution added in to 100 *Hydra vulgaris AEP* polyps on a petri dish. It was shaken at 200 rpm at room temperature for 1 hour or until big tissue particles could not be seen. Pipette was used for mixing the solution 4-5 times during the shaking. 3 ml dissociation solution was added into the sample of total animal cell suspension, which was used for neuron separation immediately.

5.5.2 Neuron separation

Neuron population was enriched by three times of centrifugation and details of the process are indicated in Figure 5-1. Method is developed together with Andrea Murillo.

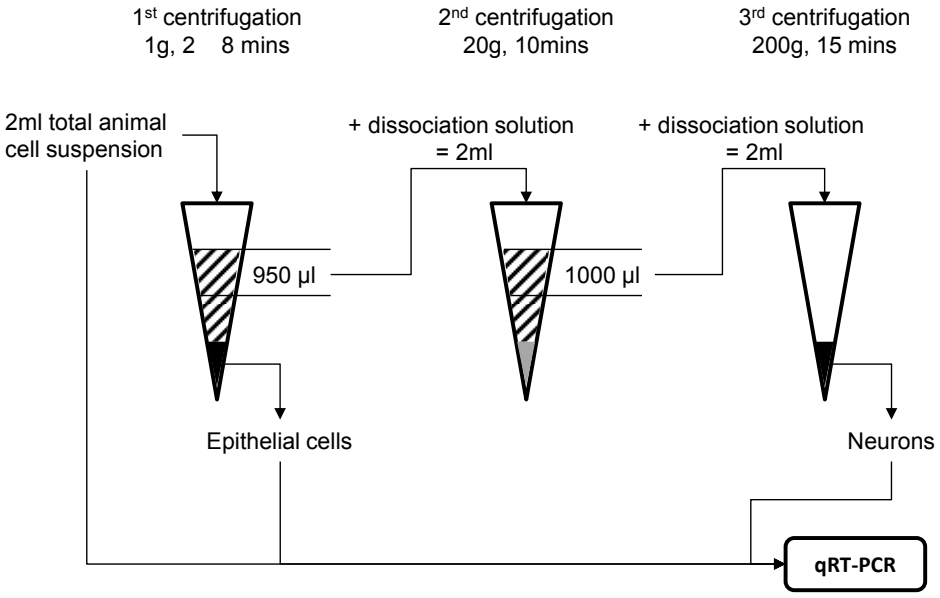

Figure 5-1 Neuron population enrichment

5.6 5 Bromo-deoxy-uridine (BrdU) labelling and detection

BrdU is a thymidin analogues base, which is incorporated into the DNA instead of thymidin in the Sphase of the cell cycle, therefore, was used to determine the proliferation activity of cell types. The protocol has been established according to both (Holstein et al. 1991) and (David 1973).

Day 1

30 polyps of transgenic and control *Hydra* were exposed to 5 mM BrdU in Hydra medium for 3 h after the solution initially has been injected into the gastric cavity. Afterwards, every 2 polyps were transferred into a tube with 150 µl maceration solution and incubate in water bath at 32 °C for 30 min. The cells were dissociated by flipping the tube and fixed by the addition of an equal volume of an 8% paraformaldehyde solution. Two spots of 100 µl suspension were placed onto gelatine-covered glass-slides with a droplet of a 1% Tween20 solution. Slides were air-dried overnight.

Day 2

The slides with the dried cell suspension were rinsed three times for 10 min with PBS and for 1 h incubated in 2 N HCl at 37 °C. After three times washing for 10 min in PBT the preparations were incubated with 100 µl of monoclonal anti-BrdU-mouse-Ig (1:100 diluted in PBT/1% BSA) at 8 °C in a humid chamber. In order to ensure an even distribution of the antibody parafilm was used to cover the slides.

Day 3

The slides were washed three times for 10 min in PBT (0.5% Tween & 0.5% BSA) and 2 h incubated with 100 µl of anti-mouse-IgG-AP (1:5000 diluted in PBT/1% BSA) under parafilm at RT in a humid chamber. The preparations were again washed three times for 10 min in PBT (0.5% Tween & 0.5% BSA). Afterwards, they were equilibrated three times for 5 with NTMT buffer and incubated in 300 µl NBT/BCIP (1:200 diluted in NTM) until the desired staining intensity was reached (15-25 mins). The reaction was stopped with three times washing for 10 min with Millipore H2O. The slides were embedded in Glycerol/PBS (1:9) for analysis with the microscope.

5.7 *In situ* hybridization

5.7.1 Generation of a labelled RNA probe

The transcript fragments were amplified from cDNA, cloned into the pGEM®-T vector, propagated in bacteria and sequenced afterwards. Next, a PCR was performed with vector-specific primers (M13_F/M13_R). A total of 0.5 µg purified PCR product was used as template for the DIG RNA Labeling Kit (SP6/T7) according to the manufacturer's protocol. The antisense probe was used to detect the transcript. The sense probe was used as negative control.

5.7.2 Whole mount *in situ* hybridization

The protocol was based on previous work (Grens et al. 1999).

Day 1

Polyps were starved for at least two days prior to relaxation in freshly prepared urethane relaxing solution for 2-3 min. The solution was replaced by a 4 % paraformaldehyde solution prior to the overnight fixation at 8 °C.

Day 2

The following steps were performed at room temperature. The animals were washed three times for 10 min with Millipore H2O and subsequently treated in methanol until they were completely decolorized. The samples were rehydrated with decreasing amounts of ethanol diluted with PBT for 5 min per step. Afterwards, the samples were washed three times with PBT for 10 min followed by a treatment with proteinase K in PBT (end concentration 10 µg/ml) for 20 min. The reaction was stopped by the adding glycine working solution and the samples were incubated for 10 min in new glycine working solution. The samples were washed three times with PBT for 10 min and afterwards treated twice with triethanolamine for 10 min. The triethanolamine was exchanged and 2.5 µl/ml acetic anhydride were added. After 5 min additional 2.5 µl/ml acetic anhydride were added. After three washing steps with PBT for 5 min the animals were re-fixed with 4 % paraformaldehyde in PBT overnight at 8 °C.

Day 3

The paraformaldehyde was removed by washing the samples three times with PBT for 10 mins. Afterwards the animals were washed twice in 2x SSC for 10 min followed by a heating step in 2x SSC for 20 min at 70 °C. The following steps were performed at hybridization temperature of 57 °C. All solutions were pre-warmed prior to use. The animals were washed with 50% hybridization solution/50% 2x SSC for 10 min, followed by a washing step with 100% hybridization solution for 10 min. Afterwards the samples were pre-hybridized for 2 h in hybridization solution containing 20µl/ml tRNA. 2 µl of 1:15 diluted probe was denatured in 50 µl solution containing 50% Formamide/25% 20x SSC/25% Millipore H2O for 10 min at 70 °C. The hybridization solution on the samples was replaced with new hybridization solution with tRNA, and the probe was added. The hybridization was performed for 16-36 h. Sense and antisense probe were always used in parallel.

Day 4

The probe was removed by the following washing steps of 10 min each at 57 °C: 100% hybridization solution, 75% hybridization solution/25% 2x SSC, 50% hybridization solution/50% 2x SSC and 25% hybridization solution/75% 2x SSC. Afterwards, the animals were incubated twice in 2x SSC/0.1% CHAPS for 30 min. The following steps were performed at room temperature. The samples were washed twice with MAB-T for 10 min followed by a 1 h treatment in MAB-B. The samples were incubated in blocking solution for 2 h at 8 °C. Binding of the anti-DIG-alkaline phosphatase linked Fab fragments (1:2000 diluted in blocking solution) was performed overnight at 8 °C.

Day 5

The samples were washed eight times for 15 min with MAB-T and then rinsed with NTMT for 5 min and treated with NTMT/1 mM Levamisole for 5 min. The solution was replaced by the staining solution containing 2% NBT/BCIP in NTMT. The samples were incubated in the dark until a clear staining was detectable. The reaction was stopped by washing three times for 10 min with Millipore H2O. The animals were dehydrated with increasing amounts of ethanol prior to embedding in Euparal.

5.8 Phylogenetic analysis

Phylogenetic analysis of ILPs was based on the amino acid sequences of ILP without signal peptide domain. The alignment of these sequences was achieved by Clustal Omega (Sievers et al. 2011) with default settings. The result file was saved as ".clustal" and used for BioEdit in order to align the cysteine of ILPs, then saved as a ".phy" file. After converting the ".phy" result file into ".meg" file, Mega 6 is used to find the best model for visualizing a phylogenetic tree by Maximum likelihood method with 1000 bootstraps (Tamura et al. 2013).

5.9 Anti-HyILP-A and anti-HyILP-B antibodies design

Amino acids sequences from A domain of HyILP-A and HyILP-B were sent to GenScript for antigen design and synthesis, as well as generating Antibodies for HyILP-A and HyILP-B. Sequence of "SIFSGKLDNADEEC" was selected as HyILP-A antigen peptide and sequence of "PDVYPTDINVHDEC" was selected as HyILP-B antigen through analysis of several sequence properties such as antigenicity, hydrophilicity and disordered region (Figure 5-2).

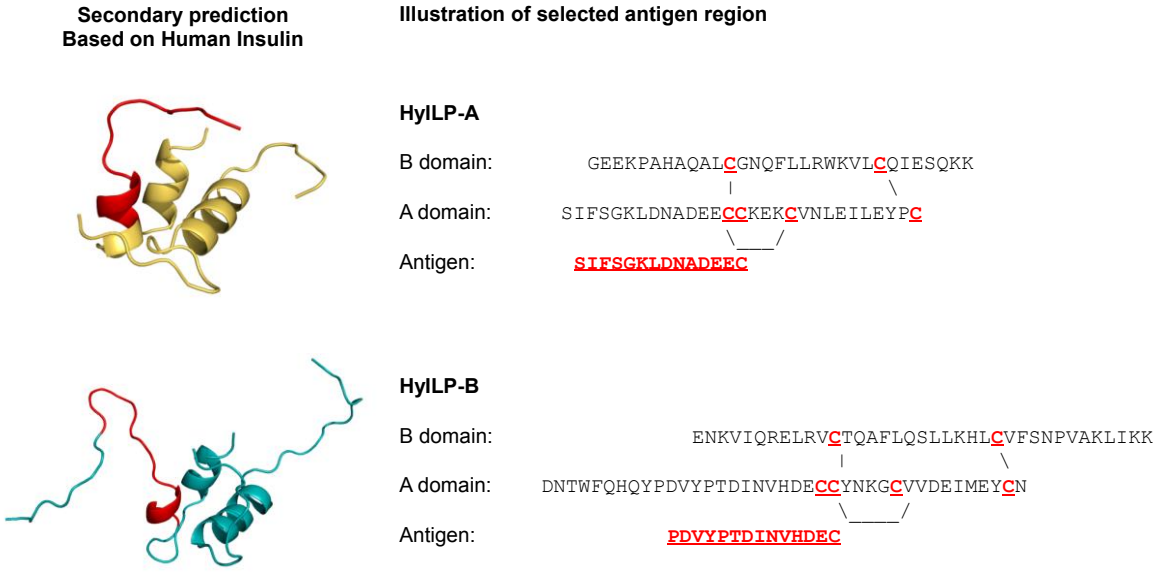

Figure 5-2 Design Antibody targeting ILPA and ILPB

3D protein modelling was performed for *Hydra* ILPs using human pro-insulin as template model with the help of Jan Taubenheim. Red region indicate the region selected as antigen.

5.10 Generation of transgenic *Hydra vulgaris (AEP)*

5.10.1 Construct for overexpression of HyILP-B fused with GFP

To achieve an overexpression of *hyilp-B* fused with *gfp*, a construct containing the coding region of *hyilp-B* cloned into ConsJL-13 expression vector in front of *gfp* was generated (for sequence of complete HyILP-B-GFP overexpression vector see Appendix Figure 8-6). The *hyilp-B* sequence is flanked by a *SbfI* and *PvuI* cutting site for site-directed mutagenesis. The *hyilp-B* coding part was amplified from cDNA with primers containing the *SbfI* and *PvuI* cutting site, digested with the corresponding enzymes and substituted the Dlp1 from ConsJL13 vector (Figure 5-3) prior to

electroporation into *E. coli*. Afterwards, the uptake of the plasmid by bacteria was checked by colony check PCR. A selected clone was propagated in an LB liquid culture and submitted to plasmid mini-preparation. Subsequently, the correctness of the construct was proven by sequencing. Prior to the injection into Hydra embryos, a plasmid midi-preparation was performed. Embry with both GFP and dsRED signals was selected and treated as an initial founder. By selecting for both GFP and dsRED-expression using an Olympus SZX16 stereomicroscope, mass cultures of both, polyps with no transgenic cells (HyILP-B-GFP control) and polyps with full endodermal and ectodermal expression of GFP (HyILP-B-GFP overexpression), were generated.

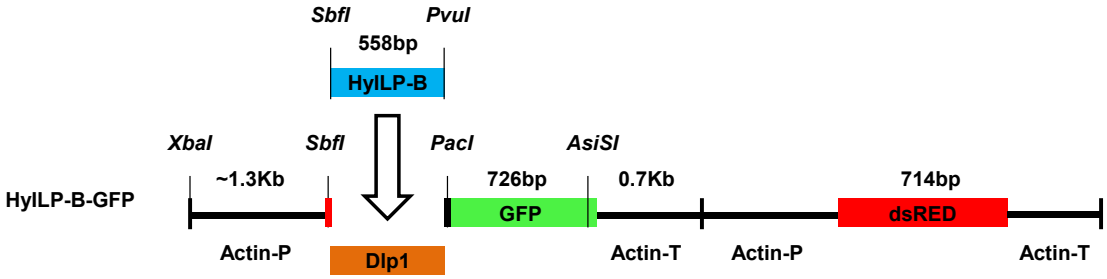

Figure 5-3 Construction of HyILP-B-GFP construct.

5.10.2 Construct for overexpression of HyILP-B fused with cMyc

To achieve an overexpression of *hyilp-B* fused with *cMyc*, a construct containing the coding region of *hyilp-B* fused with *cMyc* cloned into ConsJL-13 expression vector by substituting the Dlp1-GFP was generated (for sequence of complete HyILP-B-cMyc overexpression vector see Appendix Figure 8-7). The *hyilp-B-cMyc* sequence is flanked by a *SbfI* and *AsiSI* cutting site for site-directed mutagenesis. The *hyilp-B* coding part was amplified from cDNA with primers containing the *SbfI* and *cMyc-AsiSI* cutting site, digested with the corresponding enzymes and substituted the *Dlp1-GFP* from ConsJL13 vector (Figure 5-4) prior to electroporation into *E. coli*. Afterwards, the uptake of the plasmid by bacteria was checked by colony check PCR. A selected clone was propagated in an LB liquid culture and submitted to plasmid mini-preparation. Subsequently, the correctness of the construct was proven by sequencing. Prior to the injection into Hydra embryos, a plasmid midi-preparation was performed. Embry with dsRED signal was selected and treated as an initial founder. By selecting for dsRED-expression using an Olympus SZX16 stereomicroscope, mass cultures of both, polyps with no transgenic cells (HyILP-B-cMyc control) and polyps with full ectodermal expression of dsRED (HyILP-B-cMyc overexpression), were generated.

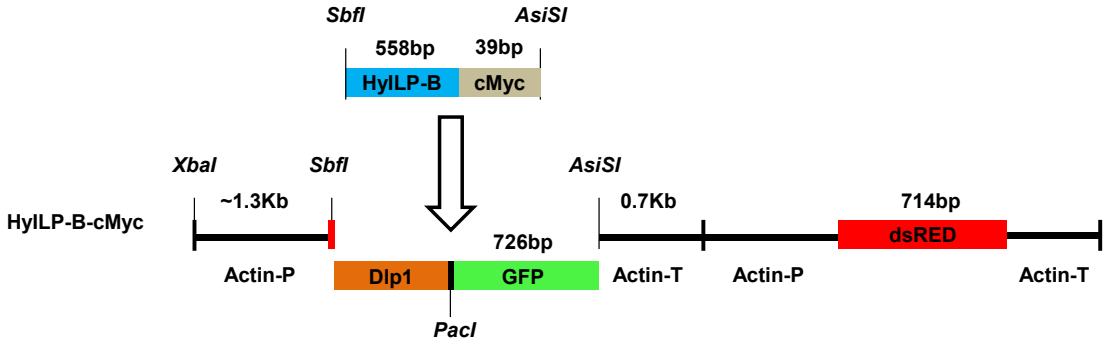

Figure 5-4 Construction of HylLP-B-cMyc construct.

5.10.3 Construct for knockdown of HylLP-B

For stable knockdown of *hyilp-B*, a hairpin construct containing a sense and antisense sequence from *hyilp-B*, separated by a linker sequence, cloned into LigAF expression vector behind GFP was generated (for sequence of complete HylLP-B-Hairpin see Appendix Figure 8-8). The *hyilp-B* hairpin is flanked by an *AsiSI* and *EcoRI* cutting site for site-directed mutagenesis. After transcription this sequence will form a hairpin structure which binds to the *HylLP-B* transcript, leading to degradation of the hybrid by the RNAi machinery. The 433 bp HylLP-B sense sequence from a highly variable part of the gene was amplified from cDNA including a 117 bp linker using primers containing the *EcoRI* and *kpnI* cutting site. The corresponding antisense sequence was amplified using primers containing the *kpnI* and *AsiSI* cutting site. Afterwards, both products were digested with *kpnI* and ligated. The ligation product was sub-cloned into pGEM®-T vector, digested with *AsiSI* and *EcoRI* and ligated into LigAF vector (Figure 5-5) prior to electroporation into E. coli. Afterwards, the uptake of the plasmid by bacteria was checked by colony check PCR. A selected clone was propagated in an LB liquid culture and submitted to plasmid mini-preparation. Subsequently, the correctness of the construct was proven by sequencing. Prior to the injection into Hydra embryos, a plasmid midi-preparation was performed.

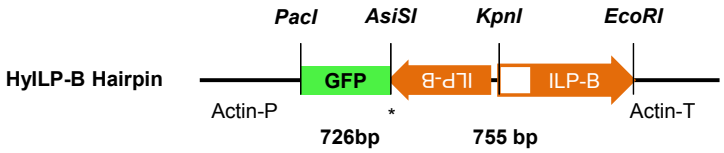

Figure 5-5 Construction of HylLP-B Hairpin construct

5.10.4 Embryo microinjection

Transgenic H. vulgaris strain AEP were generated at the University of Kiel Transgenic Hydra Facility (http://www.unikiel.de/zoologie/bosch/transgenic.htm) as described by Wittlieb et al (Wittlieb et al., 2006). A plasmid concentration of 1 µg/µl was used and 1% Rhodamine B Isothiocyanate-Dextran R9379 were added as tracer. The solution was injected into Hydra embryos within the 2 to 4 cell developmental stage.

5.11 Immunohistochemical staining of proteins in *Hydra*

Immunohistochemistry of transgenic polyps was performed following standard procedures (Engel et al. 2002). Animals were relaxed in freshly prepared urethane relaxing solution for 1-2 min and fixed by the addition of 4% paraformaldehyde in Hydra medium for 30 min. Afterwards, animals were washed four times for 15 min with PBT followed by a washing step with PBS/0.5% TritonX100 for 30 min. Blocking was performed with PBT / 1% BSA for overnight at 4 °C. The incubation with the first antibody was performed overnight at 4 °C. The samples were washed four times with PBT / 1% BSA for 15 min. Then the samples were treated with the fluorescence-labelled secondary antibody in PBT/1% BSA for 2 h. The samples were washed four times with PBS/0.5% Tween20 / 1% BSA for 15 min. Subsequently, the animals were treated with phalloidin (1:1000 in PBS / 1% BSA / 0.5% TritonX100 / 0.5% Tween20) for 1 h, followed by four times washing with PBS / 1% BSA / 0.5% Tween20 for 15 min. Subsequently, the

samples were treated with TO-PRO (1:1000 diluted in PBS / 1% BSA / 0.5% Tween20) and directly embedded in Mowiol and stored at 4 °C prior to microscopically analysis using the confocal laser scanning microscope. The antibodies were listed in Table 12.

Proteins	1st Antibodies	2nd Antibodies
GFP	Rabbit anti-GFP (1:500)	anti-rabbit_AF488 (1:500)
cMyc	Mouse-anti-MycTag #05-724 (1:500)	Donkey-anti-mouse_AF488 (1:500)
HyILP-A	Rabbit-anti-HyILPA (1:3000)	anti-rabbit_AF488 (1:500)
HyILP-B	Rabbit-anti-HyILPB (1:1000)	anti-rabbit_AF488 (1:500)

Table 12 proteins detection by antibodies in Immunohistochemical staining

5.12 Population growth rate analysis

All animals were cultured according to Method 5.1.2, however, every polyp was cultured separately. See Results 2.4.2 and 2.4.4 for population growth rate analysis.

5.13 Western Blot

5.13.1 Preparation of samples

Calculating 20 µg protein based on the OD600, a certain volume of the bacterial culture medium was taken. After centrifugation, the pellet was resuspended by adding 16 µl ddH2O and 4 µl 5x SDS-PAGE loading buffer. Then the sample was boiled for 5 min and centrifuged at max speed for 5 min. Finally, 10µl sample was loaded on the SDS-Gel.

5.13.2 SDS-PAGE

The glass plates were cleaned and assembled. 10% separating-gels were made by mixing the following reagents as shown in

Component	Volume
40% Acrylamid/Bisacrylamid 29:1	2.5 ml
3x Gel Buffer	3.3 ml
Glycerol	1 ml
Millipore water	3.2 ml
25% APS	24 µl
TEMED	5.3 µl
Final volume	**10 ml**

Table 13. 25% APS and TEMED were added just before pouring the gel

Component	Volume
40% Acrylamid/Bisacrylamid 29:1	2.5 ml
3x Gel Buffer	3.3 ml
Glycerol	1 ml
Millipore water	3.2 ml
25% APS	24 µl

TEMED	5.3 µl
Final volume	**10 ml**

Table 13 Pipetting scheme for two 15% separating-gels

Isopropanol was layered on the top of the gels to prevent dehydration and allow polymerizing. After 30 min-1 h, isopropanol was removed by washing with Millipore water and the glass plates were dried by filter paper. Then stacking-gel was overlaid on the top with inserting comb. Table 14 contains the pipetting scheme for two 5% stacking-gels. 25% APS and TEMED were added just before pouring the gel.

Component	**Volume**
40% Acrylamid/Bisacrylamid 29:1	0.6 ml
3x Gel Buffer	1.7 ml
Glycerol	-
Millipore water	2.7 ml
25% APS	17 µl
TEMED	3.8 µl
Final volume	3.38 ml

Table 14 Pipetting scheme for two 4% stacking-gels

30 min later, the combs were removed carefully, and the glass plates were assembled into the device filled with 1x SDS-PAGE running buffer. After loading the samples, 75V was used to run the stacking-gel, and then increased the voltage to 150V to run the separating-gels until the marker reached the bottom. The size of protein bands was estimated using the PageRuler™ Plus Prestained Protein Ladder (Fermentas).

5.13.3 Coomassie brilliant blue staining

The SDS-Gels were transferred into Coomassie brilliant blue staining solution and shook overnight at room temperature. Afterwards the SDS-Gels were destained by Coomassie brilliant blue destaining solution until weakened background.

5.13.4 Transfer membranes

After SDS-PAGE, the SDS-Gels were soaked in Transfer buffer for 15 min. PVDF membranes (Roth) were activated in methanol for 1 min and then incubated in Transfer buffer for 5 min as 8x Waterman papers. The transfer sandwich was assembled as following: 4x Waterman papers, PVDF membrane, SDS-Gel and another 4x Waterman papers at the top. Any air bubble was rolled out after each layer. The transblot was run using 2 mA / cm^2 for 1-1.5 h.

5.13.5 Western blot

The membranes were taken out and washed with TBS-T for 5 min following with incubation in 1% BSA / 4% milk / TBT-T for 4 min at room temperature. Adding first Antibody to replaced 1% BSA/ 4% milk / TBS-T, the membranes was incubated overnight at 4°C with rotation. Afterwards the membranes were washed 3 times with TBS-T for 10 min. New 1% BSA/ 4% milk / TBS-T with second antibody was used to incubate the membranes for 2 h at room temperature with rotation. To thoroughly wash away the Antibody, the membranes incubated with Goat-anti-Rabbit*HRP were washed three times with TBS-T for 10 min at RT. Then the membranes were stained with TMB solution; the membrane incubated with Sheep-anti-Mouse*AP were washed three times with NTMT for 5 min. Afterwards the solution was replaced by the staining solution containing 0.5 % NBT/BCIP in NTMT. Both type of membranes were kept in dark until a clear staining was detectable. The reaction was stopped by washing two times with Millipore water for 10 min. Finally, the membranes were dried by filter paper. The antibodies were listed in Table 15.

Protein	**1st Antibodies**
GFP	Rabbit anti-GFP (1:500)
HylLP-B	Rabbit-anti-ILPB (1:800)
HylLP-B (Blocked by A)	Rabbit-anti-ILPB (1:800) + HylLPA Peptide (1:400) 1:40
HylLP-B (Blocked by B)	Rabbit-anti-ILPB (1:800) + HylLPB Peptide (1:500) 1:40

Protein	**2nd Antibodies**
GFP	Sheep-anti-Mouse-AP 1:3,000
HylLP-B	Goat-anti-Rabbit*HRP (JacksonIR) 1:10,000
HylLP-B (Blocked by A)	Goat-anti-Rabbit*HRP (JacksonIR) 1:10,000
HylLP-B (Blocked by B)	Goat-anti-Rabbit*HRP (JacksonIR) 1:10,000

Table 15 proteins detection by antibodies in *western blot*

5.14 Imaging techniques

In vivo observations were made and documented using Olympus SZX16 and Olympus DP71 digital camera. Laser-scanning confocal data were acquired using Leica CLSM TCS SP/UV and Leica DC300F digital camera. Light microscopic analyses were performed using Zeiss Axioskop 2 and Zeiss AxioCam digital camera.

6. References

Anctil, M. (2009). "Chemical transmission in the sea anemone Nematostella vectensis: A genomic perspective." Comp Biochem Physiol Part D Genomics Proteomics **4**(4): 268-289.

Augustin, R., et al. (2009). "Activity of the novel peptide arminin against multiresistant human pathogens shows the considerable potential of phylogenetically ancient organisms as drug sources." Antimicrob Agents Chemother **53**(12): 5245-5250.

Bai, H., et al. (2012). "Drosophila insulin-like peptide-6 (dilp6) expression from fat body extends lifespan and represses secretion of Drosophila insulin-like peptide-2 from the brain." Aging Cell **11**(6): 978-985.

Bairoch, A. and R. Apweiler (1997). "The SWISS-PROT protein sequence data bank and its supplement TrEMBL." Nucleic Acids Res **25**(1): 31-36.

Bathgate, R. A. D., et al. (2013). "Relaxin Family Peptides and Their Receptors." Physiological Reviews **93**(1): 405-480.

Bayne, M. L., et al. (1989). "The C region of human insulin-like growth factor (IGF) I is required for high affinity binding to the type 1 IGF receptor." J Biol Chem **264**(19): 11004-11008.

Bode, H. R. (1992). "Continuous conversion of neuron phenotype in hydra." Trends Genet **8**(8): 279-284.

Bode, H. R. (2009). "Axial patterning in hydra." Cold Spring Harb Perspect Biol **1**(1): a000463.

Boehm, A. M., et al. (2012). "FoxO is a critical regulator of stem cell maintenance in immortal Hydra." Proc Natl Acad Sci U S A **109**(48): 19697-19702.

Bosch, T. C. (2007). "Symmetry breaking in stem cells of the basal metazoan Hydra." Prog Mol Subcell Biol **45**: 61-78.

Bosch, T. C. (2009). "Hydra and the evolution of stem cells." Bioessays **31**(4): 478-486.

Bosch, T. C. (2013). "Cnidarian-microbe interactions and the origin of innate immunity in metazoans." Annu Rev Microbiol **67**: 499-518.

Bosch, T. C. (2014). "Rethinking the role of immunity: lessons from Hydra." Trends Immunol **35**(10): 495-502.

Bosch, T. C., et al. (2010). "The Hydra polyp: nothing but an active stem cell community." Dev Growth Differ **52**(1): 15-25.

Bosch, T. C., et al. (2009). "Uncovering the evolutionary history of innate immunity: the simple metazoan Hydra uses epithelial cells for host defence." Dev Comp Immunol **33**(4): 559-569.

Bosch, T. C. G. (2009). "Hydra and the evolution of stem cells." Bioessays **31**(4): 478-486.

Bosch, T. C. G., et al. (2010). "The Hydra polyp: Nothing but an active stem cell community." Development Growth & Differentiation **52**(1): 15-25.

Bosch, T. C. G. and C. N. David (1984). "Growth-Regulation in Hydra - Relationship between Epithelial-Cell Cycle Length and Growth-Rate." Dev Biol **104**(1): 161-171.

Bosch, T. C. G. and C. N. David (1986). "Male and Female Stem-Cells and Sex Reversal in Hydra Polyps." Proc Natl Acad Sci U S A **83**(24): 9478-9482.

Bosch, T. C. G. and C. N. David (1990). "Cloned Interstitial Stem-Cells Grow as Contiguous Patches in Hydra." Dev Biol **138**(2): 513-515.

Bottger, A., et al. (2006). "Genetic screen for signal peptides in Hydra reveals novel secreted proteins and evidence for non-classical protein secretion." Eur J Cell Biol **85**(9-10): 1107-1117.

Brogiolo, W., et al. (2001). "An evolutionarily conserved function of the Drosophila insulin receptor and insulin-like peptides in growth control." Curr Biol **11**(4): 213-221.

Broun, M., et al. (2005). "Formation of the head organizer in hydra involves the canonical Wnt pathway." Development **132**(12): 2907-2916.

Calnan, D. R. and A. Brunet (2008). "The FoxO code." Oncogene **27**(16): 2276-2288.

Campbell, R. D. (1967). "Tissue dynamics of steady state growth in Hydra littoralis. II. Patterns of tissue movement." J Morphol **121**(1): 19-28.

Campbell, R. D. (1987). "Organization of the Nematocyst Battery in the Tentacle of Hydra - Arrangement of the Complex Anchoring Junctions between Nematocytes, Epithelial-Cells, and Basement-Membrane." Cell Tissue Res **249**(3): 647-655.

Chapman, J. A., et al. (2010). "The dynamic genome of Hydra." Nature **464**(7288): 592-596.

Chen, Z., et al. (2013). "Two insulin-like peptides antagonistically regulate aversive olfactory learning in C. elegans." Neuron **77**(3): 572-585.

Claeys, I., et al. (2002). "Insulin-related peptides and their conserved signal transduction pathway." Peptides **23**(4): 807-816.

Clemmons, D. R., et al. (1998). "Modifications of insulin-like growth factor binding proteins and their role in controlling IGF actions." Endocrine Journal **45**: S1-S8.

Cohen, E. and A. Dillin (2008). "The insulin paradox: aging, proteotoxicity and neurodegeneration." Nat Rev Neurosci **9**(10): 759-767.

Collins, A. G., et al. (2006). "Medusozoan phylogeny and character evolution clarified by new large and small subunit rDNA data and an assessment of the utility of phylogenetic mixture models." Syst Biol **55**(1): 97-115.

Colombani, J., et al. (2012). "Secreted peptide Dilp8 coordinates Drosophila tissue growth with developmental timing." Science **336**(6081): 582-585.

Combet, C., et al. (2000). "NPS@: Network Protein Sequence Analysis." Trends in Biochemical Sciences **25**(3): 147-150.

David, C. N. (1973). "Quantitative Method for Maceration of Hydra Tissue." Wilhelm Roux Archiv Fur Entwicklungsmechanik Der Organismen **171**(4): 259-268.

David, C. N. (2012). "Interstitial stem cells in Hydra: multipotency and decision-making." Int J Dev Biol **56**(6-8): 489-497.

David, C. N. and S. Murphy (1977). "Characterization of interstitial stem cells in hydra by cloning." Dev Biol **58**(2): 372-383.

Davis, L. E., et al. (1968). "Histological and ultrastructural study of the muscular and nervous systems in Hydra. II. Nervous system." J Exp Zool **167**(3): 295-331.

Domazet-Loso, T., et al. (2014). "Naturally occurring tumours in the basal metazoan Hydra." Nat Commun **5**: 4222.

Duckert, P., et al. (2004). "Prediction of proprotein convertase cleavage sites." Protein Eng Des Sel **17**(1): 107-112.

Edgar, B. A. (2006). "How flies get their size: genetics meets physiology." Nature Reviews Genetics **7**(12): 907-916.

Engel, U., et al. (2002). "Nowa, a novel protein with minicollagen cys-rich domains, is involved in nematocyst formation in Hydra (vol 115, pg 3923, 2002)." J Cell Sci **115**(23): 4719-4719.

Fernandez, A. M. and I. Torres-Aleman (2012). "The many faces of insulin-like peptide signalling in the brain." Nat Rev Neurosci **13**(4): 225-239.

Fernandez, R., et al. (1995). "The Drosophila insulin receptor homolog: a gene essential for embryonic development encodes two receptor isoforms with different signaling potential." EMBO J **14**(14): 3373-3384.

Fielenbach, N. and A. Antebi (2008). "C. elegans dauer formation and the molecular basis of plasticity." Genes Dev **22**(16): 2149-2165.

Franzenburg, S., et al. (2012). "MyD88-deficient Hydra reveal an ancient function of TLR signaling in sensing bacterial colonizers." Proc Natl Acad Sci U S A **109**(47): 19374-19379.

Franzenburg, S., et al. (2013). "Distinct antimicrobial peptide expression determines host species-specific bacterial associations." Proc Natl Acad Sci U S A **110**(39): E3730-3738.

Fraune, S. and T. C. Bosch (2007). "Long-term maintenance of species-specific bacterial microbiota in the basal metazoan Hydra." Proc Natl Acad Sci U S A **104**(32): 13146-13151.

Fujisawa, T. (2008). "Hydra peptide project 1993-2007." Dev Growth Differ **50 Suppl 1**: S257-268.

Fujisawa, T. and E. Hayakawa (2012). "Peptide signaling in Hydra." Int J Dev Biol **56**(6-8): 543-550.

Garelli, A., et al. (2012). "Imaginal discs secrete insulin-like peptide 8 to mediate plasticity of growth and maturation." Science **336**(6081): 579-582.

Garofalo, R. S. (2002). "Genetic analysis of insulin signaling in Drosophila." Trends Endocrinol Metab **13**(4): 156-162.

Gee, L., et al. (2010). "beta-catenin plays a central role in setting up the head organizer in hydra." Dev Biol **340**(1): 116-124.

Gorczyca, M., et al. (1993). "Insulin-Like Receptor and Insulin-Like Peptide Are Localized at Neuromuscular-Junctions in Drosophila." Journal of Neuroscience **13**(9): 3692-3704.

Grasis, J. A., et al. (2014). "Species-specific viromes in the ancestral holobiont Hydra." PLoS One **9**(10): e109952.

Grens, A., et al. (1999). "The novel signal peptides, pedibin and Hym-346, lower positional value thereby enhancing foot formation in hydra." Development **126**(3): 517-524.

Grimmelikhuijzen, C. J. P., et al. (2002). "Neuropeptides in cnidarians." Canadian Journal of Zoology-Revue Canadienne De Zoologie **80**(10): 1690-1702.

Gronke, S., et al. (2010). "Molecular evolution and functional characterization of Drosophila insulin-like peptides." PLoS Genet **6**(2): e1000857.

Gu, Z., et al. (2002). "Extent of gene duplication in the genomes of Drosophila, nematode, and yeast." Mol Biol Evol **19**(3): 256-262.

Gu, Z., et al. (2003). "Role of duplicate genes in genetic robustness against null mutations." Nature **421**(6918): 63-66.

Habetha, M., et al. (2003). "The Hydra viridis/Chlorella symbiosis. Growth and sexual differentiation in polyps without symbionts." Zoology (Jena) **106**(2): 101-108.

Halls, M. L., et al. (2006). "Relaxin family peptide receptors RXFP1 and RXFP2 modulate cAMP signaling by distinct mechanisms." Molecular Pharmacology **70**(1): 214-226.

Halls, M. L., et al. (2007). "Comparison of signaling pathways activated by the relaxin family peptide receptors, RXFP1 and RXFP2, using reporter genes." J Pharmacol Exp Ther **320**(1): 281-290.

Halls, M. L., et al. (2015). "International Union of Basic and Clinical Pharmacology. XCV. Recent Advances in the Understanding of the Pharmacology and Biological Roles of Relaxin Family Peptide Receptors 1-4, the Receptors for Relaxin Family Peptides." Pharmacological Reviews **67**(2): 389-440.

Halls, M. L., et al. (2009). "Relaxin family peptide receptor (RXFP1) coupling to G(alpha)i3 involves the C-terminal Arg752 and localization within membrane Raft Microdomains." Molecular Pharmacology **75**(2): 415-428.

Hansen, G. N., et al. (2000). "Two-color double-labeling in situ hybridization of whole-mount Hydra using RNA probes for five different Hydra neuropeptide preprohormones: evidence for colocalization." Cell Tissue Res **301**(2): 245-253.

Hansen, G. N., et al. (2002). "A new case of neuropeptide coexpression (RGamide and LWamides) in Hydra, found by whole-mount, two-color double-labeling in situ hybridization." Cell Tissue Res **308**(1): 157-165.

Hemmrich, G., et al. (2007). "Molecular phylogenetics in Hydra, a classical model in evolutionary developmental biology." Molecular Phylogenetics and Evolution **44**(1): 281-290.

Hemmrich, G. and T. C. Bosch (2008). "Compagen, a comparative genomics platform for early branching metazoan animals, reveals early origins of genes regulating stem-cell differentiation." Bioessays **30**(10): 1010-1018.

Hemmrich, G., et al. (2012). "Molecular Signatures of the Three Stem Cell Lineages in Hydra and the Emergence of Stem Cell Function at the Base of Multicellularity." Mol Biol Evol **29**(11): 3267-3280.

Herold, M., et al. (2002). "Cloning and characterisation of PKB and PRK homologs from Hydra and the evolution of the protein kinase family." Dev Genes Evol **212**(11): 513-519.

Holstein, T. W., et al. (1991). "Pattern of epithelial cell cycling in hydra." Dev Biol **148**(2): 602-611.

Hsu, S. Y. (1999). "Cloning of two novel mammalian paralogs of relaxin/insulin family proteins and their expression in testis and kidney." Molecular Endocrinology **13**(12): 2163-2174.

Hsu, S. Y., et al. (2000). "The three subfamilies of leucine-rich repeat-containing G protein-coupled receptors (LGR): Identification of LGR6 and LGR7 and the signaling mechanism for LGR7." Molecular Endocrinology **14**(8): 1257-1271.

Huang, H. C. and P. S. Klein (2004). "The Frizzled family: receptors for multiple signal transduction pathways." Genome Biol **5**(7): 234.

Hughes, A. L. (1994). "The Evolution of Functionally Novel Proteins after Gene Duplication." Proceedings of the Royal Society B-Biological Sciences **256**(1346): 119-124.

Hwang, W. Y., et al. (2013). "Efficient genome editing in zebrafish using a CRISPR-Cas system." Nat Biotechnol **31**(3): 227-229.

Ikeya, T., et al. (2002). "Nutrient-dependent expression of insulin-like peptides from neuroendocrine cells in the CNS contributes to growth regulation in Drosophila." Curr Biol **12**(15): 1293-1300.

Iwami, M. (2000). "Bombyxin: An insect brain peptide that belongs to the insulin family." Zoological Science **17**(8): 1035-1044.

Jekely, G. (2013). "Global view of the evolution and diversity of metazoan neuropeptide signaling." Proc Natl Acad Sci U S A **110**(21): 8702-8707.

Jones, O. R., et al. (2014). "Diversity of ageing across the tree of life." Nature **505**(7482): 169-173.

Jung, S., et al. (2009). "Hydramacin-1, structure and antibacterial activity of a protein from the basal metazoan Hydra." J Biol Chem **284**(3): 1896-1905.

Kaletsky, R. and C. T. Murphy (2010). "The role of insulin/IGF-like signaling in C. elegans longevity and aging." Dis Model Mech **3**(7-8): 415-419.

Kelley, L. A., et al. (2015). "The Phyre2 web portal for protein modeling, prediction and analysis." Nat Protoc **10**(6): 845-858.

Kersey, P. J., et al. (2016). "Ensembl Genomes 2016: more genomes, more complexity." Nucleic Acids Res **44**(D1): D574-580.

Khalturin, K., et al. (2009). "More than just orphans: are taxonomically-restricted genes important in evolution?" Trends Genet **25**(9): 404-413.

Kimura, K. D., et al. (1997). "daf-2, an insulin receptor-like gene that regulates longevity and diapause in Caenorhabditis elegans." Science **277**(5328): 942-946.

King, N., et al. (2008). "The genome of the choanoflagellate Monosiga brevicollis and the origin of metazoans." Nature **451**(7180): 783-788.

Koizumi, O. (2007). "Nerve ring of the hypostome in hydra: is it an origin of the central nervous system of bilaterian animals?" Brain Behav Evol **69**(2): 151-159.

Koizumi, O. and H. R. Bode (1986). "Plasticity in the nervous system of adult hydra. I. The position-dependent expression of FMRFamide-like immunoreactivity." Dev Biol **116**(2): 407-421.

Koizumi, O. and H. R. Bode (1991). "Plasticity in the nervous system of adult hydra. III. Conversion of neurons to expression of a vasopressin-like immunoreactivity depends on axial location." J Neurosci **11**(7): 2011-2020.

Koizumi, O., et al. (1988). "Plasticity in the nervous system of adult hydra. II. Conversion of ganglion cells of the body column into epidermal sensory cells of the hypostome." Dev Biol **129**(2): 358-371.

Kooijman, R. (2006). "Regulation of apoptosis by insulin-like growth factor (IGF)-I." Cytokine Growth Factor Rev **17**(4): 305-323.

Krishnan, A. and H. B. Schioth (2015). "The role of G protein-coupled receptors in the early evolution of neurotransmission and the nervous system." J Exp Biol **218**(Pt 4): 562-571.

Lang, B. F., et al. (2002). "The closest unicellular relatives of animals." Curr Biol **12**(20): 1773-1778.

Laron, Z. (2001). "Insulin-like growth factor 1 (IGF-1): a growth hormone." Journal of Clinical Pathology-Molecular Pathology **54**(5): 311-316.

Lasi, M., et al. (2010). "Apoptosis in pre-Bilaterians: Hydra as a model." Apoptosis **15**(3): 269-278.

Lenhoff, H. M. and R. D. Brown (1970). "Mass culture of hydra: an improved method and its application to other aquatic invertebrates." Lab Anim **4**(1): 139-154.

Lespinet, O., et al. (2002). "The role of lineage-specific gene family expansion in the evolution of eukaryotes." Genome Res **12**(7): 1048-1059.

Li, C. and K. Kim (2008). "Neuropeptides." WormBook: 1-36.

Li, W., et al. (2015). "The EMBL-EBI bioinformatics web and programmatic tools framework." Nucleic Acids Res **43**(W1): W580-584.

Littlefield, C. L. (1985). "Germ-Cells in Hydra-Oligactis Males .1. Isolation of a Subpopulation of Interstitial-Cells That Is Developmentally Restricted to Sperm Production." Dev Biol **112**(1): 185-193.

Littlefield, C. L., et al. (1991). "Spermatogenesis in Hydra-Oligactis .2. How Temperature Controls the Reciprocity of Sexual and Asexual Reproduction." Dev Biol **146**(2): 292-300.

Livak, K. J. and T. D. Schmittgen (2001). "Analysis of relative gene expression data using real-time quantitative PCR and the 2(T)(-Delta Delta C) method." Methods **25**(4): 402-408.

Ma, Y., et al. (2006). "Prevalence of off-target effects in Drosophila RNA interference screens." Nature **443**(7109): 359-363.

MacNeil, L. T., et al. (2013). "Diet-induced developmental acceleration independent of TOR and insulin in C. elegans." Cell **153**(1): 240-252.

Manning, B. D. and L. C. Cantley (2007). "AKT/PKB signaling: Navigating downstream." Cell **129**(7): 1261-1274.

Manuel, G. C., et al. (2006). "PI3K and ERK 1-2 regulate early stages during head regeneration in hydra." Dev Growth Differ **48**(2): 129-138.

Martin, V. J., et al. (1997). "Embryogenesis in hydra." Biological Bulletin **192**(3): 345-363.

Masumura, M., et al. (2000). "Glucose stimulates the release of bombyxin, an insulin-related peptide of the silkworm Bombyx mori." Gen Comp Endocrinol **118**(3): 393-399.

Matsuno, T. and T. Kageyama (1984). "The Nervous-System in the Hypostome of Pelmatohydra-Robusta - the Presence of a Circumhypostomal Nerve Ring in the Epidermis." J Morphol **182**(2): 153-168.

Meinhardt, H. (2012). "Modeling pattern formation in hydra: a route to understanding essential steps in development." Int J Dev Biol **56**(6-8): 447-462.

Mitgutsch, C., et al. (1999). "Expression and developmental regulation of the Hydra-RFamide and Hydra-LWamide preprohormone genes in Hydra: evidence for transient phases of head formation." Dev Biol **207**(1): 189-203.

Mombaerts, P. (2001). "The human repertoire of odorant receptor genes and pseudogenes." Annu Rev Genomics Hum Genet **2**: 493-510.

Moreland, R. T., et al. (2014). "A customized Web portal for the genome of the ctenophore Mnemiopsis leidyi." BMC Genomics **15**: 316.

Moroz, L. L. and A. B. Kohn (2016). "Independent origins of neurons and synapses: insights from ctenophores." Philos Trans R Soc Lond B Biol Sci **371**(1685): 20150041.

Murphy, C. T. and P. J. Hu (2013). "Insulin/insulin-like growth factor signaling in C. elegans." WormBook: 1-43.

Nakae, J., et al. (2001). "Distinct and overlapping functions of insulin and IGF-I receptors." Endocr Rev **22**(6): 818-835.

Nguyen, B. T. and C. W. Dessauer (2005). "Relaxin stimulates protein kinase C zeta translocation: Requirement for cyclic adenosine 3 ',5 '-monophosphate production." Molecular Endocrinology **19**(4): 1012-1023.

Nguyen, B. T., et al. (2003). "Phosphoinositide 3-kinase activity is required for biphasic stimulation of cyclic adenosine 3 ',5 '-monophosphate by relaxin." Molecular Endocrinology **17**(6): 1075-1084.

Nielsen, C., et al. (1996). "Cladistic analyses of the animal kingdom." Biological Journal of the Linnean Society **57**(4): 385-410.

Nikitin, M. (2015). "Bioinformatic prediction of Trichoplax adhaerens regulatory peptides." Gen Comp Endocrinol **212**: 145-155.

Nowak, M. A., et al. (1997). "Evolution of genetic redundancy." Nature **388**(6638): 167-171.

Okamoto, N., et al. (2009). "An ecdysteroid-inducible insulin-like growth factor-like peptide regulates adult development of the silkmoth Bombyx mori." FEBS J **276**(5): 1221-1232.

Pierce, S. B., et al. (2001). "Regulation of DAF-2 receptor signaling by human insulin and ins-1, a member of the unusually large and diverse C-elegans insulin gene family." Genes Dev **15**(6): 672-686.

Pierre De Meyts, et al. (2000-2013). Madame Curie Bioscience Database [Internet]. Insulin and IGF-I Receptor Structure and Binding Mechanism, Austin (TX): Landes Bioscience.

Pisani, D., et al. (2015). "Genomic data do not support comb jellies as the sister group to all other animals." Proc Natl Acad Sci U S A **112**(50): 15402-15407.

PROSITE (2004). "Insulin family signature." from http://prosite.expasy.org/PDOC00235.

Putnam, N. H., et al. (2007). "Sea anemone genome reveals ancestral eumetazoan gene repertoire and genomic organization." Science **317**(5834): 86-94.

Ritter, A. D., et al. (2013). "Complex expression dynamics and robustness in C. elegans insulin networks." Genome Res **23**(6): 954-965.

Robitzki, A., et al. (1989). "Demonstration of an endocrine signaling circuit for insulin in the sponge Geodia cydonium." EMBO J **8**(10): 2905-2909.

Rubin, G. M., et al. (2000). "Comparative genomics of the eukaryotes." Science **287**(5461): 2204-2215.

Rulifson, E. J., et al. (2002). "Ablation of insulin-producing neurons in flies: growth and diabetic phenotypes." Science **296**(5570): 1118-1120.

Ryan, J. F., et al. (2013). "The genome of the ctenophore Mnemiopsis leidyi and its implications for cell type evolution." Science **342**(6164): 1242592.

Saltiel, A. R. and C. R. Kahn (2001). "Insulin signalling and the regulation of glucose and lipid metabolism." Nature **414**(6865): 799-806.

Sanger, F. (1959). "Chemistry of insulin; determination of the structure of insulin opens the way to greater understanding of life processes." Science **129**(3359): 1340-1344.

Sanger, F., et al. (1977). "DNA sequencing with chain-terminating inhibitors." Proc Natl Acad Sci U S A **74**(12): 5463-5467.

Satake, S., et al. (1997). "Bombyxin, an insulin-related peptide of insects, reduces the major storage carbohydrates in the silkworm Bombyx mori." Comp Biochem Physiol B Biochem Mol Biol **118**(2): 349-357.

Schaible, R., et al. (2015). "Constant mortality and fertility over age in Hydra." Proc Natl Acad Sci U S A **112**(51): 15701-15706.

Schwentner, M. and T. C. G. Bosch (2015). "Revisiting the age, evolutionary history and species level diversity of the genus Hydra (Cnidaria: Hydrozoa)." Molecular Phylogenetics and Evolution **91**: 41-55.

Sciacca, L., et al. (2012). "Insulin analogs and cancer." Front Endocrinol (Lausanne) **3**: 21.

Shingleton, A. W., et al. (2005). "The temporal requirements for insulin signaling during development in Drosophila." PLoS Biol **3**(9): e289.

Siddle, K. (2011). "Signalling by insulin and IGF receptors: supporting acts and new players." J Mol Endocrinol **47**(1): R1-10.

Sievers, F., et al. (2011). "Fast, scalable generation of high-quality protein multiple sequence alignments using Clustal Omega." Mol Syst Biol **7**.

Skorokhod, A., et al. (1999). "Origin of insulin receptor-like tyrosine kinases in marine sponges." Biological Bulletin **197**(2): 198-206.

Slaidina, M., et al. (2009). "A Drosophila insulin-like peptide promotes growth during nonfeeding states." Dev Cell **17**(6): 874-884.

Slautterback, D. B. (1967). "The cnidoblast-musculoepithelial cell complex in the tentacles of hydra." Z Zellforsch Mikrosk Anat **79**(2): 296-318.

Smit, A. B., et al. (1998). "Towards understanding the role of insulin in the brain: lessons from insulin-related signaling systems in the invertebrate brain." Prog Neurobiol **54**(1): 35-54.

Srivastava, M., et al. (2008). "The Trichoplax genome and the nature of placozoans." Nature **454**(7207): 955-960.

Srivastava, M., et al. (2010). "The Amphimedon queenslandica genome and the evolution of animal complexity." Nature **466**(7307): 720-726.

Steele, R. E., et al. (1996). "Response to insulin and the expression pattern of a gene encoding an insulin receptor homologue suggest a role for an insulin-like molecule in regulating growth and patterning in Hydra." Dev Genes Evol **206**(4): 247-259.

Steiner, D. F., et al. (1985). "Structure and evolution of the insulin gene." Annu Rev Genet **19**: 463-484.

Steiner, D. F., et al. (1984). "Golgi/granule processing of peptide hormone and neuropeptide precursors: a minireview." J Cell Biochem **24**(2): 121-130.

Taguchi, A. and M. F. White (2008). "Insulin-like signaling, nutrient homeostasis, and life span." Annu Rev Physiol **70**: 191-212.

Takahashi, T., et al. (2003). "Identification of a new member of the GLWamide peptide family: physiological activity and cellular localization in cnidarian polyps." Comp Biochem Physiol B Biochem Mol Biol **135**(2): 309-324.

Takahashi, T. and N. Takeda (2015). "Insight into the Molecular and Functional Diversity of Cnidarian Neuropeptides." International Journal of Molecular Sciences **16**(2): 2610-2625.

Tamura, K., et al. (2013). "MEGA6: Molecular Evolutionary Genetics Analysis Version 6.0." Mol Biol Evol **30**(12): 2725-2729.

Tardent, P. (1995). "The Cnidarian Cnidocyte, a High-Tech Cellular Weaponry." Bioessays **17**(4): 351-362.

Trembley, A. (1744). "Mémoires, pour servir à l'historie d'un genre de polypes d'eau douce, à bras en forme de cornes." (Jean and Herman Verbeek).

van der Westhuizen, E. T., et al. (2010). "H2 Relaxin Is a Biased Ligand Relative to H3 Relaxin at the Relaxin Family Peptide Receptor 3 (RXFP3)." Molecular Pharmacology **77**(5): 759-772.

van der Westhuizen, E. T., et al. (2007). "The relaxin family peptide receptor 3 activates extracellular signal-regulated kinase 1/2 through a protein kinase C-dependent mechanism." Molecular Pharmacology **71**(6): 1618-1629.

Van Hiel, M. B., et al. (2015). "Cloning, constitutive activity and expression profiling of two receptors related to relaxin receptors in Drosophila melanogaster." Peptides **68**: 83-90.

van Leeuwenhoek, A. (1702). "The Collected Letters of Antoni van Leeuwenhoek. Palm, L.C. (Ed.)." (Swets and Zeitlinger, 1996) **XIV**: 169-173.

Vandesompele, J., et al. (2002). "Accurate normalization of real-time quantitative RT-PCR data by geometric averaging of multiple internal control genes." Genome Biol **3**(7): RESEARCH0034.

Veenstra, J. A. (2011). "Neuropeptide evolution: neurohormones and neuropeptides predicted from the genomes of Capitella teleta and Helobdella robusta." Gen Comp Endocrinol **171**(2): 160-175.

Wagner, A. (1994). "Evolution of Gene Networks by Gene Duplications - a Mathematical-Model and Its Implications on Genome Organization." Proc Natl Acad Sci U S A **91**(10): 4387-4391.

Wagner, A. (2001). "The yeast protein interaction network evolves rapidly and contains few redundant duplicate genes." Mol Biol Evol **18**(7): 1283-1292.

Wang, S., et al. (2014). "Identification of putative insulin-like peptides and components of insulin signaling pathways in parasitic platyhelminths by the use of genome-wide screening." FEBS J **281**(3): 877-893.

Wenger, Y., et al. (2016). "Loss of neurogenesis in Hydra leads to compensatory regulation of neurogenic and neurotransmission genes in epithelial cells." Philos Trans R Soc Lond B Biol Sci **371**(1685): 20150040.

Whelan, N. V., et al. (2015). "Error, signal, and the placement of Ctenophora sister to all other animals." Proc Natl Acad Sci U S A **112**(18): 5773-5778.

Wilicox, B. J., et al. (2008). "FOXO3A genotype is strongly associated with human longevity." Proc Natl Acad Sci U S A **105**(37): 13987-13992.

Winter, B. (2013) Linear models and linear mixed effects models in R with linguistic applications.

Wittlieb, J., et al. (2006). "Transgenic Hydra allow in vivo tracking of individual stem cells during morphogenesis." Proc Natl Acad Sci U S A **103**(16): 6208-6211.

Wolkow, C. A., et al. (2002). "Insulin receptor substrate and p55 orthologous adaptor proteins function in the Caenorhabditis elegans daf-2/insulin-like signaling pathway." J Biol Chem **277**(51): 49591-49597.

Wood, R. L. and P. L. Novak (1982). "The anchoring of nematocysts and nematocytes in the tentacles of hydra." J Ultrastruct Res **81**(1): 104-116.

Yegorov, S., et al. (2014). "The relaxin family peptide receptors and their ligands: New developments and paradigms in the evolution from jawless fish to mammals." General and Comparative Endocrinology **209**: 93-105.

Zhang, J. Z. (2003). "Evolution by gene duplication: an update." Trends in Ecology & Evolution **18**(6): 292-298.

Zhang, X. and S. Firestein (2002). "The olfactory receptor gene superfamily of the mouse." Nat Neurosci **5**(2): 124-133.

7. Acknowledgements

The completion of this thesis would not be possible without the guidance, support and encouragement from many people. I would like to give my highest respects for my supervisor, Prof. Thomas Bosch. I still remember when I was quite touched by your paper revealing your research career and I was eager to be your PhD student. Time has proved that you are a fond supervisor with very strict demands on both yourself and the people around you. Thank you so much for preparing me for my future career.

To Dr. Alexander Klimovich, you have provided me a best example of a knowledgeable scientist with kindness, firmness and flexibility. Our discussions are my precious gifts from you as you shared your insightful advices about both work and life selflessly. Thank you for your guide in the lab work as well as my writing and presentation skills. It was a great pleasure for me to work with you.

I would like to thank the entire Bosch lab, past and current members, for sharing your scientific expertise and creating a friendly and cheerful working environment. Dr. Anna-Marei Böhm, thank you for orientating me to the lab environment and teaching me experimental techniques in my initial period in the lab, as well as your work which provided a part of basal part for my thesis. Dr. René Augustin, Dr. Sebastian Fraune, Dr. Konstantin Khalturin, Dr. Friederike Anton-Erxleben, Dr. Juris Grasis, Dr. Mayuko Hamada, Dr. Tim Lachnit, Dr. Peter Deines, thank you for your comments on my naive questions on protocols, data analysis and much more. Jan Taubenheim and Andrea Murillo, I appreciate your time when we discussed and developed methods together. Doris Willoweit-Ohl, Jörg Wittlieb, Antje Thomas, Eva-Maria Herbst, Maria Franck, Daniel Freyer and Antika Hintz, thank you for all the behind-the-scene work to keep things in order for the lab. Dr. Cleo Pietschke, Dr. Sören Franzenburg, Dr. Wei Wang, Katja Schröder, Javier Andrés López Quintero, Santiago Insua, Kai Rathje, Benedikt Mortzfeld, Timo Minten, Janina Lange, Jinru He, Laura Baldassarre, Mehdi Harmi and Hanna Englert, thank you for all the helps and continuous encouragement and moral support.

I appreciate International Max Planck research school for evolutionary biology for its supports during my PhD study by providing practical courses, financial supports and

a warm social community. Dr. Kerstin Mehnert, special thank you for your helps and suggestions during my study and living in Kiel. To my other thesis committee members: Prof. Thomas Roeder, Prof. Hinrich Schulenburg and Prof. John Baines, thank you for your wise advices and guide during the development of my PhD thesis.

My most grateful thanks are extended to my parents Fudi Xiang and Min Zhu. Thank you for your unconditional love to me and encouragement to whatever I am doing. Thank you for your echoic reminders over the phone of staying warm and healthy. In nowhere I can find a place better than home.

8. Appendix

8.1 Amino acid sequences alignment

8.1.1 Sixteen ILPs

No.	Name	Species	Gene ID/UniProtKB/Swiss-Prot
1	Hs INS	Homo sapiens (human)	3630
2	Mm INS2	Mus musculus (house mouse)	16334
3	Gg INS	Gallus gallus (chicken)	396145
4	Xl INSa	Xenopus laevis (African clawed frog)	378696
5	Mg INS	Myxine glutinosa	P01342.1
6	Dr INS	Danio rerio (zebrafish)	30262
7	Dm ILP1	Drosophila melanogaster (fruit fly)	39149
8	Dm ILP2	Drosophila melanogaster (fruit fly)	39150
9	Dm ILP3	Drosophila melanogaster (fruit fly)	39151
10	Dm ILP4	Drosophila melanogaster (fruit fly)	39152
11	Dm ILP5	Drosophila melanogaster (fruit fly)	2768992
12	Dm ILP6	Drosophila melanogaster (fruit fly)	31220
13	Ce INS1	Caenorhabditis elegans	177936
14	Ac INS	Aplysia californica (California sea hare)	100533403
15	Lm IRP	Locusta migratoria	P15131.2
16	Ls IRP1	Lymnaea stagnalis	P07223.2

Table 16 16 initial ILPs for extraction of ILPs cysteine pattern

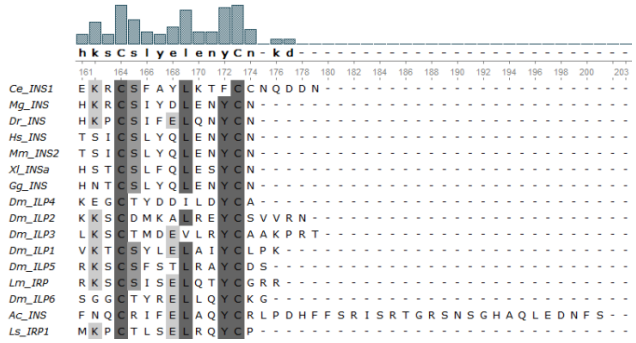

Figure 8-1 alignment of 16 initial ILPs

Species name abbreviations: Hs, *Homo sapiens*; Mm, *Mus musculus*; Dm *Drosophila melanogaster*; Ce, *Caenorhabditis elegans*; Xl, *Xenopus laevis*; Dr *Danio rerio*; Gg *Gallus gallus*; Ac, *Aplysia californica*; Mg, *Myxine glutinosa*; Lm, *Locusta migratoria*; Ls, *Lymnaea stagnalis*.

8.1.2 HylLPs

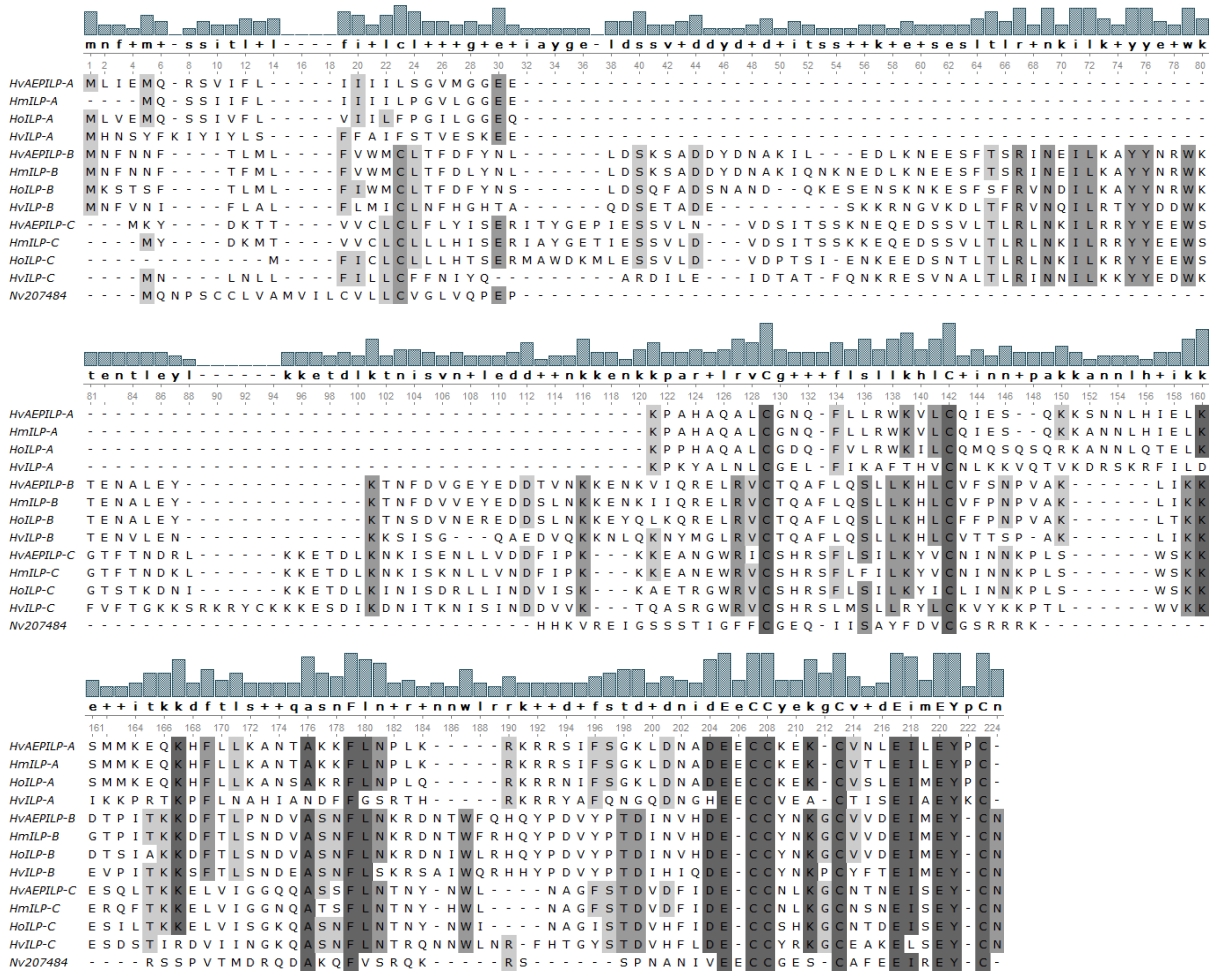

Figure 8-2 HylLPs alignment with *Nematostella vectensis* ILP 207484 (UniProt)

Abbreviations: *HvAEP*, *Hydra vulgaris AEP*; Hm, *Hydra magnipapillata*; Ho, *Hydra oligactis*; Hv, *Hydra viridissima*; Nv: *Nematostella vectensis*

8.1.3 Cnidarian ILPs

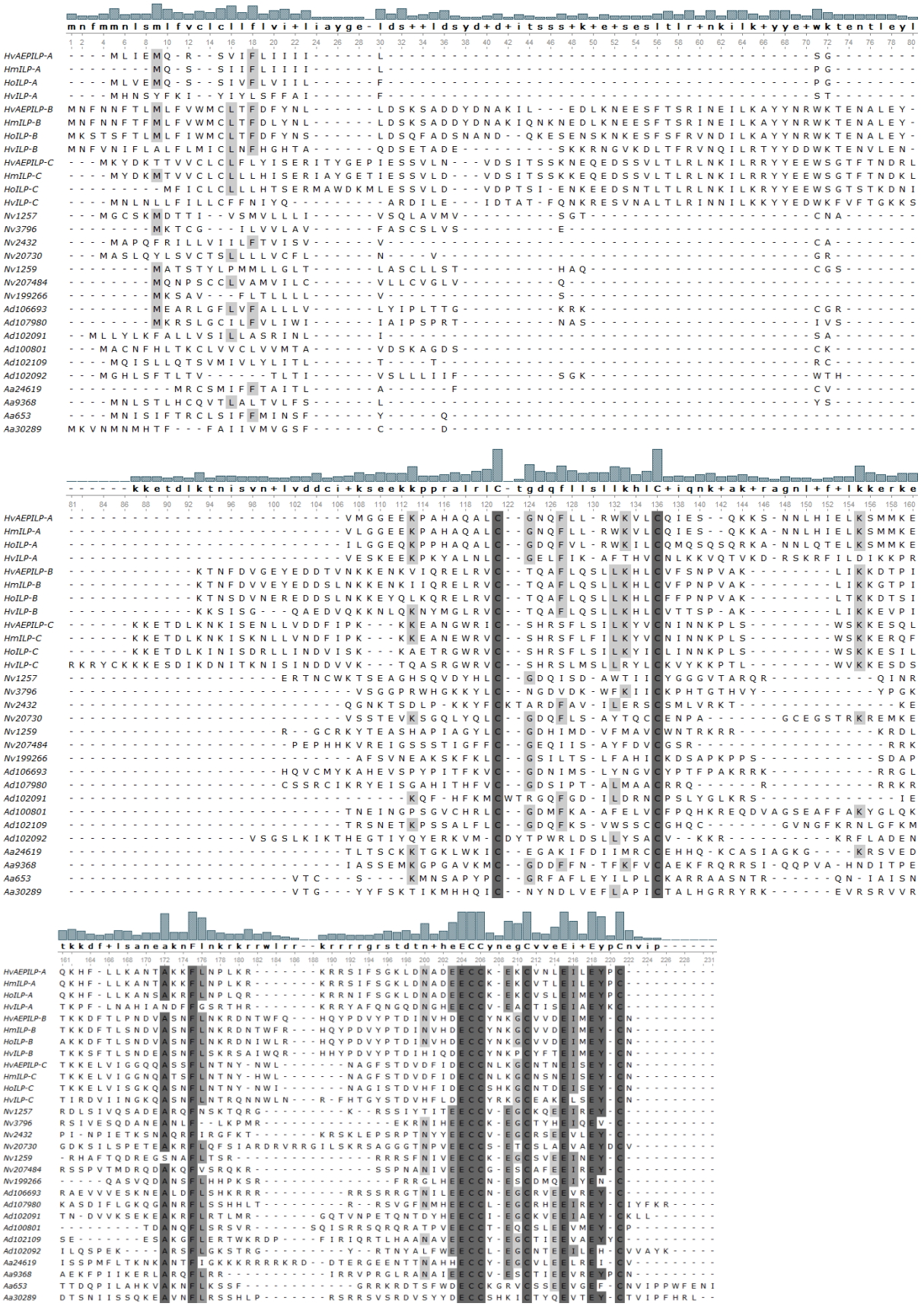

Figure 8-3 Cnidarian ILPs

Abbreviations: *HvAEP*, *Hydra vulgaris AEP*; Hm, *Hydra magnipapillata*; Ho, *Hydra oligactis*; Hv, *Hydra viridissima*; Nv: *Nematostella vectensis; Ad*, *Acropora digitfera* and Aa *Aurelia aurita*

8.2 Phylogenetic analysis

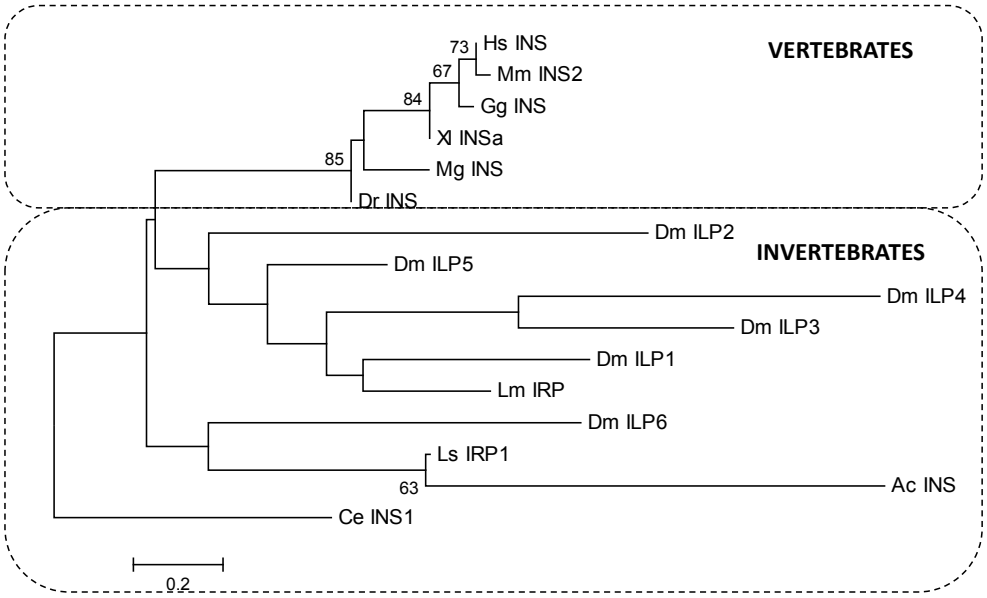

Figure 8-4 Phylogenetic analysis of 16 ILPs as an initial seed for ILPs pattern searching

Maximum likelihood phylogram of 16 ILPs from 11 animals. Numbers at nodes are bootstrap support values calculated by 1000 replicates of Maximum likelihood using Dayhoff model with a discrete Gamma distribution with 5 rate categories. Bootstrap values under 50 are not shown. ILPs were subdivided into two main clusters. Species name abbreviations: Hs, *Homo sapiens*; Mm, *Mus musculus*; Dm *Drosophila melanogaster*; Ce, *Caenorhabditis elegans*; Xl, *Xenopus laevis*; Dr *Danio rerio*; Gg *Gallus gallus*; Ac, *Aplysia californica*; Mg, *Myxine glutinosa*; Lm, *Locusta migratoria*; Ls, *Lymnaea stagnalis*.

8.3 Analysis of 5' prime sequence *Hydra magnipapillata* ILPs.

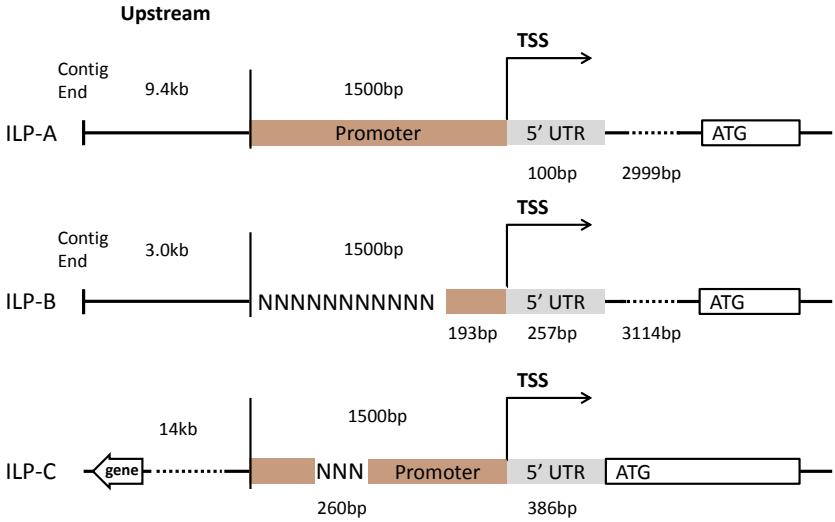

Figure 8-5 5' prime sequence analysis of *Hydra magnipapillata* ILPs

NNN: no base assigned in sequences; TSS: transcription start site;

8.4 Oligonucleotides (primers)

Description	Primers	Sequence (5' -> 3')	TM(°C)
Primers for standard PCR or qRT-PCR			
ef1 alpha	EF1a_F_qRT	GCAGTACTGGTGAGTTTGAAG	57.9
	EF1a_R_qRT	CTTCGCTGTATGGTGGTTCAG	59.8
actin	SF_actin_RT_F	GAATCAGCTGGTATCCATGAAAC	58.9
	SF_actin_RT_R	AACATTGTCGTACCACCTGATAG	58.9
HylLP-A (AEP)	XX_ILPAq_F	AAACCTGCTCACGCACAAGC	59.4
	XX_ILPAq_R	GCTCCTTCATCATACTTTTAAGCTC	59.7
HylLP-B (AEP)	ILP2_F_qRT	CCGGATGTTTATCCAACTGACA	58.4
	ILP2_R_qRT	CAAAATAGGTCCTCACTGTCAC	58.4
HylLP-C (AEP)	ILP3_F_qRT	GGAGGTATTACGAAGAATGGAG	58.4
	ILP3_R_qRT	GATGCGAACAAATTCGCCATCC	60.3
HylNSR (AEP)	INSR_F_qRT	CTGGCAATGGTTCATGGACAG	59.8
	INSR_R_qRT	CAGCAAGGCAACAATTACTGCAG	60.6
NDA-1	NDA-1F	Provided by Katja Schröder	
	NDA-1R	Provided by Katja Schröder	
FoxO	FoxO3_qRT_F	GGATTCTACATCAAGTGCAGG	57.9
	FoxO3_qRT_R	GATTTCCCTGCTTTTGCATCTG	58.4
Hydramacin	SF_Macin_qRT_F	GCCTTCCGATACACAAGCTG	59.4
	SF_Macin_qRT_R	ACTATGTCCGAGCTCTTTACAAC	58.9
GFP	XX_GFPqRT_F	GAGAGGGTGAAGGTGATGCA	59.4
	XX_GFPqRT_R	AGTCATGCCGTTTCATATGATCTG	59.3
Chordin1	AK_Chordin1qF1	AGATGAATGGTCCCCTGATTC	57.9
	AK_Chordin1qR1	GACGACATCAGTATAGGACATG	58.4
Total HylLP-B	XX_ILPBqRTNewF	CTCTACCTAATGATGTCGCTTCC	60.6
	XX_ILPBqRTNewR	GTCGTGGACATTAATGTCAGTTG	58.9
HylLP-B-GFP	XX_ILPBGFPqRTF	CAACTGACATTAATGTCCACGAC	58.9
	GFP_R (75)	GTGCCCATTAACATCACCATC	57.9
HylLP-B-cMyc	XX_ILPBGFPqRTF	CAACTGACATTAATGTCCACGAC	58.9
	XX_MycTag_qRT_R	CGCGATCGCTAAATCTTCTTCAG	60.6
Endogenous HylLP-B	ILP2_F_qRT	CCGGATGTTTATCCAACTGACA	58.4
	ILP2_R_qRT	CAAAATAGGTCCTCACTGTCAC	58.4
M13	M13F	GTAAAACGACGGCCAGT	52.8
	M13R	GGAAACAGCTATGACCATG	54.5
T7	T7	GTAATACGACTCACTATAGGG	55.9
	T7_IRD800	GTAATACGACTCACTATAGGG	55.9
SP6	SP6	AAGCTATTTAGGTGACACTATAG	55.3
	SP6_IRD700	AAGCTATTTAGGTGACACTATAG	55.3
GFP	GFP629F	ATCCCAACGAAAAGAGAGAC	55.3

	GFP75R	GTGCCCATTAACATCACCATC	57.9
actin terminator	HAT_R(2342)	GGACGTCTTTTATATTACAGC	54
	HAT_R_IRD800	GGACGTCTTTTATATTACAGC	54
HyILP-A ORF (H.mag)	XXHmagIlpAORF_F	GTTATAATCAAATCAAACCGC	52
	XXHmagIlpAORF_R	GACATTAAATGACATCCAGAG	54
HyILP-A ORF (H.oli)	XXHoliIlpAORF_F	CCCTAGATTTTATTGTGTTTAC	52.8
	XXHoliIlpAORF_R	CAGTTGACACCCAAGGATTGC	59.8
HyILP-A ORF (H.vir)	XXHvirIlpAORF_F	CACTGTGTATTAAGATGCATAAC	55.3
	XXHvirIlpAORF_R	TAGTCACAAAACTGAAGGCG	55.3
HyILP-B ORF (H.mag)	XX_HmIlPBmRNAF1	ATCCTGAGTAAAAAACTGGT	51.2
	XX_HmIlpBmRNAR	ATAGGTCCTTACTGTCACCGTG	60.3
HyILP-B ORF (H.oli)	XXHoliIlpBORF_F	GTCtAAaTAAGATATCCTGTGC	54.7
	XXHoliIlpBORF_R	GATCTCTGTCTTTGCCGCG	58.8
HyILP-B ORF (H.vir)	XXHvirIlpBORF_F	CAAACATAGCGATGAACTTCG	55.9
	XXHvirIlpBORF_R	CTCCTACACTCAACCACATG	57.3
HyILP-C ORF (H.mag)	XXHmagIlpCORF_F	TACAGAAGCATCGGAAACCG	57.3
	XXHmagIlpCORF_R	CATTGTATCTCAACGAATCTC	54
HyILP-C ORF (H.oli)	XXHoliIlpCORF_F	CATGTTTATATGTCTTTGTCTTC	53.5
	XXHoliIlpCORF_R	GTCGACAAATAGTCTAATATTC	52.8
HyILP-C ORF (H.vir)	XXHvirIlpCORF_F	CTTGATGTCACATCTTTCACGG	58.4
	XXHvirIlpCORF_R	TATTGATGGACTTCTTGCTAC	54
HyILP-C cds	XX_ilpCcdsF:	ATGAAATACGATAAAACGACGG	54.7
	XX_ilpCcdsR:	GTTACAGTATTCAGATATCTC	52
Primers for transgenic *Hydra*			
HyILP-B shortarm	ILPBshortF_AsiSI	gcgatcgcgtagCAAAATAGGTCCTCACTGTC	70.8
	ILPBshortR_kpnI	ggtaccTACAAAGAGAATTAAGAGTT	58.5
HyILP-B longtarm	ILPBlongF_kpnI	ggtaccAAATACTTAAGGCCTATTAT	58.5
	ILPBlongR_EcoRI	gaattcCAAAATAGGTCCTCACTGTC	61.6
	ILP-BlinkerR	CTTCGTATTCGCCAACGTC	56.7
HyILP-A cds	XX_ilpAcdsF_Sbf	CCTGCAGGAATGCTTATTGAAATGCAACGTTCAG	68.3
	XX_ilpAcdsR_Pac	TTAATTAAACATGGATACTCCAATATTTCTAG	59.2
HyILP-B cds	XX_ilpBcdsF_Sbf	CCTGCAGGAATGAATTTTAACAATTTCAC	61
	XX_ilpBcdsR_Pvu	CGATCGAATTACAATATTCCATAATTTCG	59.6
HyILP-C cds	XX_ilpCcdsF_Sbf:	CCTGCAGGAATGAAATACGATAAAACGACGG	66.8
	XX_ilpCcdsR_Pac:	TTAATTAAGTTACAGTATTCAGATATCTC	56.8
Primers for HyILP promoter region detection			
HyILP-A Promoter	XX_ILPA_Pro_F2	CTGTTAACAATCTTATCGGC	53.2
	XX_ILPA_Pro_R-2	AACTCGAGTTACACAACAG	52.4
	XX_ILPA_Pro_F3	CTGTTGTGTAACTCGAGTT	52.4
	XX_ILPA_Pro_R-1	GCTTTATTAAATGCTAGCGTAC	54.7

	XX_ILPA_Pro_F4	gtACGCTAGCATTTAATAAAGC	54.7
	XX_ILPA_Pro_R2	CGTGTGTGTTTATGTGTTCC	55.3
HylLP-C Promoter	XX_ILPC_Pro_F3	ATACTTCAAAACTGGCCAAC	53.2
	XX_ILPC_Pro_R3	GATAAAACTCCAACAACGAG	53.2
HylLP-B Promoter	XX_HmllPB5UTRF3	CAACAACTATTTCTTGACGCC	55.9
	XX_HmllPB5UTRR	CTAAGAATGATTTATCCAAAGC	52.8

8.5 Transgenic construct sequence

8.5.1 Sequence of construct for overexpression of HylLP-B fused with GFP

AATACGACTCACTATAGGGCGAATTGAGCTCGACAGCTGTCTCTTATACACAAGTGCGGCCGCG
CATGGTGCACGTCGACTCTAGAGGATCCCCCATCGATCTGACTAACCTAACCAGTGCAAAAAAA
TTTAAAAGATTTGCATTGTGAAAGTTAGAATATTATAAAAAATCTAAAACGAGTATTACTCGAGTAA
ATGTTATACGATCTATAGATTAAATATATTAAAAATGTATAGCGAATGTTAAACTAAATATATAATAT
AAACTTGAAAACTTACTAAATTGCAAAAACTCAAAACCGACTGTATCATTTTTACAGGAAACCGTT
ATTCAAGATACTTAAGTTGTTTACTACATTATTATAACATCTTGCAATTAGCAAGACAATCGTTATT
TTAACATCACGGTATCGAAAGGATTTTGAGAAATTTTATTGAAACATTTTAAACAAAAAATATCATA
TTTAGATGCATTTTAAGCCGAGATGCAGGATTCTGAATGAAAAAGAAAAAAAGAAGTCTCGGTAG
AGTAAAAGTGATCGGTTTGCAACTGYAAAATTTATTGAAGTACCAATAATTTTATTTAAAATAAAAC
TGAAATATAAAGTTAAAGTTGCTGTTCTATAAGTTTACTCGAATTTTAAAACCATTGTAACGCTAGA
GTAATATTTGAGTCTACTAAGTTAGTCCCCGCACTTTTTAATCAAGCAATAAATACCCAAAYTTTGC
TTATTCAAATCAATAAACCAATATATCTCTTAAAATAAAGTAAAAACTTCTGAAATTCTATAAAAAAA
AATTTAATTTCGAAATATCAAATGTAACTTCAACACCGCACTATTTTCTTTTAAACAACTGATATAG
TAATTACTTCTCAAAAACGTTATCTCAAGGTTTGTGATGTACTTAAAACCACTCCTATTTTGTTACG
CGTTTAAAAAAGCAAACATAAGTTGGTTTCTATTGATGAATGAGAACATATTTCATTTAAAGTTAAA
ATCCTACCAGTGGTTTCACTGTACGTAAACACCGTCAAAAAAACAGGAACGTTTTTAAAGATTAAT
AATTGAAGTAAAAAAAATTTAATACCGGGGGTTAAAAAAATCTTTTAAAATAATTATAAATATATATA
TTAAAATTTATAAATTTTTAAACACATTTAAAATATATATTAAGTATAATAAAAGTAATATTATAAAAA
AAAATTTAATTTTATAATTATTTTTATTAAATTTATAAATAATAGGTAAAACTTACATATCCGTTTTAT
TTTTTCTTAATAAAATAACGCGTGCAAATTTTTGTCCATATAAAGACCTTTTCGAACAATAACTTTTT
TGCTTAGCCGTTTTTTTTCTTATATGGTCAAAAAAGCGCTCAAGCGATTCACCATAAAAAGCGCAA
TTAGTTCAGCGTTCGTTATTCAGAAGCTTCAGCTTTGCTTGATACTCAGCTCTTCTCTTTTTAAACA
AAACACTTAATCAAAATGGCCGATCCTGCAGGAATGAATTTTAACAATTTCACTTTAATGTTATTTG
TTTGGATGTGTTTAACATTTGACTTTTACAATTTACTTGATTCAAAATCTGCGGATGATTACGACAA
CGCGAAAATTCTAGAAGACTTAAAAAATGAAGAAAGTTTTACTTCTCGCATCAATGAAATACTTAA
GGCCTATTATAACCGTTGGAAAACTGAAAATGCATTAGAATACAAAACAAATTTTGACGTTGGCGA
ATACGAAGATGATACTGTAAATAAAAAAGAAAACAAAGTCATACAAAGAGAATTAAGAGTTTGCAC
GCAAGCTTTTTTGCAATCATTGCTCAAGCACTTGTGCGTTTTTTCAAATCCAGTGGCAAAGTTAAT
TAAAAAAGATACGCCAATCACAAAGAAAGATTTTACTCTACCTAATGATGTCGCTTCCAATTTTCT
GAATAAACGAGATAATACCTGGTTCCAACACCAATATCCGGATGTTTATCCAACTGACATTAATGT

CCACGACGAATGTTGTTATAACAAAGGGTGCGTCGTTGACGAAATTATGGAATATTGTAATTCGA
TTAATGAAAAAATGAGTAAAGGAGAAGAACTTTTCACTGGAGTTGTCCCAATTCTTGTTGAATTAG
ATGGTGATGTTAATGGGCACAAATTTTCTGTCAGTGGAGAGGGTGAAGGTGATGCAACATACGG
AAAACTTACCCTTAAATTTATTTGCACTACTGGAAAACTACCTGTTCCATGGCCAACACTTGTCAC
TACTTTCTGTTATGGTGTTCAATGCTTTTCAAGATACCCAGATCATATGAAACGGCATGACTTTTT
CAAGAGTGCCATGCCCGAAGGTTATGTACAGGAAAGAACTATATTTTTCAAAGATGACGGGAACT
ACAAGACACGTGCTGAAGTCAAGTTTGAAGGTGATACCCTTGTTAATAGAATCGAGTTAAAAGGT
ATTGATTTTAAAGAAGATGGAAACATTCTTGGACACAAATTGGAATACAACTATAACTCACACAAT
GTATACATCATGGCAGACAAACAAAAGAATGGAATCAAAGTTAACTTCAAAATTAGACACAACATT
GAAGATGGAAGCGTTCAACTAGCAGACCATTATCAACAAAATACTCCAATTGGCGATGGCCCTGT
CCTTTTACCAGACAACCATTACCTGTCCACACAATCTGCCCTTTCGAAAGATCCCAACGAAAAGA
GAGACCACATGGTCCTTCTTGAGTTTGTAACAGCTGCTGGGATTACACATGGCATGGATGAACTA
TACAAAGCGATCGCGTAGAATTCACAATTCGATTATATTTATACTGGACTATTTTTACATCTGTTCG
GTTATTTTCACATTTATTTTTCTATATATATCTTATAAACGTTTTAAAACCCATGTAATTTTTGTTAAG
CTGTAATATAAAAGACGTCCTAACAAACTTCTTTTATTACTGAATTTCCTTTAATTATAATAAATAAC
AAGTTTTAAAATAAATTCAGGCAATTAAGGCGCTCCTGAGGTACTAAAATTAATGTAAACATTTAAA
ATTAACTTGGATGGTCTTAAGTACTGTACTCGTGATTTTGTTATACTTTATTATTAGAAAAGTCGTC
TATTAACTTTTTGTTCCTTAATTTACTTGATTAAATTGTCGCTTAATTTATCAAATCAGGTTTTGCGC
GTTATTTTAGAGAAAAACTTATTAGAAAAATGAATAAGCAAAGTTTAGGCTAACATGTTTTTTTATT
ATTTTAAATAGTTCAAGTCAATGACGTATAAAATGCATTTGCAAAAAATTTTAAGTAACCCTATAAA
CTTAGCAATAGTAGATACTGGATGCAAGCATTCAGTAGCAGCATTGCATATCTGCTGTCTTTACGT
ACAAATAACAGCAAAAATGGACCTTTATTGGCTTCACATCGTCGTAAAACATGTGTTATTGGACTT
GTCACAAATGTGTTAAGTATACAGAGCTTAGCTCTTGATGTTGATCACTAGTGTAAAAGTGATCG
GTTTGCAACTGTAAAATTTATTGAAGTACCAATAATTTTATTTAAAATAAAACTGAAATATAAAGTTA
AAGTTGCTGTTCTATAAGTTTACCGAATTTTAAAACCATTGTAACGCTAGAGTAATATTTGAGTCTA
CTAAGTTAGTCCCCGCACTTTTTAATCAAGCAATAAATACCCAAACTTTGCTTATTCAAATCAATAA
ACCAATATATCTCTTAAAATAAAGTAAAAACTTCTGAAATTCTATAAAAAAAAATTTAATTTCGAAAT
ATCAAATGTAACTTCAACACCGCACTATTTTCTTTTAAACAACTGATATAGTAATTACTTCTCAAAA
ACGTTATCTCAAGGTTTGTGATGTACTTAAAACCACTCCTATTTTGTTACGCGTTTAAAAAAGCAA
ACATAAGTTGGTTTCTATTGATGAATGAGAACATATTTCATTTAAAGTTAAAATCCTACCAGTGGTT
TCACTGTACGTAAACACCGTCAAAAAAACAGGAACGTTTTTAAAGATTAATAATTGAAGTAAAAAA
AATTTAATACCGGGGGTTAAAAAAATCTTTTAAAATAATTATAAATATATATATTAAAATTTATAAAT
TTTTAAACACATTTAAAATATATATTAAGTATAATAAAAGTAATATTATAAAAAAAAATTTAATTTTAT
AATTATTTTTATTAAATTTATAAATAATAGGTAAAACTTACATATCCGTTTTATTTTTTCTTAATAAAA
TAACGCGTGCAAATTTTTGTCCATATAAAGACCTTTTCGAACAATAACTTTTTTGCTTAGCCGTTTT
TTTTCTTATATGGTCAAAAAAGCGCTCAAGCGATTCACCATAAAAAGCGCAATTAGTTCAGCGTTC
GTTATTCAGAAGCTTCAGCTTTGCTTGATACTCAGCTCTTCTCTTTTTAAACAAAACACTTAATCAA
AATGGCCGATGATGAAGTTGCCGCCCTCGGCCGGCCAATGGCTTCATCAGAAAATGTTATTACA
GAATTTATGAGATTTAAAGTTAGAATGGAAGGTACAGTTAATGGACATGAATTTGAAATTGAGGGA
GAAGGAGAAGGTAGACCATATGAAGGACATAATACAGTTAAATTAAAGGTTACAAAAGGAGGACC

ATTACCATTTGCGTGGGATATTTTATCACCACAATTTCAATATGGATCAAAGGTTTACGTTAAACAT
CCAGCTGATATTCCAGATTATAAAAAATTATCTTTTCCAGAAGGATTTAAATGGGAAAGAGTTATG
AATTTTGAAGATGGTGGAGTTGCTACAGTTACACAAGATTCATCATTACAAGATGGTTGTTTTATT
TATAAAGTTAAATTTATTGGGGTTAATTTTCCATCAGACGGACCAGTTATGCAAAAAAAAACAATG
GGATGGGAAGCTAGTACAGAAAGATTATATCCAAGAGACGGGGTTTTAAAGGGAGAAACACATA
AAGCTCTAAAATTAAAGGACGGAGGACATTATTTAGTTGAATTTAAATCAATTTATATGGCTAAAAA
ACCAGTTCAATTACCAGGATATTATTATGTAGATGCTAAGTTAGATATTACATCACATAATGAAGAT
TATACAATTGTTGAACAATATGAAAGAACAGAAGGTAGACATCATTTATTTTTATAGCATTCGTAGA
ATTCACAATTCGATTATATTTATACTGGACTATTTTTACATCTGTTCGGTTATTTTCACATTTATTTT
TCTATATATATCTTATAAACGTTTTAAAACCCATGTAATTTTTGTTAAGCTGTAATATAAAAGACGTC
CTAACAAACTTCTTTTATTACTGAATTTCCTTTAATTATAATAAATAACAAGTTTTAAAATAAATTCA
GGCAATTAAGGCGCTCCTGAGGTACTAAAATTAATGTAAACATTTAAAATTAACTTGGATGGTCTT
AAGTACTGTACTCGTGATTTTGTTATACTTTATTATTAGAAAAGTCGTCTATTAACTTTTTGTTCCTT
AATTTACTTGATTAAATTGTCGCTTAATTTATCAAATCAGGTTTTGCGCGTTATTTTAGAGAAAAAC
TTATTAGAAAAATGAATAAGCAAAGTTTAGGCTAACATGGTTTAAACGAATGCGGCCGCACTTGT
GTATAAGAGACAGCTGTCGAGCTCCCAACGCGTTGGATGCATAGCTTGAGTATTCTATAGTGTC
ACCTAAATAGCTTGGCGTAATCATGGTCATAGCTGTTTCCTGTGTGAAATTGTTATCCGCTCACAA
TTCCACACAACATACGAGCCGGAAGCATAAAGTGTAAAGCCTGGGGTGCCTAATGAGTGAGCTA
ACTCACATTAATTGCGTTGCGCTCACTGCCCGCTTTCCAGTCGGGAAACCTGTCGTGCCAGCTG
CATTAATGAATCGGCCAACGCGCGGGGAGAGGCGGTTTGCGTATTGGGCGCTCTTCCGCTTCCT
CGCTCACTGACTCGCTGCGCTCGGTCGTTCGGCTGCGCGAGCGGTATCA

Figure 8-6 Sequence of overexpression of HylLP-B fused with GFP

ATGAATTTTAA…: hylp-B ORF; ATGAGTAAAGG…: GFP; ATGGCCGATGA…: DsRed; TAG : Stop codon; GCGGCCGC or GAGCTC: restriction sites: GAGCTC - SacI restriction site; CAGCTG - PvuII restriction site; GCGGCCGC - NotI restriction site; GTGCAC - ApaLI restriction site; GTCGAC - SalI restriction site; TCTAGA - XbaI restriction site; GGATCC - BamHI restriction site; ATCGAT - BspDI/ClaI restriction site; CTCGAG - XhoI/ PaeR7I restriction site; GCGATCGC - AsiSI restriction site; ACTAGT - SpeI restriction site; GTTTAAAC - PmeI restriction site; ACGCGT - MluI restriction site; CCTGCAGG - SbfI restriction site.

8.5.2 Sequence of construct for overexpression of HylLP-B fused with cMyc

AATACGACTCACTATAGGGCGAATTGAGCTCGACAGCTGTCTCTTATACACAAGTGCGGCCGCG
CATGGTGCACGTCGACTCTAGAGGATCCCCCATCGATCTGACTAACCTAACCAGTGCAAAAAAA
TTTAAAAGATTTGCATTGTGAAAGTTAGAATATTATAAAAAATCTAAAACGAGTATTACTCGAGTAA
ATGTTATACGATCTATAGATTAAATATATTAAAAATGTATAGCGAATGTTAAACTAAATATATAATAT
AAACTTGAAAACTTACTAAATTGCAAAAACTCAAAACCGACTGTATCATTTTTACAGGAAACCGTT
ATTCAAGATACTTAAGTTGTTTACTACATTATTATAACATCTTGCAATTAGCAAGACAATCGTTATT
TTAACATCACGGTATCGAAAGGATTTTGAGAAATTTTATTGAAACATTTTAAACAAAAAATATCATA
TTTAGATGCATTTTAAGCCGAGATGCAGGATTCTGAATGAAAAAGAAAAAAAGAAGTCTCGGTAG
AGTAAAAGTGATCGGTTTGCAACTGYAAAATTTATTGAAGTACCAATAATTTTATTTAAAATAAAAC
TGAAATATAAAGTTAAAGTTGCTGTTCTATAAGTTTACTCGAATTTTAAAACCATTGTAACGCTAGA

GTAATATTTGAGTCTACTAAGTTAGTCCCCGCACTTTTTAATCAAGCAATAAATACCCAAAYTTTGC
TTATTCAAATCAATAAACCAATATATCTCTTAAAATAAAGTAAAAACTTCTGAAATTCTATAAAAAAA
AATTTAATTTCGAAATATCAAATGTAACTTCAACACCGCACTATTTTCTTTTAAACAACTGATATAG
TAATTACTTCTCAAAAACGTTATCTCAAGGTTTGTGATGTACTTAAAACCACTCCTATTTTGTTACG
CGTTTAAAAAAGCAAACATAAGTTGGTTTCTATTGATGAATGAGAACATATTTCATTTAAAGTTAAA
ATCCTACCAGTGGTTTCACTGTACGTAAACACCGTCAAAAAAACAGGAACGTTTTTAAAGATTAAT
AATTGAAGTAAAAAAAATTTAATACCGGGGGTTAAAAAAATCTTTTAAAATAATTATAAATATATATA
TTAAAATTTATAAATTTTTAAACACATTTAAAATATATATTAAGTATAATAAAAGTAATATTATAAAAA
AAAATTTAATTTTATAATTATTTTTATTAAATTTATAAATAATAGGTAAAACTTACATATCCGTTTTAT
TTTTTCTTAATAAAATAACGCGTGCAAATTTTTGTCCATATAAAGACCTTTTCGAACAATAACTTTTT
TGCTTAGCCGTTTTTTTTCTTATATGGTCAAAAAAGCGCTCAAGCGATTCACCATAAAAAGCGCAA
TTAGTTCAGCGTTCGTTATTCAGAAGCTTCAGCTTTGCTTGATACTCAGCTCTTCTCTTTTTAAACA
AAACACTTAATCAAAATGGCCGATCCTGCAGGAATGAATTTTAACAATTTCACTTTAATGTTATTTG
TTTGGATGTGTTTAACATTTGACTTTTACAATTTACTTGATTCAAAATCTGCGGATGATTACGACAA
CGCGAAAATTCTAGAAGACTTAAAAAATGAAGAAAGTTTTACTTCTCGCATCAATGAAATACTTAA
GGCCTATTATAACCGTTGGAAAACTGAAAATGCATTAGAATACAAAACAAATTTTGACGTTGGCGA
ATACGAAGATGATACTGTAAATAAAAAAGAAAACAAAGTCATACAAAGAGAATTAAGAGTTTGCAC
GCAAGCTTTTTTGCAATCATTGCTCAAGCACTTGTGCGTTTTTTCAAATCCAGTGGCAAAGTTAAT
TAAAAAAGATACGCCAATCACAAAGAAAGATTTTACTCTACCTAATGATGTCGCTTCCAATTTTCT
GAATAAACGAGATAATACCTGGTTCCAACACCAATATCCGGATGTTTATCCAACTGACATTAATGT
CCACGACGAATGTTGTTATAACAAAGGGTGCGTCGTTGACGAAATTATGGAATATTGTAATTCGA
TTAATGAACAAAAATTAATTTCTGAAGAAGATTTAGCGATCGCGTAGAATTCACAATTCGATTATAT
TTATACTGGACTATTTTTACATCTGTTCGGTTATTTTCACATTTATTTTTCTATATATATCTTATAAAC
GTTTTAAAACCCATGTAATTTTTGTTAAGCTGTAATATAAAAGACGTCCTAACAAACTTCTTTTATT
ACTGAATTTCCTTTAATTATAATAAATAACAAGTTTTAAAATAAATTCAGGCAATTAAGGCGCTCCT
GAGGTACTAAAATTAATGTAAACATTTAAAATTAACTTGGATGGTCTTAAGTACTGTACTCGTGATT
TTGTTATACTTTATTATTAGAAAAGTCGTCTATTAACTTTTTGTTCCTTAATTTACTTGATTAAATTG
TCGCTTAATTTATCAAATCAGGTTTTGCGCGTTATTTTAGAGAAAAACTTATTAGAAAAATGAATAA
GCAAAGTTTAGGCTAACATGTTTTTTTATTATTTTAAATAGTTCAAGTCAATGACGTATAAAATGCA
TTTGCAAAAAATTTTAAGTAACCCTATAAACTTAGCAATAGTAGATACTGGATGCAAGCATTCAGT
AGCAGCATTGCATATCTGCTGTCTTTACGTACAAATAACAGCAAAAATGGACCTTTATTGGCTTCA
CATCGTCGTAAAACATGTGTTATTGGACTTGTCACAAATGTGTTAAGTATACAGAGCTTAGCTCTT
GATGTTGATCACTAGTGTAAAAGTGATCGGTTTGCAACTGTAAAATTTATTGAAGTACCAATAATT
TTATTTAAAATAAAACTGAAATATAAAGTTAAAGTTGCTGTTCTATAAGTTTACCGAATTTTAAAACC
ATTGTAACGCTAGAGTAATATTTGAGTCTACTAAGTTAGTCCCCGCACTTTTTAATCAAGCAATAA
ATACCCAAACTTTGCTTATTCAAATCAATAAACCAATATATCTCTTAAAATAAAGTAAAAACTTCTG
AAATTCTATAAAAAAAAATTTAATTTCGAAATATCAAATGTAACTTCAACACCGCACTATTTTCTTTT
AAACAACTGATATAGTAATTACTTCTCAAAAACGTTATCTCAAGGTTTGTGATGTACTTAAAACCAC
TCCTATTTTGTTACGCGTTTAAAAAAGCAAACATAAGTTGGTTTCTATTGATGAATGAGAACATATT
TCATTTAAAGTTAAAATCCTACCAGTGGTTTCACTGTACGTAAACACCGTCAAAAAAACAGGAACG

TTTTTAAAGATTAATAATTGAAGTAAAAAAAATTTAATACCGGGGGTTAAAAAAATCTTTTAAAATAA
TTATAAATATATATATTAAAATTTATAAATTTTTAAACACATTTAAAATATATATTAAGTATAATAAAA
GTAATATTATAAAAAAAAATTTAATTTTATAATTATTTTTATTAAATTTATAAATAATAGGTAAAACTT
ACATATCCGTTTTATTTTTTCTTAATAAAATAACGCGTGCAAATTTTTGTCCATATAAAGACCTTTTC
GAACAATAACTTTTTTGCTTAGCCGTTTTTTTTCTTATATGGTCAAAAAAGCGCTCAAGCGATTCAC
CATAAAAAGCGCAATTAGTTCAGCGTTCGTTATTCAGAAGCTTCAGCTTTGCTTGATACTCAGCTC
TTCTCTTTTTAAACAAAACACTTAATCAAAATGGCCGATGATGAAGTTGCCGCCCTCGGCCGGCC
AATGGCTTCATCAGAAAATGTTATTACAGAATTTATGAGATTTAAAGTTAGAATGGAAGGTACAGT
TAATGGACATGAATTTGAAATTGAGGGAGAAGGAGAAGGTAGACCATATGAAGGACATAATACAG
TTAAATTAAAGGTTACAAAAGGAGGACCATTACCATTTGCGTGGGATATTTTATCACCACAATTTC
AATATGGATCAAAGGTTTACGTTAAACATCCAGCTGATATTCCAGATTATAAAAAATTATCTTTTCC
AGAAGGATTTAAATGGGAAAGAGTTATGAATTTTGAAGATGGTGGAGTTGCTACAGTTACACAAG
ATTCATCATTACAAGATGGTTGTTTTATTTATAAAGTTAAATTTATTGGGGTTAATTTTCCATCAGA
CGGACCAGTTATGCAAAAAAAAACAATGGGATGGGAAGCTAGTACAGAAAGATTATATCCAAGAG
ACGGGGTTTTAAAGGGAGAAACACATAAAGCTCTAAAATTAAAGGACGGAGGACATTATTTAGTT
GAATTTAAATCAATTTATATGGCTAAAAAACCAGTTCAATTACCAGGATATTATTATGTAGATGCTA
AGTTAGATATTACATCACATAATGAAGATTATACAATTGTTGAACAATATGAAAGAACAGAAGGTA
GACATCATTTATTTTTATAGCATTCGTAGAATTCACAATTCGATTATATTTATACTGGACTATTTTTA
CATCTGTTCGGTTATTTTCACATTTATTTTTCTATATATATCTTATAAACGTTTTAAAACCCATGTAA
TTTTTGTTAAGCTGTAATATAAAAGACGTCCTAACAAACTTCTTTTATTACTGAATTTCCTTTAATTA
TAATAAATAACAAGTTTTAAAATAAATTCAGGCAATTAAGGCGCTCCTGAGGTACTAAAATTAATGT
AAACATTTAAAATTAACTTGGATGGTCTTAAGTACTGTACTCGTGATTTTGTTATACTTTATTATTA
GAAAAGTCGTCTATTAACTTTTTGTTCCTTAATTTACTTGATTAAATTGTCGCTTAATTTATCAAATC
AGGTTTTGCGCGTTATTTTAGAGAAAAACTTATTAGAAAAATGAATAAGCAAAGTTTAGGCTAACA
TGGTTTAAACGAATGCGGCCGCACTTGTGTATAAGAGACAGCTGTCGAGCTCCCAACGCGTTGG
ATGCATAGCTTGAGTATTCTATAGTGTCACCTAAATAGCTTGGCGTAATCATGGTCATAGCTGTTT
CCTGTGTGAAATTGTTATCCGCTCACAATTCCACACAACATACGAGCCGGAAGCATAAAGTGTAA
AGCCTGGGGTGCCTAATGAGTGAGCTAACTCACATTAATTGCGTTGCGCTCACTGCCCGCTTTC
CAGTCGGGAAACCTGTCGTGCCAGCTGCATTAATGAATCGGCCAACGCGCGGGGAGAGGCGGT
TTGCGTATTGGGCGCTCTTCCGCTTCCTCGCTCACTGACTCGCTGCGCTCGGTCGTTCGGCTGC
GCGAGCGGTATCA

Figure 8-7 Sequence of overexpression of HylLP-B fused with cMyc

ATGAATTTTAA…: hyilp-B ORF; ATGAGTAAAGG…: GFP; ATGGCCGATGA…: DsRed; TAG : Stop codon; cMyc: GAACAAAAATTAATTTCTGAAGAAGATTTA; GCGGCCGC or GAGCTC: restriction sites: GAGCTC - SacI restriction site; CAGCTG - PvuII restriction site; GCGGCCGC - NotI restriction site; GTGCAC - ApaLI restriction site; GTCGAC - SalI restriction site; TCTAGA -XbaI restriction site; GGATCC - BamHI restriction site. ATCGAT - BspDI/ClaI restriction site; CTCGAG - XhoI/ PaeR7I restriction site; GCGATCGC - AsiSI restriction site; ACTAGT - SpeI restriction site; GTTTAAAC - PmeI restriction site; ACGCGT - MluI restriction site; CCTGCAGG - SbfI restriction site.

8.5.3 Sequence of construct for HylLP-B Hairpin construct

gagctcccaacgcgttggatgcatagcttgagtattctatagtgtcacctaaatagcttggcgtaatcatggtcatagctgtttcctgtgtgaaattgtt
atccgctcacaattccacacaacatacgagccggaagcataaagtgtaaagcctggggtgcctaatgagtgagctaactcacattaattgcgt
tgcgctcactgcccgctttccagtcgggaaacctgtcgtgccagctgcattaatgaatcggccaacgcgcggggagaggcggtttgcgtattgg
gcgctcttccgcttcctcgctcactgactcgctgcgctcggtcgttcggctgcggcgagcggtatcagctcactcaaaggcggtaatacggttatc
cacagaatcaggggataacgcaggaaagaacatgtgagcaaaaggccagcaaaaggccaggaaccgtaaaaaggccgcgttgctggc
gtttttccataggctccgccccctgacgagcatcacaaaaatcgacgctcaagtcagaggtggcgaaacccgacaggactataaagatac
caggcgtttccccctggaagctccctcgtgcgctctcctgttccgaccctgccgcttaccggatacctgtccgcctttctcccttcgggaagcgtgg
cgctttctcatagctcacgctgtaggtatctcagttcggtgtaggtcgttcgctccaagctgggctgtgtgcacgaacccccccgttcagcccgacc
gctgcgccttatccggtaactatcgtcttgagtccaacccggtaagacacgacttatcgccactggcagcagccactggtaacaggattagca
gagcgaggtatgtaggcggtgctacagagttcttgaagtggtggcctaactacggctacactagaagaacagtatttggtatctgcgctctgctg
aagccagttaccttcggaaaaagagttggtagctcttgatccggcaaacaaaccaccgctggtagcggtggttttttgtttgcaagcagcagatt
acgcgcagaaaaaaaggatctcaagaagatcctttgatcttttctacggggtctgacgctcagtggaacgaaaactcacgttaagggattttgg
tcatgagattatcaaaaaggatcttcacctagatccttttaaattaaaaatgaagttttaaatcaatctaaagtatatatgagtaaacttggtctgac
agttaccaatgcttaatcagtgaggcacctatctcagcgatctgtctatttcgttcatccatagttgcctgactccccgtcgtgtagataactacgata
cgggagggcttaccatctggccccagtgctgcaatgataccgcgagacccacgctcaccggctccagatttatcagcaataaaccagccag
ccggaagggccgagcgcagaagtggtcctgcaactttatccgcctccatccagtctattaattgttgccgggaagctagagtaagtagttcgcc
agttaatagtttgcgcaacgttgttgccattgctacaggcatcgtggtgtcacgctcgtcgtttggtatggcttcattcagctccggttcccaacgatc
aaggcgagttacatgatcccccatgttgtgcaaaaaagcggttagctccttcggtcctccgatcgttgtcagaagtaagttggccgcagtgttatc
actcatggttatggcagcactgcataattctcttactgtcatgccatccgtaagatgcttttctgtgactggtgagtactcaaccaagtcattctgaga
atagtgtatgcggcgaccgagttgctcttgcccggcgtcaatacgggataataccgcgccacatagcagaactttaaaagtgctcatcattgga
aaacgttcttcggggcgaaaactctcaaggatcttaccgctgttgagatccagttcgatgtaacccactcgtgcacccaactgatcttcagcatct
tttactttcaccagcgtttctgggtgagcaaaaacaggaaggcaaaatgccgcaaaaaagggaataagggcgacacggaaatgttgaatac
tcatactcttcctttttcaatattattgaagcatttatcagggttattgtctcatgagcggatacatatttgaatgtatttagaaaaataaacaaataggg
gttccgcgcacatttccccgaaaagtgccacctgatgcggtgtgaaataccgcacagatgcgtaaggagaaaataccgcatcaggaaattgt
aagcgttaatattttgttaaaattcgcgttaaatttttgttaaatcagctcatttttttaaccaataggccgaaatcggcaaaatcccttataaatcaaaa
gaatagaccgagatagggttgagtgttgttccagtttggaacaagagtccactattaaagaacgtggactccaacgtcaaagggcgaaaaac
cgtctatcagggcgatggcccactacgtgaaccatcaccctaatcaagttttttggggtcgaggtgccgtaaagcactaaatcggaaccctaaa
gggagcccccgatttagagcttgacggggaaagccggcgaacgtggcgagaaaggaagggaagaaagcgaaaggagcgggcgctag
ggcgctggcaagtgtagcggtcacgctgcgcgtaaccaccacacccgccgcgcttaatgcgccgctacagggcgcgtccattcgccattcag
gctgcgcaactgttgggaagggcgatcggtgcgggcctcttcgctattacgccagctggcgaaaggggatgtgctgcaaggcgattaagttg
ggtaacgccagggttttcccagtcacgacgttgtaaaacgacggccagtgaattgtaatacgactcactatagggcgaattgagctcgacagc
tgtctcttatacacaagtgcggccgcgcatggtgcacgtcgactctagaggatccccatcgatctgactaacctaaccagtgcaaaaaaatttt
aaaagatttgcattgtgaaagttagaatattataaaaaatctaaaacgagtattactcgagtaaatgttatacgatctatagattaaatatattaaa
aatgtatagcgaatgttaaactaaatatataatataaacttgaaaacttactaaattgcaaaaactcaaaaccgactgtatcatttttacaggaaa
ccgttattcaagatacttaagttgtttactacattattataacatcttgcaattagcaagacaatcgttatttttaacatcacggtatcgaaaggattttga
gaaattttattgaaacattttaaacaaaaaatatcatatttagatgcattttaagccgagatgcaggattctgaatgaaaaagaaaaaaagaagt
ctcggtagagtaaaagtgatcggtttgcaactgyaaaatttattgaagtaccaataatttttatttaaaataaaactgaaatataaagttaaagttgct
gttctataagtttactcgaattttaaaaccattgtaacgctagagtaatatttgagtctactaagttagtccccgcacttttttaatcaagcaataaatac
ccaaaytttgcttattcaaatcaataaaccaatatatctcttaaaataaagtaaaaacttctgaaattctataaaaaaaaatttaatttcgaaatatc

aaatgtaacttcaacaccgcactattttcttttaaacaactgatatagtaattacttctcaaaaacgttatctcaaggtttgtgatgtacttaaaaccac
tcctattttgttacgcgtttaaaaaagcaaacataagttggtttctattgatgaatgagaacatatttcatttaaagttaaaatcctaccagtggtttcac
tgtacgtaaacaccgtcaaaaaaacaggaacgtttttaaagattaataattgaagtaaaaaaaatttaataccgggggttaaaaaaatcttttaa
aataattataaatatatatattaaaatttataaatttttaaacacatttaaaatatatattaagtataataaaagtaatattataaaaaaaaatttaatttt
ataattatttttattaaatttataaataataggtaaaacttacatatccgttttatttttttcttaataaaataacgcgtgcaaatttttgtccatataaagacc
ttttcgaacaataacttttttgcttagccgtttttttttcttatatggtcaaaaaagcgctcaagcgattcaccataaaaagcgcaattagttcagcgttcg
ttattcagaagcttcagctttgcttgatactcagctcttctcttttaaacaaaacacttaatcaaaatggccgatgatgaagttgccgccctcctgc
aggaccggtattaattaatgaaaaaatgagtaaaggagaagaacttttcactggagttgtcccaattcttgttgaattagatggtgatgttaatgg
gcacaaattttctgtcagtggagagggtgaaggtgatgcaacatacggaaaacttacccttaaatttatttgcactactggaaaactacctgttcc
atggccaacacttgtcactactttctgttatggtgttcaatgcttttcaagatacccagatcatatgaaacggcatgactttttcaagagtgccatgcc
cgaaggttatgtacaggaaagaactatatttttcaaagatgacgggaactacaagacacgtgctgaagtcaagtttgaaggtgatacccttgtta
atagaatcgagttaaaaggtattgattttaaagaagatggaaacattcttggacacaaattggaatacaactataactcacacaatgtatacatc
atggcagacaaacaaaagaatggaatcaaagttaacttcaaaattagacacaacattgaagatggaagcgttcaactagcagaccattatc
aacaaaatactccaattggcgatggccctgtccttttaccagacaaccattacctgtccacacaatctgccctttcgaaagatcccaacgaaaa
gagagaccacatggtccttcttgagtttgtaacagctgctgggattacacatggcatggatgaactatacaaagcgatcgcgtagCAAAAT
AGGTCCTCACTGTCACCGTGACATTAATTACAATATTCCATAATTTCGTCAACGACGCACCCTTTG
TTATAACAACATTCGTCGTGGACATTAATGTCAGTTGGATAAACATCCGGATATTGGTGTTGGAAC
CAGGTATTATCTCGTTTATTCAGAAAATTGGAAGCGACATCATTAGGTAGAGTAAAATCTTTCTTT
GTGATTGGCGTATCTTTTTTAATTAACTTTGCCACTGGATTTGAAAAAACGCACAAGTGCTTGAGC
AATGATTGCAAAAAAGCTTGCGTGCAAACTCTTAATTCTCTTTGTAggtaccAAATACTTAAGGCCTA
TTATAACCGTTGGAAAACTGAAAATGCATTAGAGTACAAAACAAATTTTGACGTTGGCGAATACGA
AGATGATACTTTAAATAAAAAAGAAAACAAAGTCATACAAAGAGAATTAAGAGTTTGCACGCAAGC
TTTTTTGCAATCATTGCTCAAGCACTTGTGCGTTTTTTCAAATCCAGTGGCAAAGTTAATTAAAAAA
GATACGCCAATCACAAAGAAAGATTTTACTCTACCTAATGATGTCGCTTCCAATTTTCTGAATAAA
CGAGATAATACCTGGTTCCAACACCAATATCCGGATGTTTATCCAACTGACATTAATGTCCACGA
CGAATGTTGTTATAACAAAGGGTGCGTCGTTGACGAAATTATGGAATATTGTAATTAATGTCACG
GTGACAGTGAGGACCTATTTTGgaattcacaattcgattatatttatactggactatttttacatctgttcggttattttcacatttatttttct
atatatatcttataaacgttttaaaacccatgtaatttttgttaagctgtaatataaaagacgtcctaacaaacttcttttattactgaatttcctttaattat
aataaataacaagttttaaaataaattcaggcaattaaggcgctcctgaggtactaaaattaatgtaaacatttaaaattaacttggatggtcttaa
gtactgtactcgtgattttgttatactttattattagaaaagtcgtctattaacttttgttccttaatttacttgattaaattgtcgcttaatttatcaaatcaggt
tttgcgcgttatttttagagaaaaacttattagaaaaatgaataagcaaagtttaggctaacatgttttttattattttaaatagttcaagtcaatgacgt
ataaaatgcatttgcaaaaaattttaagtaaccctataaacttagcaatagtagatactggatgcaagcattcagtagcagcattgcatatctgct
gtctttacgtacaaataacagcaaaaatggacctttattggcttcacatcgtcgtaaaacatgtgttattggacttgtcacaaatgtgttaagtatac
agagcttagctcttgatgttgatcactagtcggcgcgccatcagtttaaacgaatgcggccgcacttgtgtataagagacagctgtc

Figure 8-8 Sequence of HylLP-B Hairpin construct

Atgagtaaaggagaagaa: GFP; AAATACTTAAGGCC: HyILP-B hairpin Linker; TAG : Stop codon; GCGGCCGC or GAGCTC: restriction sites: SalI restriction site - GTCGAC; BamHI restriction site - GGATCC; SbfI restriction site - CCTGCAGG; PacI restriction site - TTAATTAA; AsiSI restriction site - GCGATCGC; KpnI restriction site - GGTACC; EcoRI restriction site - GAATTC; SpeI restriction site - ACTAGT; PmeI restriction site - GTTTAAAC; IlpB Hairpin - CAAAATAGGTCCTC.

8.6 Overview of HyILP-B in the head region labelled by HyILP-B antibody

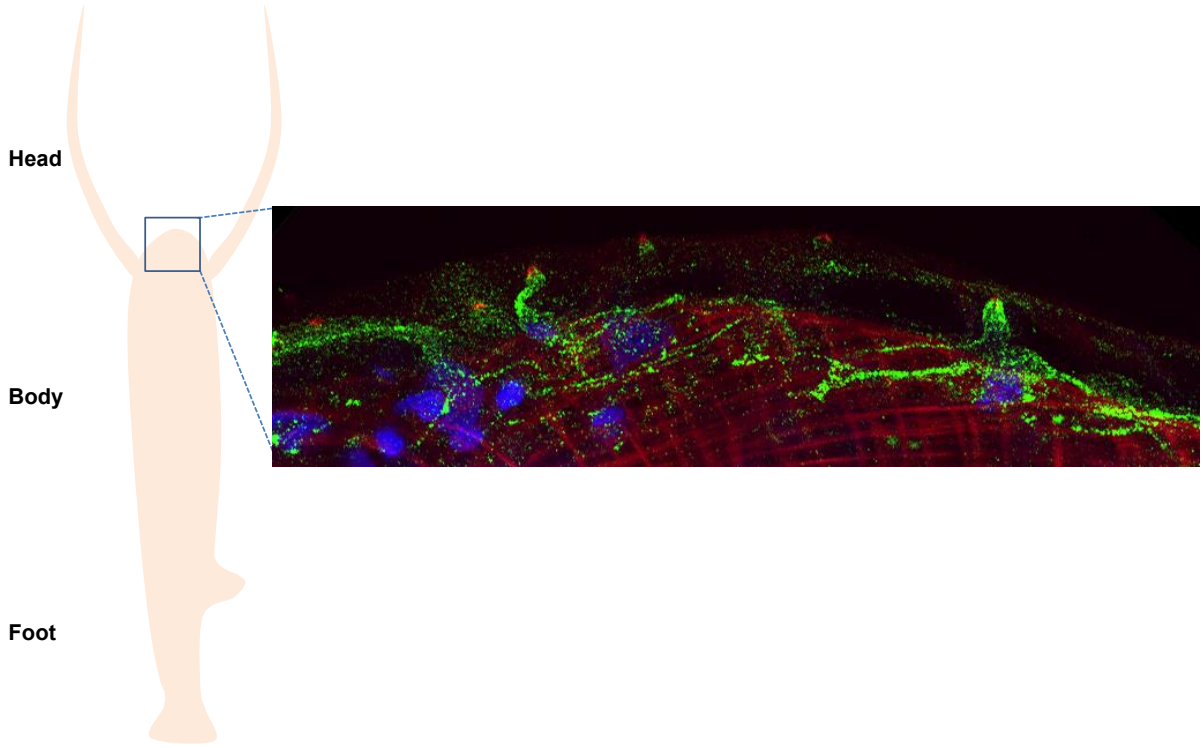

Figure 8-9 HyILP-B in the head region labelled by HyILP-B antibody

HyILP-B; Actin filament; Nuclei.

9. Erklärung

Hiermit erkläre ich, dass ich die vorliegende Dissertation nach den Regeln guter wissenschaftlicher Praxis eigenständig verfasst und keine anderen als die angegebenen Hilfsmittel und Quellen benutzt habe. Dabei habe ich keine Hilfe, außer der wissenschaftlichen Beratung durch meinen Doktorvater Prof. Dr. Dr. h.c. Thomas C. G. Bosch in Anspruch genommen. Des Weiteren erkläre ich, dass ich noch keinen Promotionsversuch unternommen habe.

Kiel, den 04. August 2016

_____

Xiaoyu Xiang